Investigations into cell polarity and trafficking in the plant model *Arabidopsis thaliana*

by

Maciej Adamowski

June, 2017

A thesis presented to the
Graduate School
of the
Institute of Science and Technology Austria, Klosterneuburg, Austria
in partial fulfillment of the requirements
for the degree of
Doctor of Philosophy

I hereby declare that this dissertation is my own work and that it does not contain other people's work without this being so stated; this thesis does not contain my previous work without this being stated, and the bibliography contains all the literature that I used in writing the dissertation.

I declare that this is a true copy of my thesis, including any final revisions, as approved by my thesis committee, and that this thesis has not been submitted for a higher degree to any other university or institution.

I certify that any republication of materials presented in this thesis has been approved by the relevant publishers and co-authors.

Signature: _____

Maciej Adamowski

June 2, 2017

Abstract

The thesis encompasses several topics of plant cell biology which were studied in the model plant *Arabidopsis thaliana*. Chapter 1 concerns the plant hormone auxin and its polar transport through cells and tissues. The highly controlled, directional transport of auxin is facilitated by plasma membrane-localized transporters. Transporters from the PIN family direct auxin transport due to their polarized localizations at cell membranes. Substantial effort has been put into research on cellular trafficking of PIN proteins, which is thought to underlie their polar distribution. I participated in a forward genetic screen aimed at identifying novel regulators of PIN polarity. The screen yielded several genes which may be involved in PIN polarity regulation or participate in polar auxin transport by other means.

Chapter 2 focuses on the endomembrane system, with particular attention to clathrin-mediated endocytosis. The project started with identification of several proteins that interact with clathrin light chains. Among them, I focused on two putative homologues of auxilin, which in non-plant systems is an endocytotic factor known for uncoating clathrin-coated vesicles in the final step of endocytosis. The body of my work consisted of an in-depth characterization of transgenic *A. thaliana* lines overexpressing these putative auxilins in an inducible manner. Overexpression of these proteins leads to an inhibition of endocytosis, as documented by imaging of cargoes and clathrin-related endocytic machinery. An extension of this work is an investigation into a concept of homeostatic regulation acting between distinct transport processes in the endomembrane system. With auxilin overexpressing lines, where endocytosis is blocked specifically, I made observations on the mutual relationship between two opposite trafficking processes of secretion and endocytosis.

In Chapter 3, I analyze cortical microtubule arrays and their relationship to auxin signaling and polarized growth in elongating cells. In plants, microtubules are organized into arrays just below the plasma membrane, and it is thought that their function is to guide membrane-docked cellulose synthase complexes. These, in turn, influence cell wall structure and cell shape by directed deposition of cellulose fibres. In elongating cells, cortical microtubule arrays are able to reorient in relation to long cell axis, and these reorientations have been linked to cell growth and to signaling of growth-regulating factors such as auxin or light. In this chapter, I am addressing the causal relationship between microtubule array reorientation, growth, and auxin signaling. I arrive at a model where array reorientation is not guided by auxin directly, but instead is only controlled by growth, which, in turn, is regulated by auxin.

Acknowledgments

I would like to thank all members of Friml lab, past and present, for the nice and scientifically stimulating atmosphere, and I would like to thank Prof. Jiří Friml for his endless patience.

About the Author

Maciej Adamowski completed MSc in Plant Biotechnology at Warsaw University of Life Sciences. In October of 2011, he joined the group of Prof. Jiří Friml, then at the Department of Plant Systems Biology (PSB) of Vlaams Instituut voor Biotechnologie (VIB) in Ghent, Belgium. He then moved to IST Austria together with Prof. Jiří Friml's group in spring of 2013, where he continued his work on several aspects of plant cell and developmental biology.

List of Publications Appearing in Thesis

1. Adamowski M, Friml J. (2015): PIN-Dependent Auxin Transport: Action, Regulation, and Evolution. Plant Cell. 27(1):20-32. (Review)

Table of Contents

List of Figures

List of Tables

List of Symbols/Abbreviations

ABP1 – auxin-binding protein 1
ALA - aminophospholipid ATPase
ALIS – ALA-interacting subunit
ANTH/ENTH - AP180 N-Terminal Homology / Epsin N-Terminal Homology
AP – adaptor protein
ARF – ADP-ribosylation factor
ARF-GEF - ADP-ribosylation factor guanine-nucleotide exchange factors
BEN - BFA-visualized endocytic trafficking defective
BFA – brefeldin A
BRI1 – brassinosteroid insensitive 1
CCV – clathrin-coated vesicle
CESA – cellulose synthase
CHC – clathrin heavy chain
CHX - cycloheximide
CK - cytokinin
CLC – clathrin light chain
CLSM – confocal laser scanning microscopy
CME – clathrin-mediated endocytosis
CMT – cortical microtubules
D6PK – D6 protein kinase
D6PKL - D6 protein kinase-like
DHNAT - DHNA-CoA thioesterase
DRP – dynamin-related protein
ER – endoplasmatic reticulum
ERAD – ER-associated degradation
ERQC – ER quality control
ESCRT - endosomal sorting complexes required for transport
FC - fusicoccin
FCHo - FCH domain only
GA – gibberellic acid
GAK - cyclin G-associated kinases
GFP – green fluorescent protein
GLV/RGF – golven/root growth factor
HA - hemagglutinin
Hsc70 – heat shock cognate 70

IAA – indole-acetic acid
IND - indehiscent
InsP3 - inositol trisphosphate
IPMS - isopropylmalate synthase
MT - microtubule
MVB – multivesicular body
NPA – N-1-Naphthylphthalamic Acid
PAT – polar auxin transport
PID - PINOID
PILS – PIN-LIKES
PIN – PIN-FORMED
PIP5K - PtdIns4P 5-kinase
PM – plasma membrane
PP2A - protein phosphatase 2A
PtdIns(4,5)P2 - phosphatidylinositol 4,5-bisphosphate
PtdIns4P - phosphatidylinositol 4-phosphate
repp – regulator of pin polarity
RFP – red fluorescent protein
SH3P – SH3-domain containing protein
TAP-MS – tandem affinity purification-mass spectrometry
TGN/EE – trans-Golgi network/early endosome
TIRF – total internal reflection
TMK – trans-membrane kinase
UGGT - UDP-Glucose:Glycoprotein Glucosyltransferase
VAEM – variable-angle epifluorescence
VAN3 - VASCULAR NETWORK DEFECTIVE3

1 Introduction

The introduction has been adapted, with modifications, from: Adamowski M, Friml J. (2015): PIN-Dependent Auxin Transport: Action, Regulation, and Evolution. Plant Cell. 27(1):20-32.

1.1 Polar auxin transport

Early experiments on plant tropisms suggested that a mobile signal exists in the plant, which has the ability to relay information about an environmental cue from the site of its perception to the tissues which react by altering their growth rates. Not only does this signal move, but it must be transported through plant tissues in a highly controlled manner, for example, to create concentration gradients between the shaded and illuminated sides of a phototropically responding coleoptile (Went, 1974). This signal is the plant hormone auxin, and further research, aided by identification of transport inhibitors, strengthened the notion of the physiological importance of auxin relocation in the plant. Auxin is distributed in the plant body by two distinct, but interconnected, transport systems. First, a fast, non-directional stream in the phloem along with photosynthetic assimilates, and second, slow and directional cell-to-cell polar auxin transport (PAT). While phloem transport provides a general way to deliver auxin from the sites of its synthesis (mostly in young leaves) to recipient organs, PAT distributes auxin in a precise manner that is critically important for the formation of local auxin maxima, mainly in developing tissues.

At the level of single cells, PAT is explained by the chemiosmotic hypothesis (reviewed in Goldsmith, 1977). This model is based on the chemical nature of the principal auxin form, indole-3-acetic acid (IAA). In the slightly acidic pH of the apoplast, a fraction of IAA exists in a protonated state (IAAH), which allows it to pass into the plasma membrane and enter the cell freely by diffusion. While in the cytosol, at a higher pH of around 7, virtually all auxin molecules are dissociated into the ionic form and thus cannot exit the cell passively. For auxin transport out of the cell to occur, the existence of plasma-membrane localized auxin efflux carriers was postulated, and the strict directionality of PAT required these transporters to be localized only on one side of the cell, thus their polar localization being decisive for the direction of auxin movement.

1.2 Discovery of PINs – the polarized auxin efflux components predicted by chemiosmotic hypothesis

The founding member of *PIN* gene family, *PIN1*, was identified following isolation of the *pin-formed1 (pin1)* mutant in *Arabidopsis thaliana*, which is characterized by a stem nearly devoid of organs such as leaves or flowers (Okada et al., 1991). The absence of organs on the stems of *pin1* mutants traces back to the shoot apical meristem, where primordia fail to form. The morphological phenotype of *pin1* could be phenocopied by a treatment with

PAT inhibitors, and *pin1* mutants showed reduced PAT. Molecular cloning of the *PIN1* gene revealed that PIN1 encodes a transmembrane protein with similarity to bacterial and eukaryotic carrier proteins (Gälweiler et al., 1998). The protein was found to be localized on the basal side of cells in the vascular tissue of the stem, just as one would predict for the auxin efflux carrier postulated by the chemiosmotic hypothesis. Around the same time, a mutant with agravitropic root was isolated independently by four labs (Chen et al., 1998; Luschnig et al., 1998; Müller at al., 1998; Utsuno et al., 1998) and the underlying gene turned out to encode a protein highly homologous to PIN1, with the same predicted membrane topology, thus named PIN2. Root gravitropism has been long associated with PAT. The agravitropic *pin2* phenotype along with the polarized localization of PIN2 in the root (Müller at al., 1998) identified PIN2 as the PAT component of root gravitropic response. The auxin efflux capacity of PIN proteins has been since shown in a number of transport assays in different systems (Petrásek et al., 2006; Yang and Murphy, 2009; Barbez et al., 2013; Zourelidou et al., 2014). An important question concerned the relation between PIN polarity and directionality of auxin transport. When PIN1 is expressed under the control of the PIN2 promoter in the agravitropic *pin2* mutant, it is, in contrast to PIN2, localized predominantly basally (towards root tip) in epidermis cells. Therefore, the auxin transport capacity in basipetal (shootward) direction, necessary for correct gravitropism, is not achieved. However, a mutant version of PIN1, containing a green fluorescent protein (GFP) insertion which presumably interferes with a polarity-determining signal, localizes more apically (shootward) and was able to rescue the agravitropism of *pin2* by mediating the auxin flux away from the root tip, similarly to PIN2 function in the wild type. Thus, by switching the polarity of ectopically expressed PIN1 in otherwise identical conditions, and observing resultant auxin redistribution and tropic response, the causal link between PIN polar localization and auxin flow direction was proven (Wiśniewska et al., 2006).

1.3 Developmental roles of PIN-driven auxin transport

The phenotypes of mutants in the first two *PIN* genes indicated that PIN-driven PAT is crucial for processes as diverse as above-ground organogenesis and the root gravitropic response. *Arabidopsis* contains a total of eight *PIN* sequences, and isolation of other *pin* mutants extended the repertoire of processes mediated by this auxin efflux carrier family. Auxin transport mediated by PINs is necessary from the very beginning of multicellular plant body development, during the laying down of the main apical-basal body axis in early embryogenesis (Friml et al., 2003). Embryos express four *PIN* genes, namely *PIN1, 3, 4* and *7*, and developmental defects in early embryogenesis can be found in single *pin4* (Friml et al., 2002a) and *pin7* mutants (Friml et al., 2003), with increasingly severe aberrations in multiple mutant combinations (Friml et al., 2003; Blilou et al. 2005; Vieten et al., 2005). Preferential accumulation of auxin is first seen in the apical cell originating after zygote division, and

auxin remains present in the apical part of the embryo until a switch occurs around the 32-cell stage, following which auxin maximum is instead detected in the basal parts of the embryo, as well as the uppermost suspensor cell (Friml et al., 2003; Figure 1C). Polar localizations of PINs correspond well with these auxin fluxes, as initially PIN7 is expressed in basal domains of the embryo and polarized towards apical cells, while later both PIN7 in the suspensor and PIN1 in provascular cells of the embryo proper exhibit basal polarity (Friml et al., 2003; Figure 1D). Recent modelling studies combined with experimental approaches revealed that the PIN polarity switches during embryogenesis occur as a result of feedback regulation by auxin sources. In this scenario, local auxin production, first in the suspensor and presumably in the maternal tissues, and later at the apical end of the embryo, polarize auxin fluxes to define the apico-basal embryonic axis (Robert et al., 2013; Wabnik et al., 2013). As embryo development progresses, additional peaks of auxin response appear at the sites of cotyledon formation. Accordingly, PIN1 protein can be detected in the epidermal layer with polarities facing towards these auxin maxima, while a canal expressing basally localized PIN1 forms in the inner embryo body, driving auxin away from the primordium and defining future vascular strands (Benková et al., 2003). Indeed, cotyledon development defects, such as single, triple, fused or improperly shaped cotyledons are observed in *pin* mutants (Friml et al., 2003; Benková et al., 2003).

When seeds germinate underground, or *in vitro* in darkness, the elongated hypocotyl forms at its apical end a curved structure called the apical hook, designed by nature to protect the all-important shoot apical meristem from physical damage in the soil. During the development of this structure, an auxin response gradient is formed with a maximum in the inner side of the hook (Friml et al., 2002b; Žádníková et al., 2010; Vandenbussche et al., 2010). The importance of PAT for generating this local auxin maximum and for the resulting differential cell elongation is evident by a complete loss of apical hook formation following treatment with PAT inhibitors (Žádníková et al., 2010). Time-lapse imaging revealed disrupted dynamics of apical hook development in *pin1, pin3, pin4* and *pin7,* as well as certain double mutant combinations. Interestingly, PIN3 and PIN4 are preferentially expressed in the outer side of the apical hook, and the increased drainage of auxin from this region may result in its predominant accumulation on the opposite side (Žádníková et al., 2010).

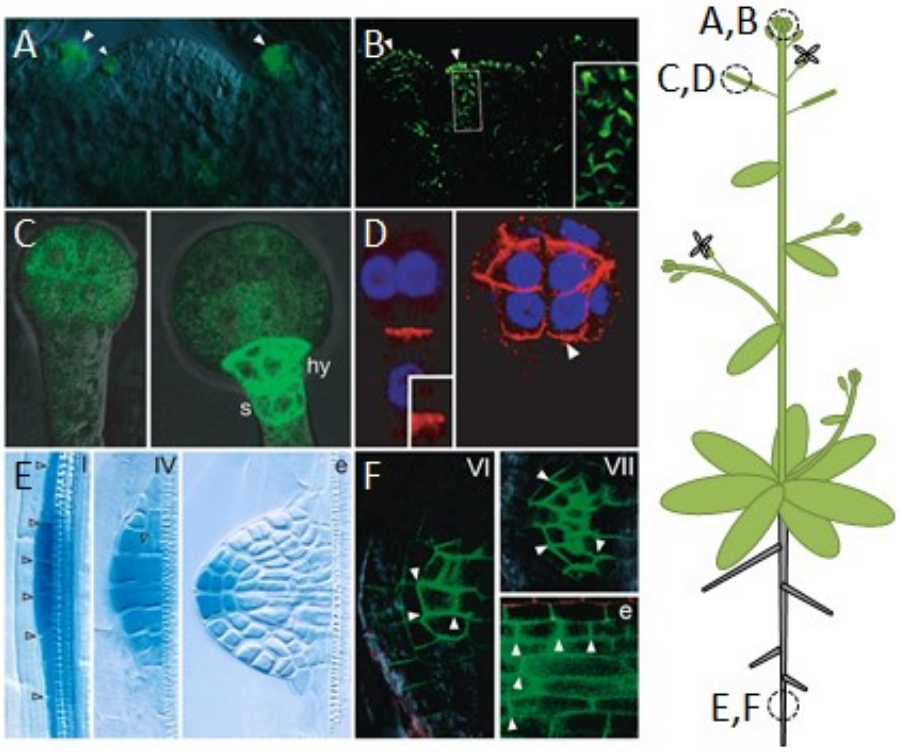

Figure 1. Examples of auxin-mediated developmental processes. Auxin response maxima (visualized by transcriptional auxin response reporters; green in A, C; blue in E) are established by the action of polarly localized PIN proteins (green in B, F; red in D) during the development of shoot apical meristem-derived primordia (A, B), embryo (C, D) and lateral root (E, F). **(A)** In the shoot apical meristem, auxin accumulates at the position of incipient primordia and in primordium tips (indicated by arrowheads in A and B). **(B)** In epidermis, PIN1 is polarized towards these auxin maxima, while in the inner tissues, basally localized PIN1 presumably drives auxin away from the primordium (inset). **(C)** During embryogenesis, auxin response is first observed in apical parts of the embryo (left; eight-cell stage) and later in the basal parts (right; globular stage). **(D)** PIN7 localizes apically in the basal cell of a 2-cell embryo (left; magnified in inset) and PIN1 basally in provascular initials at 16/32 cell stage (right; indicated by arrowhead). **(E)** Auxin concentrates at the apical end of a developing lateral root (arrowheads indicate cell division planes). **(F)** PIN1 gradually establishes polarized localizations (indicated by arrowheads) in the inner tissues of the developing lateral root. s – upper suspensor cell, hy – hypophysis, I, IV, VI, VII, e – developmental stages of lateral roots. Reproduced with modifications from Benková et al. (2003; A, B, E, F) and Friml et al. (2003; C, D).

From the seedling stage on, PINs function in maintaining the activity of the root apical meristem. The local auxin maximum in the root tip has been recognized as the pattern- and organ polarity-organizing signal (Sabatini et al., 1999) established by directional auxin transport driven by PINs (Friml et al., 2002a; Blilou et al., 2005). Joint action of PIN1, PIN2, PIN3, PIN4 and PIN7 establishes a local "reflux loop" of auxin (Blilou et al., 2005). Studies on PIN function in the root apical meristem revealed that PIN proteins exhibit partial functional redundancy in this developmental context, aided by ectopic expression of some *PIN* genes to complement lack of others in *pin* mutants (Blilou et al., 2005; Vieten et al., 2005).

The elaboration of plant body architecture at later stages of development involves auxin- and PIN-dependent postembryonic formation of new organs. The root system is extended into a branched network by the process of lateral root development. New roots arise from the pericycle layer of the primary root, at sites of elevated auxin response (Benková et al., 2003; Dubrovsky et al., 2008). The progression into a newly emerged organ involves dynamic changes in PIN-driven auxin distribution, leading to gradual concentration of auxin at the apical end of the growing lateral organ (Figure 1E, F). In *pin* mutants, lateral roots are generated at lower frequency, progress more slowly through development, or cannot be formed at all, instead resulting in a disorganized array of cells with diffuse auxin distribution (Benková et al., 2003).

While the development of underground tissues depends on the collaborative action of multiple PINs, the phenotypes of *pin1* clearly imply a less redundant role of PIN1 in aerial organogenesis. As stated above, *pin1* is characterized by the presence of nearly naked stems, which only rarely form defective cauline leaves or flowers (Okada et al., 1991). In the shoot apical meristem, where these organs originate, PIN1 is expressed in the outermost tissue layer, with polarities converging at an auxin maximum in the primordium tip (Reinhardt et al., 2003; Benková et al., 2003; Heisler et al., 2005; Figure 1A, B). Files of cells with basally localized PIN1 drain auxin from this maximum, into inner parts of the tissue. Later during development of the flower, local auxin response maxima mark the apical end of each developing floral organ. When ovules develop inside the gynoecium, their tips also show auxin accumulation, and an auxin peak is seen at the tip of each developing integument (Benková et al., 2003).

The examples of auxin-mediated formation of organs, such as cotyledons, lateral roots, leaves or flowers point at a common mode of auxin action (Benková et al., 2003), in which PIN proteins, by their coordinated polarized localizations, direct auxin transport such that auxin accumulates locally and defines sites of organogenesis. It is interesting to notice that in each case auxin is transported towards the tip of the root through the central part of the tissue, a flux which in root-derived organs supplies the local maximum with auxin, while in apical organs drains it; thus, complementary fluxes through the outer tissue layers also have opposite directions in apical and basal organs. These two patterns of auxin flow in organogenesis have been termed “fountain” and “reverse fountain” (Benková et al., 2003).

As already hinted in the previous paragraphs, the vascular tissue, which serves as a connecting tract for transport of photosynthetic assimilates, water, and minerals between the various plant organs, also forms in an auxin-dependent manner, and PIN1 appears to have a principal role in this process - at least when above-ground tissues are considered. *pin1* mutant plants show vascular abnormalities in stems and leaves (Gälweiler et al., 1998; Mattsson et al., 1999) which can be mimicked by chemical inhibition of PAT with 1-N-naphthylphthalamic acid (NPA; Mattsson et al., 1999). Accordingly, the pattern of vascular

development in leaves is preceded by expression of PIN1 and an elevated auxin response (Scarpella et al., 2006). During leaf vasculature formation, the “reverse fountain” auxin flow pattern can be observed, as PIN1 polarities converge in epidermis and form a stream reaching inside the leaf. PIN1 also controls the establishment of leaf shape, in particular the outgrowth of serrations at the leaf margin (Hay et al., 2006; Bilsborough et al., 2011). The epidermal auxin maxima which correspond to future veins in subepidermal tissues also mark sites for serration development. Consistently, *pin1* mutants as well as NPA-treated plants exhibit smooth leaf margins (Hay et al., 2006).

In contrast to the developmental processes outlined above, the opening of *Arabidopsis* fruit appears to depend on a conceptually novel local auxin minimum, rather than formation of an auxin maximum (Sorefan et al., 2009). *Arabidopsis* silique opens along thin margins between the replum and the two valves in a process dependent on the transcription factor INDEHISCENT (IND) expressed specifically at the valve margin. The proposed model suggests that fruit opening requires a localized auxin depletion resulting from IND- and phosphorylation-dependent modulation of PIN3 polarity and redirection of PAT.

1.4 Auxin transport across ER membrane

The canonical, plasma-membrane localized PINs, which consist of two transmembrane regions separated by a long hydrophilic loop, are represented in *Arabidopsis* by five members: PIN1-4 and PIN7. By contrast, PIN5, PIN6 and PIN8 are characterized by a reduction in the middle hydrophilic loop, partially in PIN6 and more pronounced in PIN5 and PIN8. Surprisingly, localization studies revealed that PIN5, PIN6 and PIN8 predominantly localize to the endoplasmic reticulum (ER; Mravec et al., 2009; Ding et al., 2012; Dal Bosco et al., 2012; Bender et al., 2013; Sawchuk et al., 2013) although instances of plasma membrane localization of PIN5 and PIN8 have been reported as well (Ganguly et al., 2014). Auxin transport and auxin content measurements indicate that PIN5 likely mediates auxin transport into the ER lumen (Mravec et al., 2009), while PIN8 appears to counteract this activity, which is further supported by antagonistic genetic interactions observed between mutants and overexpressors of these two transporters (Ding et al., 2012; Sawchuk et al., 2013). The proposed role of PINs at the ER membrane is the regulation of auxin homeostasis by subcellular auxin compartmentalization, as auxin inserted into ER lumen is likely unavailable for participation in PAT and nuclear signalling, and becomes a potential substrate for inactivation by ER-localized auxin conjugating enzymes (Mravec et al., 2009). PIN6- and PIN8-mediated translocation of auxin from the ER lumen into the nucleus has also been hypothesized (Sawchuk et al., 2013).

ER-localized PINs play both distinct and overlapping functions in plant development. PIN8, which is highly expressed in the male gametophyte, has an important role in pollen

development and functionality (Ding et al., 2012; Dal Bosco et al., 2012), while PIN6 has been ascribed a function in the production of nectar and proper development of short stamens (Bender et al., 2013) as well as root growth and lateral root development (Cazzonelli et al., 2013). PIN5 appears to be necessary for fine-tuning of auxin function, as a *pin5* mutant revealed only minor developmental phenotypes (Mravec et al., 2009). Moreover, all three ER-localized PINs are necessary in leaf vascular patterning (Sawchuk et al., 2013) where their intracellular auxin transport activity interacts with the intercellular PAT driven by PIN1.

Recently, a novel family of putative auxin transporters, designated PIN-likes (PILS), has been discovered, based on *in silico* search for proteins with predicted topology similar to that of the PINs (Barbez et al., 2012). Reduction or upregulation of PILS activity leads to alterations in auxin-mediated developmental processes, such as root and hypocotyl growth and lateral root formation. Analysis of transcriptional auxin responses suggested that PILS action leads to decreased auxin signalling, while auxin accumulation assays showed their ability to increase intracellular auxin retention, with a shift towards conjugated forms of the molecule. This mode of action is reminiscent of ER-localized PIN5, and indeed PILS transporters were found to localize to ER in all systems analysed. Thus, PILS emerged as a novel family of cellular auxin homeostasis regulators.

1.5 Evolution of PIN proteins

In the flowering plant species *Arabidopsis thaliana*, PIN proteins have become highly specialized, as evidenced by their differential expression patterns, subcellular localizations and developmental roles. An interesting question, then, arises about the evolutionary origin of this diversity in PIN function, and the roles of PIN-mediated auxin transport in taxonomic groups ancestral to the flowering plants. Recently, experimental insights into the developmental functions of PIN transporters in the moss model species *Physcomitrella patens,* have been reported. The *P. patens* genome encodes four *PIN* sequences, denoted Pp-*PINA*-*PIND*, of which Pp-*PINA*-*PINC* represent long, PIN1-type transporters, while Pp-*PIND* encodes a short, PIN5-type protein. Accordingly, Pp-PINA shows polar, plasma membrane localization at the apical ends of moss filaments and in leaves, while Pp-PIND does not colocalize with plasma membrane markers and has localization pattern reminiscent of ER (Viaene et al., 2014; Bennett et al., 2014). The auxin transport activity of Pp-PINs was verified by various means, including measurements of IAA export into the media from *P. patens* tissues.

The first stage of gametophyte development in moss is a structure consisting of one-cell wide filaments called protonemata, which grow by apical cell divisions, gradually changing their character from chlorophyll-rich chloronema to chlorophyll-poor caulonema. This developmental switch in cell identity seems to be regulated by auxin (Prigge et al.,

2010; Jang and Dolan, 2011). Presumably, Pp-PINs mediate auxin transport from the base of protonema filaments to their tips, influencing auxin content in each cell and thus their developmental fates (Viaene et al., 2014).

During later development, mosses generate gametophores with leaves consisting of two-dimensional sheets of cells. Auxin transport inhibition, external auxin application and long-type *pin* knockouts suggest that PIN-driven auxin transport is required for multiple aspects of gametophore development, such as apical meristem activity, leaf initiation and growth, and tropisms (Bennett et al., 2014; Viaene et al., 2014). Furthermore, development of the *P. patens* sporophyte depends on Pp-PIN function (Bennett et al., 2014), consistent with the presence of long-range PAT in moss sporophytes (Fujita et al., 2008)

The first experimental insights into PIN protein function in *P. patens*, a representative of most basal land plants, indicate that auxin transport mediated by polarly localized PINs has been recruited in the dominant gametophyte stage of moss, controlling a suite of processes including the development of relatively simple morphologies such as one-dimensional protonemal filaments or two-dimensional cell sheets which are the moss leaves.

1.6 Subcellular trafficking for PIN polar localization

Every plasma membrane localized PIN protein in *Arabidopsis* exhibits polarized localization in some instances. How is that achieved? Today, there is mounting evidence supporting subcellular trafficking of PINs as the primary factor in the establishment of their polarities. Although one may presume that PIN proteins are statically deposited at the plasma membrane, in fact PINs turned out to be continuously, dynamically cycling between their polar domain at the plasma membrane and endosomal compartments (Figure 2). This conclusion was first drawn from observations that the fungal toxin brefeldin A (BFA) triggers intracellular accumulation of PIN1 in so called “BFA compartments”, which is fully reversible after removal of BFA (Geldner et al., 2001). BFA inhibits ADP-ribosylation factor guanine-nucleotide exchange factors (ARF-GEFs), which activate ADP-ribosylation factors (ARFs), molecular players necessary for formation of coated vesicles mediating various trafficking events in the endomembrane system.

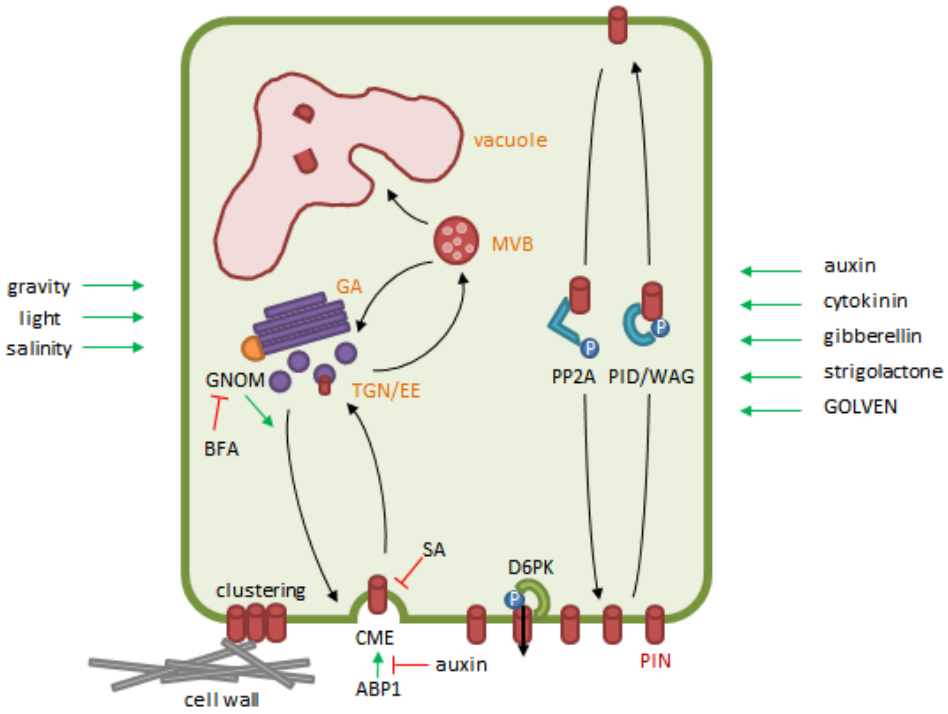

Figure 2. Subcellular trafficking and polarity maintenance of PIN proteins. Polar localization of PIN proteins is established by GNOM-mediated recycling and clathrin-mediated endocytosis (CME) and maintained by clustering in the plasma membrane as well as cell wall-plasma membrane connections. Apical-basal polarity is determined by reversible phosphorylation by PID/WAG kinases and PP2A phosphatase. Auxin transport activity of PIN is mediated by D6PK. PINs undergo trafficking through multivesicular body (MVB) for degradation in the lytic vacuole. Endogenous (hormones and signal peptides) and environmental (light, gravity, salinity) signals influence various aspects of PIN trafficking. GA – Golgi apparatus, TGN/EE – Trans-Golgi network/early endosome

Putting these facts together, a BFA-sensitive ARF-GEF action mediates constitutive recycling of PIN1 from an endosomal compartment to the polar domain at the plasma membrane, and when this recycling step is blocked, the constitutive internalization of PIN1 is revealed by its intracellular accumulation. A candidate for the protein which may mediate this BFA-sensitive polar delivery of PIN1 is the ARF-GEF GNOM. *gnom* mutants demonstrate severe defects in development, characterized, in extreme cases, by a complete loss of apical-basal body plan (Mayer et al., 1991; Shevell et al., 1994). These defects originate at embryogenesis, where coordinated cell polarities are not correctly established, as manifested by the loss of correct polarization of PIN1 (Steinmann et al., 1999). BFA-sensitive PIN1 recycling was conclusively linked with GNOM function with the use of an engineered, BFA-resistant, yet fully functional variant of GNOM (Geldner et al., 2003). While originally a model was proposed in which GNOM mediates the recycling step from a hypothetical “recycling endosome”, recent in-depth analyses using high-end microscopy revealed that GNOM in fact acts at the Golgi apparatus (Naramoto et al., 2014). Thus, GNOM may be

indirectly influencing the function of Trans-Golgi network/early endosome (TGN/EE) compartment, from where polar cargoes might be recycled. The GNOM-mediated pathway is to a large extent responsible specifically for the basal targeting of PIN proteins, while the apical pathway may be mediated by other, BFA-resistant ARF-GEFs (Kleine-Vehn et al., 2008a). Additional components of PIN delivery to the plasma membrane, namely the ARF family member ARF1A1C (Tanaka et al., 2014) and a small GTPase RabA1b (Feraru et al., 2012), were identified in a forward genetic screen based on PIN1-GFP fluorescence imaging (reviewed in Zwiewka and Friml, 2012).

PIN proteins are internalized from the plasma membrane by clathrin-mediated endocytosis (Dhonukshe et al., 2007). Interference with clathrin-coated vesicle formation by expression of a dominant-negative truncated variant of clathrin heavy chain (CHC), referred to as HUB, abolished the BFA-visualized internalization of PIN1 and PIN2 (Dhonukshe et al., 2007; Kitakura et al., 2011), while a similar, but weaker effect on PIN2 was observed in *clathrin light chain2 clathrin light chain3 (clc2 clc3)* double mutants (Wang et al., 2013). The relevance of clathrin-mediated PIN endocytosis for correct auxin transport and auxin-mediated development is illustrated by improper auxin distribution in the above-mentioned HUB line, concomitant with root gravitropism and lateral root formation defects, embryo patterning defects in the *clathrin heavy chain2* (*chc2*) mutant which leads to development of seedlings with improperly formed cotyledons and root apical meristems (Kitakura et al., 2011), as well as deficiencies in auxin transport and distribution in *clc2 clc3* mutant (Wang et al., 2013). Other than clathrin, ARF machinery has also been implicated in endocytosis. The ARF-GEF GNOM, apart from regulating recycling, functions in endocytosis in concert with ARF-GTPase activating protein (ARF-GAP) VASCULAR NETWORK DEFECTIVE3 (VAN3; Naramoto et al., 2010), while the related ARF-GEF GNOM-LIKE1 participates more specifically in endocytosis of PIN2 (Teh and Moore, 2007). Downstream of endocytosis, the early endosomal trafficking of PINs is controlled by another ARF-GEF, BFA-visualized endocytic trafficking defective1 (BEN1), and the Sec1/Munc18 family protein BEN2 (Tanaka et al., 2009; Tanaka et al., 2013).

The proposed role of constitutive internalization of PIN proteins is to maintain, in concert with polar recycling, the polarized localization of PINs at the plasma membrane. Presumably this is necessary to counteract lateral diffusion in the absence of diffusion barriers, such as junctions which separate polar domains in polarized animal cells (for a comparison of polarity determination mechanisms in animal and plant cells, see Kania et al., 2014). Indeed, PIN proteins are depolarized in the dominant negative clathrin HUB line as well as *chc2* embryos (Kitakura et al., 2011). Experimental and modelling approaches suggest that endocytosis of PINs, necessary for maintenance of its polarity, may take place preferentially at lateral cell sides (Kleine-Vehn et al., 2011). The dynamic nature of PIN trafficking could be also highly relevant for rapid changes in PIN polar localization, occurring

during embryo development (Friml et al., 2003), lateral root formation (Benková et al., 2003), root gravitropic response (Friml et al., 2002b; Kleine-Vehn et al., 2010) and hypocotyl tropic responses (Ding et al., 2011; Rakusová et al., 2011). In support of the notion of PINs being dynamically redistributed to new polar domains, a transcytosis-like process, in which the same PIN protein molecules undergo trafficking from one polar domain to another, was documented (Kleine-Vehn et al., 2008a) and implicated in gravity-induced PIN3 relocation in the root tip columella (Kleine-Vehn et al., 2010).

Endocytosis and polar recycling jointly establish the polar localization of PINs at the plasma membrane. An additional layer of regulation comes from ubiquitination-dependent PIN degradation in the vacuole (Kleine-Vehn et al., 2008b; Leitner et al., 2012), a process which requires proteasome function (Abas et al., 2006). Multiple trafficking components participate in vacuolar PIN sorting, including the adaptor protein complex 3 (AP-3; Feraru et al., 2010; Zwiewka et al., 2011), the retromer (Nodzyński et al., 2013) and the endosomal sorting complexes required for transport (ESCRT; Spitzer et al., 2009; Gao et al., 2014).

1.7 PIN polarity maintenance by clustering and the cell wall

Apart from the subcellular trafficking events describe above, an additional factor which might be important for polarity maintenance during the residence of PIN in the plasma membrane has been uncovered (Kleine-Vehn et al., 2011). PIN proteins have been observed to exhibit only limited lateral diffusion in the plasma membrane, when compared to non-polar plasma membrane markers. Following a detailed confocal and high-resolution microscopic analyses, PIN1 and PIN2 were found to be unevenly distributed in the plasma membrane, with a large fraction of the protein residing in so-called clusters, defined as agglomerations of PIN signals 100-200 nm in diameter. These clusters were immobile in the membrane, and since less clustering of non-polar membrane markers was observed, clustering was proposed as a factor limiting the lateral diffusion of PIN proteins out of their polar domains (Kleine-Vehn et al., 2011).

Another line of investigation aimed at identification of novel components of PIN polarity was the *regulator of pin polarity (repp)* forward genetic screen, designed to identify mutants with a basal-to-apical switch in localization of PIN1 ectopically expressed in root tip epidermis. Because the screen was performed in the agravitropic *pin2* mutant background (PIN2:PIN1-HA, *pin2* line), such apicalization of PIN1 in the epidermis could be identified easily, since it would lead, by mimicking native function of apically localized PIN2, to restoration of a correct auxin flow and hence root gravitropism (Feraru et al., 2011). The first mutant identified in this screen, *repp3*, was mapped to the *CELLULOSE SYNTHASE 3* (*CESA3*) locus, and independent pharmacological or genetic interference with cellulose biosynthesis phenocopied *repp3.* This unexpected function of the cell wall for PIN polarity was substantiated by observations that PIN proteins are associated with domains which are

physically connected to the cell wall, and by the rapid loss of PIN polarization after cell wall digestion. Furthermore, the lateral diffusion of PIN2 was much faster when cell wall connections were lost following pharmacological inhibition of cellulose synthesis or cell plasmolysis (Feraru et al., 2011). The role of the plant cell wall in limiting lateral diffusion of plasma membrane proteins has been since further confirmed (Martinière et al., 2012). In summary, clustering and cellulose-based cell wall-to-polar domain connections presumably contribute to the maintenance of PIN proteins at their polar domains (Figure 2). The possible relationship between these two processes remains an open question for future research.

1.8 Phosphorylation-based regulation of PIN-mediated auxin transport

In a genetic screen for mutants that have lost the ability to generate flower primordia, a mutant named *pinoid* was found, with phenotypic characteristics resembling those of *pin1* (Bennett et al., 1995). The PINOID (PID) protein encodes a member of AGCVIII family of protein kinases (Christensen et al., 2000). Although initially a role in auxin signalling was ascribed (Christensen et al., 2000), further analyses implicated PID in an auxin transport-related function (Benjamins et al., 2001). Overexpression of PID led to frequent collapse of the main root (Benjamins et al., 2001; Friml et al., 2004) which correlated with loss of local auxin maximum in the root apex. This phenotype was preceded by basal-to-apical switch of polarities of PIN1, PIN2 and PIN4 (Friml et al., 2004) resulting in draining of auxin out of the root tip. Conversely, the *pinoid* mutant exhibits the opposite, apical-to-basal, polarity switch of PIN1 in the shoot apical meristem (Friml et al., 2004), confirming the function of PID in PIN apical versus basal polarity determination. PID and its homologues directly phosphorylate PIN protein hydrophilic loops at three highly conserved motifs and the importance of these phosphorylation sites for PIN polarity determination was confirmed *in planta* by the analysis of phosphomutant versions of PINs (Michniewicz et al., 2007; Huang et al., 2010; Zhang et al., 2010).

The search for phosphatase activity which antagonizes PID function led to the identification of protein phosphatase 2A (PP2A) as an important factor in PIN polarity regulation. Initially, a mutant in one of the three *Arabidopsis* paralogues of the PP2A regulatory subunit A (PP2AA1) was isolated in a forward genetic screen for altered response to the PAT inhibitor NPA (Garbers et al., 1996). This and other phenotypes that indicated the involvement of PP2AA1 in auxin-mediated processes (Rashotte et al., 2001) prompted a more complete analysis which revealed severe auxin-related developmental defects during embryo and seedling development in multiple *pp2aa* mutants and artificial microRNA lines targeting PP2AA (Michniewicz et al., 2007). Genetic interactions supported the notion that PP2AA phosphatase function antagonizes that of PID kinase. Crucially, a basal-to-apical polarity shift of PIN1, PIN2 and PIN4 was observed in PP2AA-deficient plants (Michniewicz et

al., 2007), indicating that dephosphorylation of PINs by PP2A promotes their basal localization.

Taken all these data together, a model emerged in which PID-mediated phosphorylation promotes apical PIN localization, whereas dephosphorylation by PP2A leads to basal PIN polarity (Figure 2). However, it remains unclear at which stage of the polar sorting processes and where in the cell these regulatory steps take place, or whether they are relatively stable, or more transient.

Recently, another group of proteins from the same AGCVIII family of protein kinases, consisting of D6 protein kinase (D6PK) and D6 protein kinase-likes (D6PKL), has been implicated in the regulation of PAT. Loss of D6PK activity led to typical auxin-related phenotypes which correlated with reduced PAT rates (Zourelidou et al., 2009; Willige et al., 2013; Zourelidou et al., 2014). D6PKs phosphorylate PM-localized PINs (Zourelidou et al., 2014), but, unlike PID, do not affect their polar localizations (Willige et al., 2013). Instead, D6PKs act as activators of auxin efflux activity of PIN proteins: in *Xenopus* oocytes, auxin was actively transported only when PINs were coexpressed with D6PK (Zourelidou et al., 2014). *In planta,* this transport activation presumably occurs at basal polar domains, where D6PK localizes (Barbosa et al., 2014; Figure 2). The auxin transport assays in *Xenopus* oocytes showed that PID and its close homologue WAG2 also activate PIN-driven auxin efflux (Zourelidou et al., 2014); showing that AGCVIII family kinases likely have both different and partially overlapping functions in regulating PINs.

1.9 Auxin feedback regulations of PIN-mediated auxin transport

The canalization hypothesis, proposed by Tsvi Sachs, suggests self-organizing properties of PAT on the level of organs and tissues (summarized in Sachs, 1991). In an undifferentiated group of cells exposed to a source and sink of auxin, the cells gradually polarize their auxin transport activities towards neighbours which already happen to transport auxin most efficiently. This feedback mechanism, in which local flow of auxin affects the cells to modify this flow's direction and strength, results in emergence of a narrow, well-defined canal of cells efficiently transporting auxin to connect the source with the sink. The canalization hypothesis is intimately linked with several developmental roles of auxin, such as *de novo* vascular tissue formation or its regeneration. Cells forming the postulated canals of PAT will differentiate into vascular tissue connecting various parts of the plant body, and indeed it is by microscopic observation of vascular cell differentiation that Sachs assumed the PAT directions in his experiments.

According to the model described above, auxin itself should have the ability to influence the directionality and capacity of a given cell's auxin transport. Nowadays, we see mechanisms which could contribute to feedback of auxin regulation on its own transport by affecting PIN polar localization and PIN protein abundance in the cell, or more specifically at

the plasma membrane. A series of experiments on wounded pea epicotyls, inspired by Sachs' ideas, but extending them by direct observations of PIN proteins, was conducted by Sauer et al. (2006). The pea homologue of PIN1 co-ordinately polarized along the presumed path of auxin flow which forms around a wound, spatially corresponding to the vascular tissue which later differentiated in order to reconnect the severed vascular strand. When an auxin source was artificially provided, PIN1 became expressed and polarized so as to create a new canal, connecting that auxin source to the sink - the pre-existing central vascular cylinder. The competition between different auxin sources has an impact on their ability to induce such canalization, providing a possible mechanism for regulation of apical dominance (Balla et al., 2011). Together, these observations show that PINs are suitable candidates to be targeted by the canalization mechanism, as both their expression and subcellular polarization are regulated by auxin itself. Auxin influence on PIN polarities can be also seen in the root apical meristem, where its external application leads to cell-type specific lateral spreading of PIN1 and PIN2 via a mechanism involving the nuclear, Aux/IAA and auxin response factor (ARF)-dependent auxin signaling pathway (Sauer et al., 2006).

As PINs are subject to dynamic subcellular trafficking, regulatory inputs of auxin into specific trafficking events could be envisioned as an efficient means for the hormone to regulate its own transport. Indeed, auxin was found to inhibit endocytosis, leading to stabilization of PIN proteins at the plasma membrane and enhancement of the cell's auxin efflux capacity (Paciorek et al., 2005). This rapid auxin effect is mediated by a non-transcriptional pathway involving the auxin receptor auxin binding protein 1 (ABP1; Robert et al., 2010). Experimental evidence suggests a model in which ABP1, when not bound to auxin, promotes clathrin-mediated endocytosis, while auxin binding would block this ABP1 activity, causing loss of clathrin from the plasma membrane and inhibition of endocytosis, including that of PIN cargoes. This extracellular ABP1 action on endocytosis, presumably coupled with PM-localized transmembrane kinase (TMK) members of receptor-like kinase family (Xu et al., 2014), seems to be the central part of the mechanism by which auxin polarizes its own flux, as recently suggested by experimental and computational modelling approaches (Rakusová et al., 2014; Figure 3). However, recent isolation of new ABP1 knock-out alleles, which, in contrast to the alleles generated thus far appear phenotypically normal (Gao et al., 2015), challenges the relevance of ABP1 for plant development and calls for re-evaluation of its role in endocytosis.

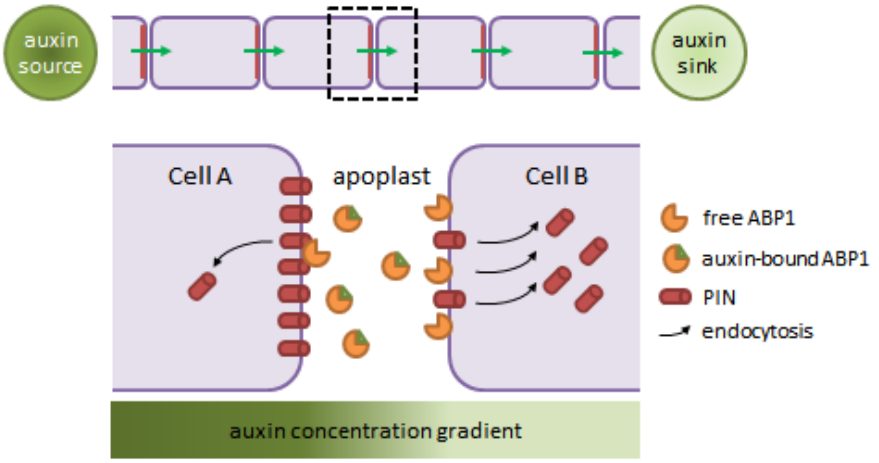

Figure 3. A model of auxin transport canalization by extracellular auxin perception by ABP1. PIN proteins gradually polarize to form a canal of auxin flow connecting auxin source to the sink. Two neighbouring cells share an apoplastic pool of ABP1 molecules. ABP1 exists in auxin-free and auxin-bound states, whereby it promotes endocytosis or is inactive, respectively. Due to an auxin concentration gradient across the apoplastic space, cell A closer to the auxin source experiences higher apoplastic auxin levels, fewer auxin-free ABP1 and thus has low PIN endocytosis rates, resulting in stabilization of PIN at the plasma membrane. The extracellular space near cell B has lower auxin concentration and more free ABP1 molecules which promote PIN removal from the plasma membrane.

Auxin also affects the abundance of PINs. Auxin influence on PIN degradation in the vacuole has been extensively studied on the model of gravistimulated root (Baster et al., 2013; Abas et al., 2006; Kleine-Vehn et al., 2008b). While auxin transiently stabilizes PIN2 by its inhibitory effect on endocytosis, both prolonged elevation and reduction of auxin levels leads to degradation of PIN2. Thus, only certain auxin optimum will not activate PIN2 degradation, and so guarantee its stabilization at the plasma membrane (Baster et al., 2013). Furthermore, multiple *PIN* genes respond transcriptionally to auxin treatments, being upregulated in a tissue- and PIN- specific manner (Vieten et al., 2005).

The data outlined above leads to a multifaceted picture of the auxin feed-back regulation of its transport directionality and capacity, and we have yet to fully understand the hierarchy of, and the interactions between, the various regulatory components involved.

1.10 Endogenous signals converging on PINs

Apart from the feedback of auxin on its own transport, other endogenous signals, among them other phytohormones and secretory peptides, can modulate PIN protein activity (Figure 2). The plant hormone cytokinin (CK) exhibits antagonistic interaction with auxin, and the cross-talk between these two molecules mediates many aspects of root development (reviewed in Schaller et al., 2015). One of the mechanisms of such interaction is the CK effect on auxin transport in the root realized by modulation of *PIN* transcription

(Dello Ioio et al., 2008; Růžička et al., 2009). Furthermore, CK has been shown to influence PIN function at the post-translational level. CK affects PIN1 trafficking, promoting its delivery to the vacuole for degradation (Marhavý et al., 2011). Since this effect seems to be preferential for PINs at certain polar domains, it enables CK to regulate the auxin transport directionality (Marhavý et al., 2014). During lateral root development, PIN1 gradually reorients to drive auxin transport towards the tip of the newly developing root, in an axis perpendicular to the apical-basal axis of the main root. CK preferentially causes the removal of PIN1 from anticlinal membranes, while having little to no effect on periclinally localized PIN1, thus potentially contributing to the establishment of a new auxin stream driving lateral root organogenesis.

In contrast to CK, the plant hormone gibberellin (GA) exhibits a stabilizing effect on plasma membrane-localized PINs (Willige et al., 2011; Löfke et al., 2013). In GA biosynthesis-deficient conditions, PINs are preferentially targeted for vacuolar degradation, while exogenously applied GA reduces vacuolar PIN trafficking and promotes its residence at the plasma membrane. Although the specific molecular components recruited by GA remain unknown, it appears that a late trafficking step on the way to the vacuole is targeted. GA's input on PIN trafficking might be relevant for regulation of the root gravitropic response, and, remarkably, involves an asymmetric distribution of GA molecules between the upper and the lower root side after gravitropic stimulation.

While it seems that CK and GA effects on subcellular trafficking are relatively specific to PINs (Marhavý et al., 2011; Löfke et al., 2013), the plant hormone salicylic acid (SA) affects endocytosis of PIN proteins as a part of its general inhibitory effect on clathrin-mediated endocytosis (Du et al., 2013). This finding represents a novel and unexpected role of SA, which is molecularly distinct from the well-established nuclear signaling pathway of this hormone, and its physiological functions remain unclear.

Strigolactone has been shown to cause depletion of PIN1 from the plasma membrane in xylem parenchyma cells of the stem (Shinohara et al., 2013). By regulating PIN1 levels at the plasma membrane, strigolactone can influence the capacity of bud-derived auxin to canalize towards the stem, and thus modulate the bud activity and shoot architecture.

Apart from hormones, plants use small secretory peptides as short-range cell-to-cell signals for regulation of multiple developmental processes. Three peptides of the GOLVEN/ROOT GROWTH FACTOR (GLV/RGF) family have been implicated in gravitropism (Whitford et al., 2012). Overexpression of *GLV1-GLV3* genes, external application of corresponding GLV peptides, as well as loss-of-function mutants of the aforementioned genes lead to alterations in root and hypocotyl gravitropism. GLV3 peptide, within minutes of application, caused elevation of plasma membrane signal of PIN2, as well as an increase in intracellular, endosomal occurrence of PIN2. Internally synthesized GLV3 in a GLV3

overexpression line similarly promoted cellular PIN2 abundance, while a *glv3* RNA silenced line exhibited decreased PIN2 signals. Thus, while the detailed aspects of GLV/RGF peptide function await clarification, GLV3 likely mediates short-range signaling to contribute to the correct PAT streams in the gravistimulated root by modulating PIN2 subcellular trafficking dynamics.

Recent work describes two membrane phospholipid species, phosphatidylinositol 4-phosphate (PtdIns4P) and phosphatidylinositol 4,5-bisphosphate [PtdIns(4,5)P_2] as important components of PIN trafficking machinery and cell polarity in plants (Ischebeck et al., 2013; Tejos et al., 2014). Interference with these phosphoinositides in knock-out mutants of PtdIns4P 5-kinases PIP5K1 and PIP5K2 led to multiple auxin-related phenotypes concomitant with defective polarization of PIN1 and PIN2. PIP5K1 and PIP5K2 participate in polarity determination presumably due to their preferential localization at apical and basal plasma membranes, where they regulate the balance between similarly locally enriched PtdIns4P and PtdIns(4,5)P_2 (Tejos et al., 2014). Such local regulation of phosphoinositides may influence the formation of clathrin-coated vesicles, thus being decisive for PIN endocytosis and so its polarity (Ischebeck et al., 2013). This provides another input avenue for signalling pathways, where PIN polarity and trafficking could be regulated via phosphoinositide metabolism and distribution.

Apart from these phosphoinositides, a role of inositol trisphosphate ($InsP_3$) dependent Ca^{2+} signalling in PIN-driven auxin distribution has been recognized in a forward genetic screen for suppressors of PIN1 overexpression phenotypes (Zhang et al., 2011). While genetic and pharmacological upregulation of $InsP_3$ and cytosolic Ca^{2+} levels interfered with basal PIN polarity, decreasing the levels of these signalling molecules affected apical PIN targeting. The intermediate steps leading to these outcomes, and thus the exact mechanism by which Ca^{2+} influences PIN sorting, remain to be elucidated, but downstream regulation of PID activity is a likely component.

1.11 Environmental influences on PIN-driven PAT

PAT is influenced by external signals in addition to endogenous regulation (Figure 2). Such regulatory inputs are necessary for auxin-mediated adaptive growth responses, clear examples of which are phototropism and gravitropism, the alignment of plant growth with light direction and gravity vector, respectively. The differential distribution of auxin between two sides of a responding organ, resulting in differences in growth rates, has been proposed by Cholodny and Went as a basis of tropic growth (summarized in Went, 1974). This auxin asymmetry has been documented during phototropism and gravitropism with auxin-inducible reporters (Luschnig et al., 1998; Rashotte et al., 2001; Friml et al., 2002b; Rakusová et al., 2011) and confirmed with a new generation of auxin sensors (Brunoud et al., 2012;

Band et al., 2012). The role of PIN-driven PAT is evident from tropism deficiencies in *pin* mutants, such as the root agravitropic phenotype of *pin2* (Luschnig et al., 1998; Müller et al., 1998; Chen et al., 1998; Utsuno et al., 1998), partial loss of root gravitropism in *pin3 pin7* (Kleine-Vehn et al., 2010) or reduced photo- and gravitropic bending of *pin3* hypocotyls (Friml et al., 2002b; Rakusová et al., 2011). Also, as seen in previous sections of this review, a number of molecular components regulating PIN trafficking and activities have been identified on the basis of tropism defects in corresponding mutants.

How can auxin transport be redirected by PINs in accordance to environmental cues? Within the PIN family, PIN3 exhibits a prominent ability to change its subcellular localization in response to gravity and light. In the columella cells of the root tip, where perception of gravity occurs (Chen et al., 1999), PIN3 is localized to the plasma membrane in an apolar manner. However, as early as several minutes after changing the gravity vector by rotating the plant, PIN3 begins to relocalize to the lateral, now lower side of the cells (Friml et al., 2002b). As such, it can redirect the auxin flow towards the lower side of the root for its further displacement by PIN2. In dark-grown hypocotyls, PIN3 shows prominent expression in the endodermis, without visible polarity. Both gravitropic stimulation (Rakusová et al., 2011) and unilateral light (Ding et al., 2011) cause polarization of the symmetrically distributed PIN3 to direct auxin flow laterally towards either the lower, or the shaded, side of the organ. Although the tissue or environmental signals concerned vary, the PIN3 polarization events described above share some similarities at the molecular level (Kleine-Vehn et al., 2010; Rakusová et al., 2011; Ding et al., 2011). In each instance, the ARF-GEF vesicle trafficking regulator GNOM was shown to be necessary for polarization to occur, and during hypocotyl tropisms, the prominent role of PID/WAG protein kinases has been shown.

Shade Avoidance Syndrome (SAS) is a growth response triggered when plants are threatened to be out-competed for light by their neighbours. It is sensed as a lowered red to far-red (R:FR) light ratio, resulting from selective light absorption by chlorophyll in leaves of surrounding plants. Similarly to the phototropic response, a light signal is transduced by PIN3 which translocates to the outer endodermis cell side, redirecting part of the PAT to the outer tissue layers and thus promoting elongation (Keuskamp et al., 2010). Accordingly, seedlings of *pin3* mutant were unable to elongate hypocotyls upon sensing low R:FR ratio.

Not only gravity and light, but also salinity is an environmental variable to which plants react in an auxin- and PIN-dependent manner. Halotropism is a recently described tropic response, wherein roots grow away from high salt concentrations (Galvan-Ampudia et al., 2013). During halotropic response, auxin accumulates differentially in the root tip, with more auxin at the side away from high salt concentration leading to asymmetric growth, analagous to the gravitropic response. This correlates with increased internalization of PIN2 at the side of salt perception, which likely leads to decreased auxin transport capacity. The proposed mechanism of this salt-induced promotion of PIN2 endocytosis

involves recruitment of clathrin to the plasma membrane by increased activity of phospholipase D, presumably through synthesis of phosphatidic acid, a phospholipid which has been shown to bind components of clathrin machinery (McLoughlin et al., 2013).

In summary, a number of environmental responses involve downstream regulation of dynamic subcellular trafficking of PINs, typically leading to polarization to specific domains in order to redirect auxin flow according to external cues. However, the exact mechanisms by which perception of signals such as gravity, light or salinity leads to regulation of PIN trafficking or polar sorting are still unclear.

1.12 Summary

Auxin mediates an impressive variety of developmental processes. In virtually all its activities, the intercellular, and possibly also intracellular transport mediated by PIN auxin transporters is of key importance. For their diverse roles to be fulfilled, PIN proteins are tightly controlled by an array of regulators at the levels of transcription as well as cellular polarity resulting from secretion, endocytosis, recycling and vacuolar trafficking. Endogenous signals, including auxin itself and other hormones, influence these regulatory steps in order to fine-tune PIN localization and function. A number of external inputs are also decisive for regulating PIN activities, thus enabling the environmental conditions to be integrated into auxin-dependent developmental programs. In conclusion, from early on in their lineage, plants have gradually evolved a complex and versatile mechanism, in which integration of endogenous and exogenous signals, converging on the PINs and distribution of auxin, provides instructions for many aspects of growth and development.

1.13 Aims and scope of the thesis

This thesis aims to elaborate our knowledge in a number of distinct topics of plant cell biology. Chapter 1 adresses the polar trafficking of PIN proteins with a forward genetic screen aimed at indentifying new regulators of this process. In Chapter 2, the aim is to identify and characterize new proteins acting in clathrin-mediated endocytosis, a fundamental process necessary for multiple cellular functions, including also the trafficking of PIN proteins. Finally, Chapter 3 dwelves into the regulation of cell growth and cortical microtubule reorientation by auxin in order to explain the cause-effect relationship of auxin’s regulation of anisotropic cell growth.

2 Forward genetic screen for regulators of PIN polarity

2.1 Introduction

This project was aimed at extending our understanding of the cellular mechanisms governing the polar localization of PIN auxin transporters. To this end, I participated in a forward genetic screen aimed at identifying novel regulators of PIN polarity. My role in the project began with several mutants that were isolated and initially characterized by Petra Marhava, as described in her doctoral thesis "Molecular mechanisms of patterning and subcellular trafficking in *Arabidopsis thaliana*".

The forward genetic screen presented here (Figure 1; Feraru et al., 2011; discussed in the introduction) is based on ectopic expression of PIN1 in the epidermis of the root, in a mutant background lacking PIN2 protein that is normally active in this tissue. Unlike PIN2, PIN1 doesn't show a preferential apical localization in epidermis, rendering the PIN2::PIN1-HA;*pin2* plants agravitropic similarly to the *pin2* mutant, due to a lack of correct shootward auxin fluxes determining root tropisms. By chemical mutagenesis, we aimed to target any potential genes necessary for basal localization of PINs, hoping to redirect the ectopic PIN1 to the apical polar domain. Such polarity switch would be manifested by a restoration of root gravitropism in the mutant line, which can be easily screened for. In the following sections, five mutants which I worked on are characterized. Each section presents the generated data as well as discussion on possible future directions.

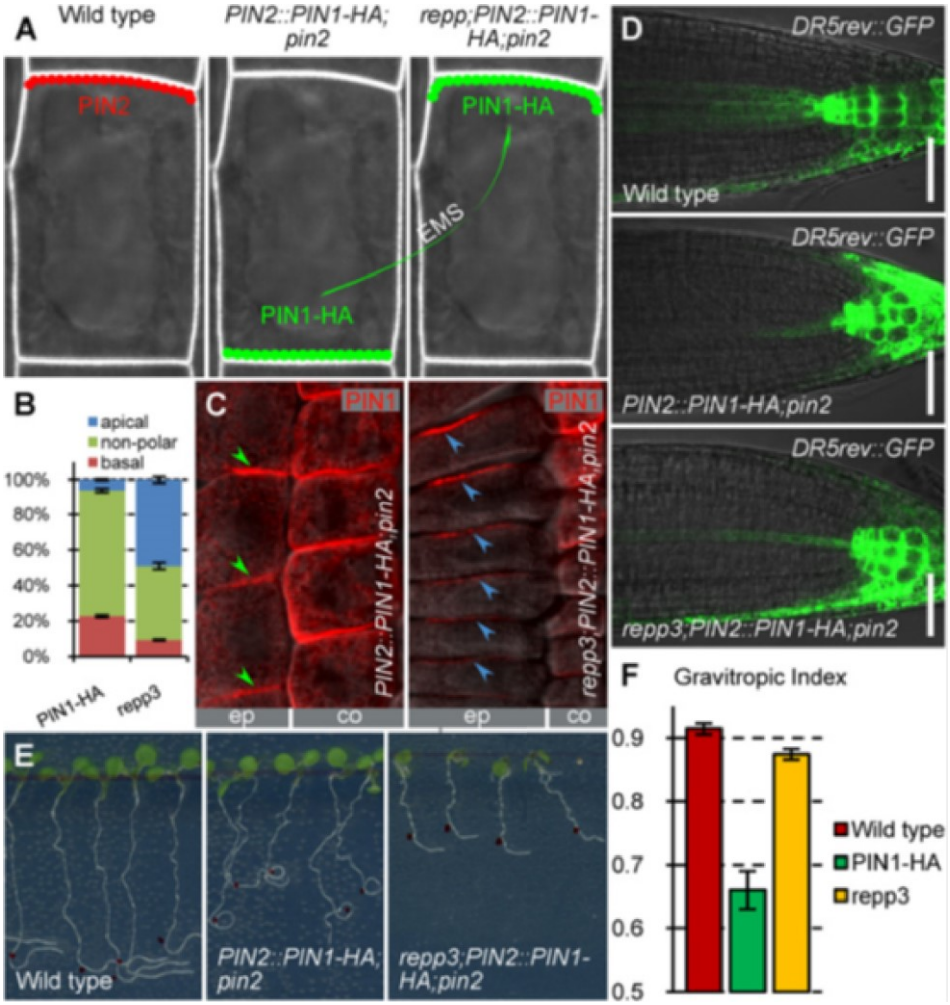

Figure 1. The principle of the forward genetic screen.

(A) Subcellular polarity of PIN proteins in the root epidermis in wild type, in the genetic background used for screening, and in the sought-after polarity mutants.

(B, C) Example of PIN1-HA polarities in a specific mutant, *repp3 (regulator of pin polarity 3).*

(D-F) Asymmetric distribution of auxin visualised by the DR5::GFP (D) and root gravitropism (E, F) as outcomes of epidermal PIN polarities in the considered genotypes.

The figure was reproduced from Feraru et al. 2011.

2.2 Results and discussion

2.2.1 repp9

In preliminary screening, the *repp9* exhibited short roots, a restored gravitropic response, and increased apical localization of PIN1-HA in the epidermis. The mapping was done by crossing the mutant (*repp9; pin2; PIN2:PIN1-HA*), which was generated in Columbia ecotype, with a *pin2* mutant allele in Landsberg ecotype (*agr1-1*). In F2 generation of this cross, seedlings with gravitropic root phenotype were selected. To map the physical position of the mutation, PCR-based SSLP (Simple Sequence Length Polymorphisms) and CAPS (Cleaved Amplified Polymorphic Sequences) genetic markers, distinguishing Columbia and

Landsberg ecotypes, were employed. With a population of 51 individuals, I searched for a chromosomal region containing exclusively Columbia sequences, wherein the mutation causing the rescue of gravitropism should be found. I narrowed down the mutant interval to a 1372 kb-long region on chromosome 5, containing 428 genes. Among these genes was CESA6, a subunit of the cellulose synthase complex. Since our genetic screen previously yielded CESA3, another subunit of this complex, and since *cesa6* mutation was also shown to cause apicalization of PIN1-HA (Feraru et al., 2011), we suspected that a mutation in CESA6 may cause the *repp9* phenotypes. Subsequently, sequencing of CESA6 gene in this mutant revealed a C to T transition in the 6th exon, producing an early STOP codon. Thus, it is very likely that *cesa6* mutation is the cause of *repp9* phenotypes. Because of this redundant finding, further work on *repp9* was abandoned.

2.2.2 repp11

The *repp11* mutant exhibited a rescue of gravitropic response of the root and concomitant increase in the apical localization of PIN1 in the root epidermis (Figure 2A, B).

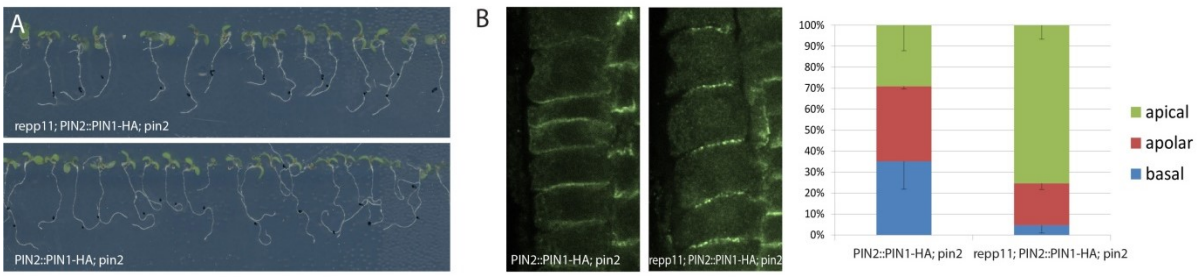

Figure 2. The *repp11* mutant. (A) The gravitropic response of the root is restored in *repp11* mutant as compared to the *PIN2::PIN1-HA; pin2* genetic background. The Petri dish was rotated by 90 degrees. Black dots represent the location of root tips before rotation. (B) Increase of apical localization of PIN1-HA in the root epidermis of *repp11* as evaluated by immunostaining of PIN1. The quantification shows an average of two experiments with a total of 232 and 166 cells scored for the genetic background and *repp11*, respectively.

The causal mutation was identified by genetic mapping where all EMS-induced point mutations were used as genetic markers, made possible due to whole-genome resequencing. The mutant was backcrossed into the PIN2::PIN1-HA;*pin2* background line, and approximately 100 seedlings showing the recessive mutant phenotype were selected in the F2 progeny. Those were pooled and whole-genome sequencing was performed in order to identify EMS-induced mutations in the pooled sample. The mutations, together with their frequencies in the mapping population, were then plotted to visualize chromosomal regions of *repp11* origin that co-segregate with the mutant phenotype (Figure 3). Based on the occurrence of high-frequency EMS-induced mutations, a mapping interval on chromosome 1 was identified. Candidate mutations were then selected inside the interval (Table 1).

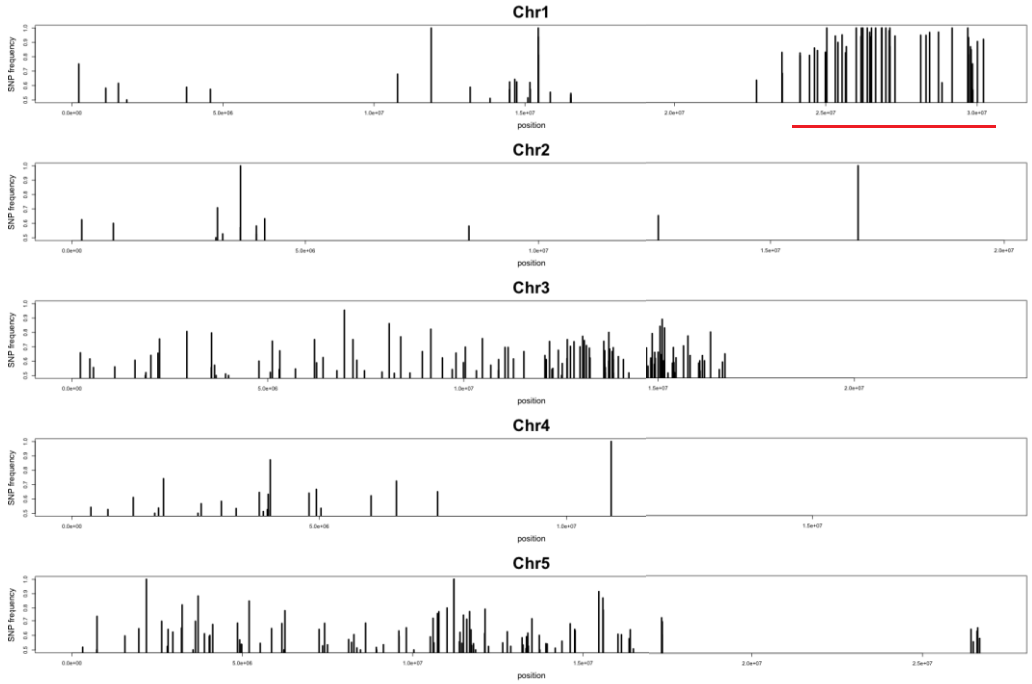

Figure 3. Mapping of *repp11*. Plots represent chromosomes of *A.thaliana* with *repp11* SNPs co-segregating with the gravitropic phenotype in the F2 generation of *repp11 x PIN2::PIN1-HA; pin2*. Heights of peaks indicate SNP frequency in the sample. Underlined is a region of chromosome 1 containing a concentration of high-frequency SNPs, where the causal mutation is likely present.

Table 1. Candidate mutations for *repp11*

Gene code	Gene name/description	Old/new codon	Old/new amino acid
AT1G69710	Regulator of chromosome condensation (RCC1) family with FYVE zinc finger domain	aGa/aAa	Arg/Lys
AT1G70360	F-BOX protein	gGa/gAa	Gly/Glu
AT1G71220	EBS1, EMS-MUTAGENIZED BRI1 SUPPRESSOR 1, PRIORITY IN SWEET LIFE 2, PSL2, UDP-GLUCOSE:GLYCOPROTEIN GLUCOSYLTRANSFERASE, UGGT	tgG/tgA	Trp/STOP
AT1G71240	Plant protein of unknown function (DUF639)	Splice site	
AT1G78955	CAMS1 (Camelliol C synthase 1); beta-amyrin synthase	aGt/aAt	Ser/Asn

Among these, AT1G71220 (henceforth called UGGT for UDP-Glucose:Glycoprotein Glucosyltransferase) is a gene that has been independently identified by Petra Marhava as a candidate mutation for another *repp* mutant. Thus, UGGT presented itself as a likely causal mutation. Two approaches were employed which confirmed UGGT as the sought-after polarity regulator. First, expression of a wild-type allele of UGGT in *repp11* background abolished the mutant phenotype, as evaluated by reversion to the agravitropic phenotype of PIN2::PIN1-HA;*pin2* (Figure 4A). Conversely, introduction of an independent *uggt* mutant

allele (*psl2-3*) into PIN2::PIN1-HA;*pin2* line caused restoration of the gravitropic response in this line (Figure 4B).

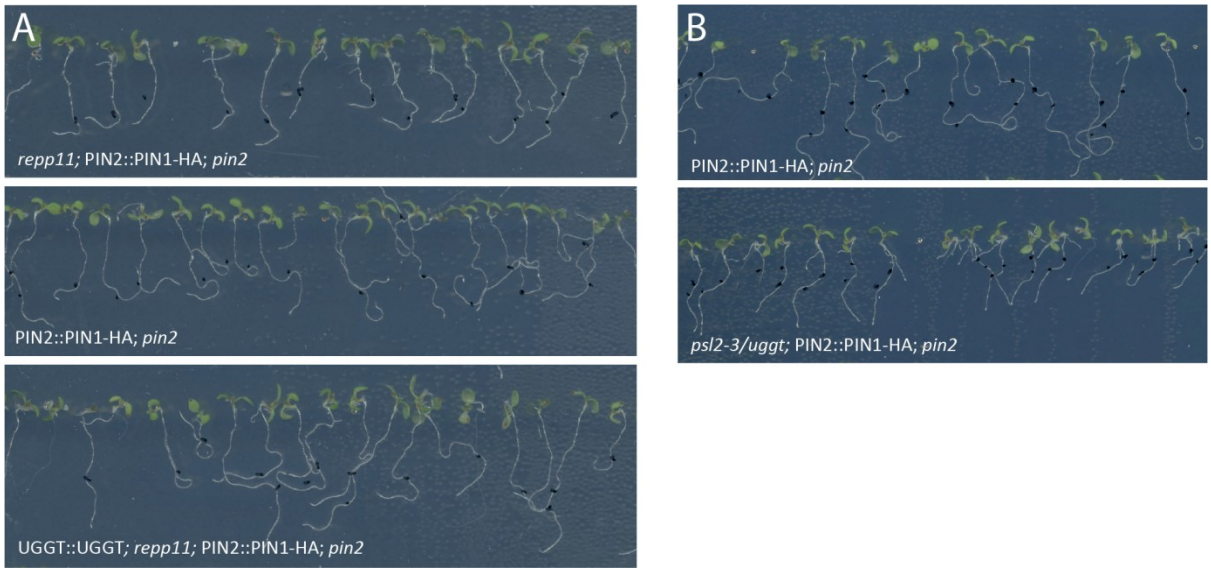

Figure 4. Confirmation of UGGT as *repp11* gene candidate.
(A) Root gravitropism is lost in *repp11* mutant which was complemented by expressing a wild-type allele of UGGT. (B) Introduction of *psl2-3*, a *uggt* allele, into the *PIN2::PIN1-HA; pin2* line, causes restoration of root gravitropism. The Petri dishes were rotated by 90 degrees once (A) or twice (B). Black dots represent the location of root tips before rotation.

UGGT is an ER-localized protein participating in late steps of protein biosynthesis, namely in the correct folding of newly synthetized proteins (Buchberger et al., 2010). The function of UGGT is thought to be specific for glycoproteins, since it is based on reversible glucosylation of N-linked glycans on the folding polypeptides. UGGT recognizes nearly-folded intermediates, which, upon glucosylation, are processed by calnexins and calreticulins, two classes of chaperones that assist their correct refolding. The function of UGGT in plants is not critical for growth and development (Blanco-Herrera et al., 2015). Knocking out AT1G71220, the only UGGT homologue in *Arabidopsis*, yields viable and fertile plants, which, however, are delayed in growth and more sensitive to certain stresses. The molecular function of UGGT in *Arabidopsis* was first demonstrated with an artificial target, a mutant version of the brassinosteroid receptor BRI1 called BRI1-9. This BRI1 variant is normally retained in the ER, but in the *uggt* mutant background it becomes secreted to the PM, where it is functional (Jin et al., 2007). This phenomenon suggests that UGGT recognizes BRI1-9 as a misfolded protein and acts to retain it in the ER. However, there does not appear to be any effect on the native BRI1 protein and brassinosteroid signaling itself, resulting from interfering with UGGT function.

One native target of UGGT, a Leu-rich receptor-like kinase EFR that functions in bacterial immunity, has been identified too (Saijo et al., 2009). Contrary to the previous

case, the function of UGGT is necessary for successful secretion of EFR, as *uggt* alleles show little or no accumulation of EFR in tissues, presumably due to its degradation by the ER-associated protein degradation pathway (ERAD). Apart from *uggt,* mutants in several other genes participating in various steps of ERQC (ER-based glycoprotein quality control) mechanism were identified in the genetic screens that assayed BRI1-9 trafficking and EFR function (Jin et al., 2009; Hong et al., 2012, 2009, Su et al., 2011, 2012; Li et al., 2009; Saijo et al., 2009; Lu et al., 2009).

To elaborate on the finding that UGGT function influences the polar localization of ectopically expressed PIN1, I searched for other independent evidence for its function in PIN polarity and polar auxin transport regulation. As explained in the introduction to this chapter, the generation of vascular tissue requires canalized flow of auxin that is mediated by PIN proteins. Therefore, I analyzed the vascular patterns of cotyledons in *uggt* and mutants of other ERQC components. I found that in these mutants the cotyledon vasculature was overall correctly developed and normal, but several features deviating from the stereotypical cotyledon venation patterning could be identified. These included atypical, additional loops and unusually positioned free ends of vascular strands (Figure 5).

A

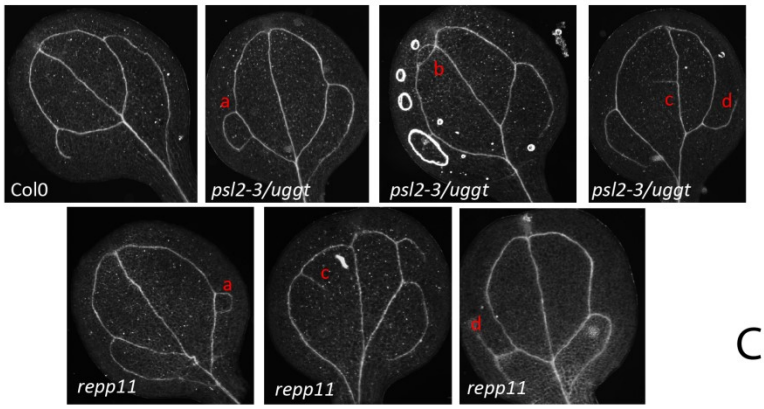

B

	psl2-3 n=102±9	Col0 n=103±7
a. loop not connected to midvein	8.5% ±1.2%	0.3% ±0.4%
b. small loop in distal position	3.0% ±1.1%	0.6% ±0.4%
c. free end inside a loop	1.4% ±1.0%	0%
d. free end directed distally	4.5% ±2.5%	1.2% ±1.1%
Sum	17.4% ±4.6%	2.2% ±1.6%

mean ± SD from 3 experiments

	repp11 n=115±4	P2:P1-HA *pin2* n=109±4
a.	6.4% ±2.2%	2.5% ±0.5%
b.	0%	2.8% ±2.0%
c.	0.9% ±0.0%	0.3% ±0.5%
d.	6.6% ±0.6%	1.8% ±0.7%
Sum	13.9% ±2.3%	7.4% ±2.7%

mean ± SD from 3 experiments

C

	mutant	control
glucIIbeta	22.2 ± 4.7%	1.5 ± 1.5%
uggt	17.4 ± 4.6%	2.2 ± 1.6%
stt3a	9.0 ± 1.4%	2.1 ± 1.7%
crt3	7.1 ± 4.9%	2.1 ± 1.7%
os9	6.5 ± 1.0%	1.2 ± 1.7%
sdf2	3.6 ± 1.4%	2.8 ± 1.3%
erdj3b	3.0 ± 0.8%	2.8 ± 1.3%
ebs5	2.2 ± 1.7%	1.9 ± 1.2%

mean ± SD from 3 experiments

Figure 5. Cotyledon vasculature patterns in the ER quality control mutants.

(A) The mutants exhibited slight alterations of cotyledon vasculature patterns, with additional small loops (a, b) and atypically looking free ends (c, d), as presented with *psl2-3* and *repp11;PIN2::PIN1-HA;pin2* alleles of *uggt*. Tables in B give frequencies of each phenotype compared to respective wild-type backgrounds in two *uggt* alleles. Table C shows combined frequency of any phenotype in all tested mutants of the ER quality control pathway.

Although these venation phenotypes were mild, and only indirectly suggest problems with PIN-driven polar auxin transport during cotyledon development, they suggested a broader involvement of ERQC in this process beyond just the function of UGGT.

Next, I crossed several ERQC mutants into PIN2::PIN1-HA;*pin2* background to test whether they are able to confer the root gravitropism rescue akin of *uggt*. In five crosses where homozygous progenies were obtained, I did not observe the root gravitropism rescue (not shown). Interestingly, then, although these mutations conferred phenotypes similar to *uggt* in the previously published genetic screens concerned with BRI1-9 and/or EFR, none of them behaved like *uggt* in our genetic screen. Regrettably, due to physical linkage, I did not manage to obtain a double homozygote between *glucIIβ* and *pin2,* which would be of particular interest as *glucIIβ* exhibited a high degree of cotyledon vasculature defects (Figure 5C).

Is UGGT truly involved in regulation of PIN polarity? The evidence collected here points only at the regulation of ectopically expressed PIN1. The idea and hope behind the genetic screen presented here was to find weak alleles of genes with strong influence on PIN trafficking, such that when knocked out, would result in strong defects in patterning and development due to defects in auxin transport. This is not the case with UGGT, as previously isolated null UGGT alleles yield relatively normal plants, and the two UGGT alleles isolated in our screen both have premature stop codons, suggesting that they are null as well. Evidently, the participation of this gene is not crucial for auxin-mediated patterning and development. Still, this project could be continued by careful examination of PIN polarities in single *uggt* mutant, outside of the model system of epidermally expressed PIN1. One hypothesis explaining the role of UGGT is that it affects PIN1 polarity indirectly, through the regulation of an unknown polarity regulator. In this scenario, the polarity regulator would be a glycoprotein whose presence is dependent on ERQC, similarly to the model reported for EFR (Saijo et al., 2009).

2.2.3 repp12

2.2.3.1 Introduction and mutant mapping

The *repp12* mutant exhibited a rescue of gravitropic response, although the root growth was often very wavy, and in this sense unlike the wild type (Figure 6A). However, the polarity of PIN1-HA did not appear to be clearly affected in *repp12*, possibly indicating that another mechanism could lead to the gravitropic rescue (Figure 6B).

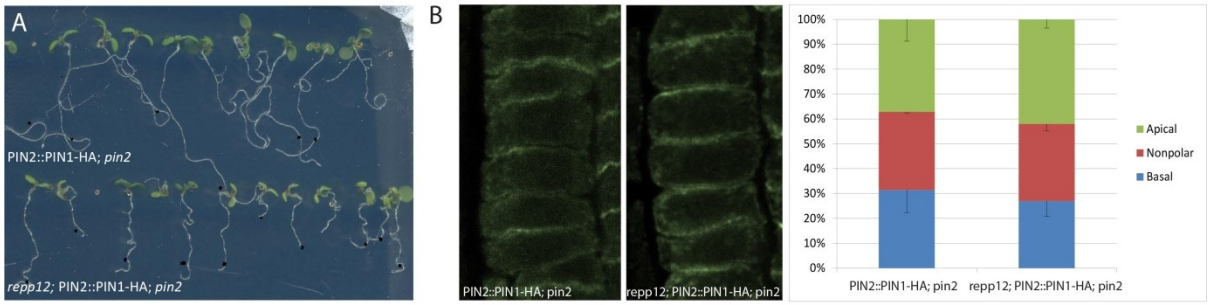

Figure 6. The *repp12* mutant. (A) The gravitropic response of the root is restored in *repp12* mutant as compared to the *PIN2::PIN1-HA; pin2* genetic background. The Petri dish was rotated by 90 degrees. Black dots represent the location of root tips before rotation. (B) No change in the polar localization of PIN1-HA in the root epidermis of *repp12.* The quantification shows an average of two experiments with a total of 166 and 173 cells scored for the genetic background and *repp12*, respectively.

Based on the gravitropic response, it was possible to map the mutation by the next generation sequencing-based approach, as described for *repp11*. The mapping revealed *repp12* mutation to be located on chromosome 1 (Figure 7), and a few candidate mutations were found in the region, listed in Table 2.

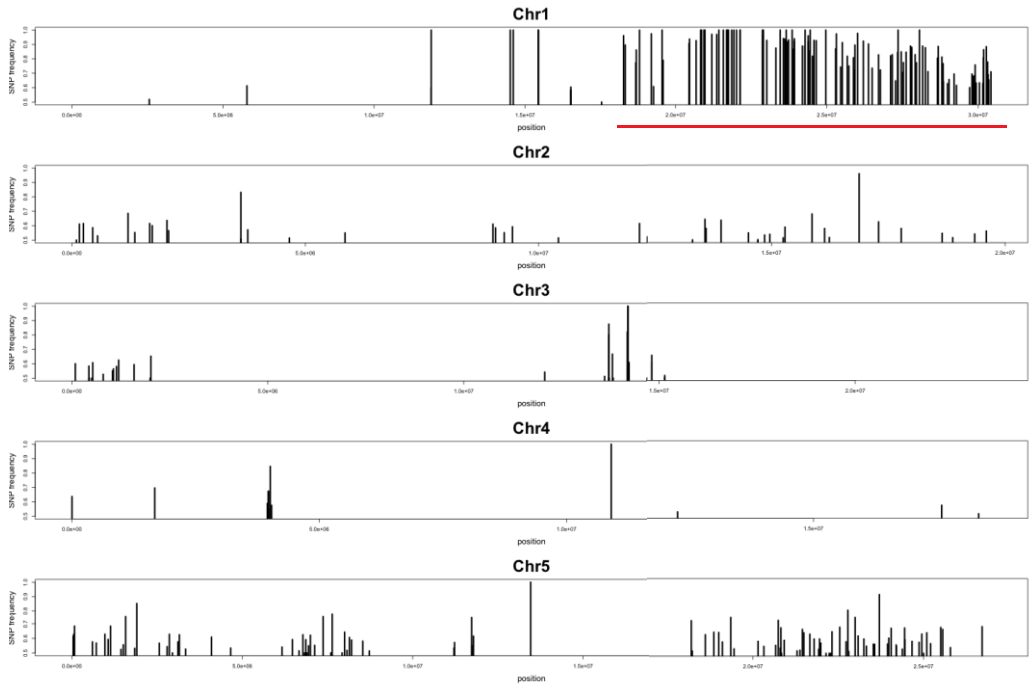

Figure 7. Mapping of *repp12*. Plots represent chromosomes of *A.thaliana* with *repp12* SNPs co-segregating with the gravitropic phenotype in the F2 generation of *repp12 x PIN2::PIN1-HA; pin2*. Heights of peaks indicate SNP frequency in the sample. Underlined is a region of chromosome 1 containing a concentration of high-frequency SNPs, where the causal mutation is likely present.

Table 2. Candidate mutations for *repp12*

Gene code	Gene name/description	Old/new codon	Old/new amino acid
AT1G55810	One of the homologous genes predicted to encode proteins with UPRT domains (Uracil phosphoribosyltransferase).	aGa/aAa	Arg/Lys
AT1G55970	HAC4 is most likely to be an expressed pseudogene that lacks HAT function.	Cag/Tag	Gln/STOP
AT1G58430	Encodes an anther-specific proline-rich protein.	Ccg/Tcg	Pro/Ser
AT1G59500	GH3.4 encodes an IAA-amido synthase that conjugates Asp and other amino acids to auxin in vitro.	Cgt/Tgt	Arg/Cys
AT1G59660	Nucleoporin subunit	tgG/tgA	Trp/STOP
AT1G59820	ALA3, a phospholipid translocase	gGg/gAg	Gly/Glu

Based on the available information about these candidate genes, AT1G59500, AT1G59660 and AT1G59820 were selected for confirmation attempts. The causal mutation was confirmed as AT1G59820 - ALA3, following two lines of evidence. First, the gravitropic phenotype of *repp12* was abolished upon expressing the wild-type allele of ALA3 in *repp12* background; second, introduction of a T-DNA insertion *ala3* allele into PIN2::PIN1-HA;*pin2* background phenocopied *repp12* (Figure 8).

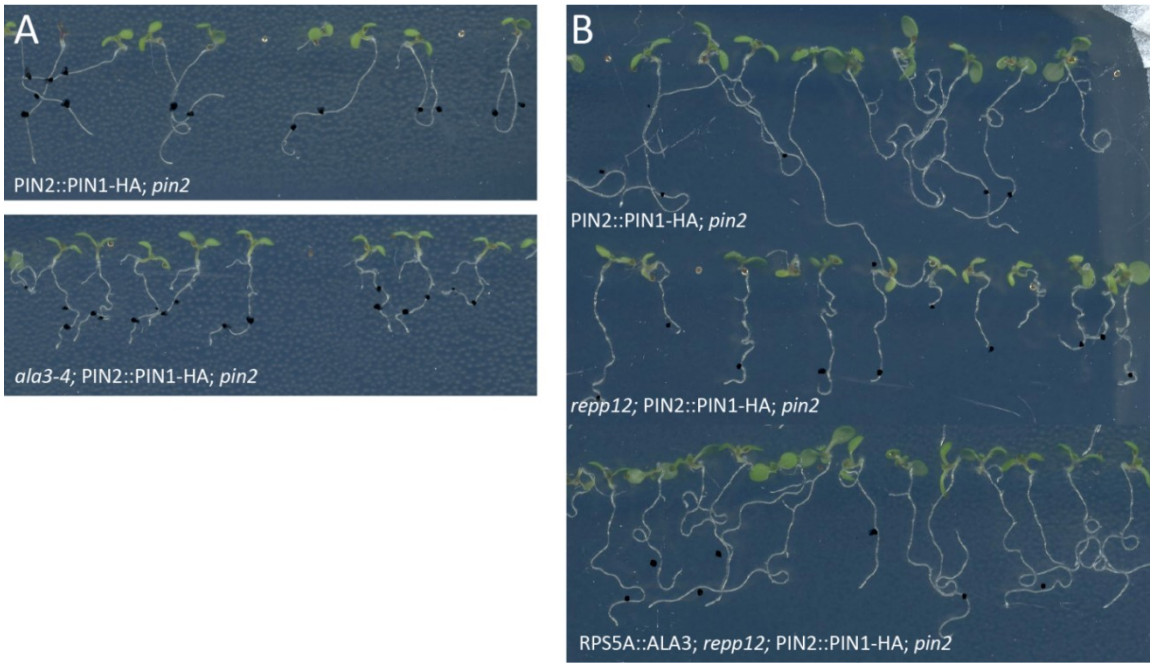

Figure 8. Confirmation of ALA3 as *repp12* gene candidate.

(A) Introduction of *ala3-4*, an *ala3* T-DNA allele, into the *PIN2::PIN1-HA; pin2* line, causes restoration of root gravitropism. (B) Root gravitropism is lost in *repp12* mutant which was complemented by expressing a wild-type allele of ALA3. The Petri dishes were rotated by 90 degrees once (B) or twice (A). Black dots represent the location of root tips before rotation.

ALA3 belongs to a family of ALA proteins – the alpha subunits of a dimeric flippase protein (Poulsen et al., 2008). Phospholipid translocases, or flippases, are a class of proteins with a proposed function in regulating the composition of lipid bilayers (Tanaka et al., 2011). Flippases are able to translocate structural phospholipids (phosphatidylserine, phosphatidylethanolamine and/or phosphatidylcholine), with various specificities, across the lipid bilayer towards the cytosolic leaflet. This transport activity thus generates an asymmetry in the distribution of specific phospholipids between the leaflets. The proposed function of these regulations relate to the physical properties of the membranes in terms of fluidity, as well as contribution to vesicle formation in the endomembrane trafficking system (Muthusamy et al., 2009).

So far, ALA3 is the best-characterized gene in the flippase alpha-subunit family of *Arabidopsis*. *ala3* mutants exhibit a range of phenotypes, including slower growth both during seedling and adult stages, reduced fertility, as well as trichome development defects (Poulsen et al., 2008; Zhang and Oppenheimer, 2009; McDowell et al., 2013). Most of these phenotypes are temperature-sensitive, as they are better expressed in cold environment. On the subcellular level, it has been reported that *ala3* fails to generate secretory structures that are specific for peripheral root cap cells: slime vesicles and hypertrophied trans-Golgi stacks (Poulsen et al., 2008). This indicates a role of ALA3 in trafficking at the Golgi apparatus. Consistently, published reports suggest that ALA3 localizes to the Golgi apparatus (Poulsen et al., 2008).

Research in the field of Arabidopsis ALA flippases focused also on ALA1 (Gomès et al., 2000), a plasma-membrane flippase species; ALA10, localized either at the PM or to the chloroplast, and which is proposed to participate in the uptake of exogenous phospholipids, as well as regulation of lipid metabolism in the chloroplast (Botella et al., 2016; Pedas et al., 2015); as well as ALA6 and ALA7 which are acting in the generative stage of development (McDowell et al., 2015).

2.2.3.2 The possible role of ALA3 in polar auxin transport

The lack of an evident apicalization of PIN1-HA in epidermis of *repp12* calls for an alternative explanation of the gravitropic rescue observed in this mutant line. To clarify whether the gravitropic rescue relates to the epidermally expressed PIN1, I have generated an *ala3 pin2* double mutant without the PIN2:PIN1-HA construct, a careful examination of which will be necessary in further efforts to characterize ALA3. As a second test helping to clarify the *repp12* phenotype, the wild-type ALA3 allele could be expressed in the *repp12* mutant specifically under the control of PIN2 promoter, in order to see whether ALA3 activity in PIN2 domain, where PIN1-HA is expressed, is sufficient. It is instead possible that the *repp12* phenotype is caused by loss of ALA3 expression in other tissues of the seedling.

These considerations appear particularly relevant if it is taken into account that root epidermis may not express ALA3 at all, or expresses it at very low levels only, as evidenced by pALA3::GUS fusion published by Poulsen et al. 2008 (reproduced in Figure 9)., ALA3 promoter activity levels are high in some of the tissues rich in auxin, such as the vasculature of cotyledons and roots, where polar auxin transport occurs, guard cells, and tips of cotyledons and roots which are considered as auxin source and sink, respectively (Figure 9).

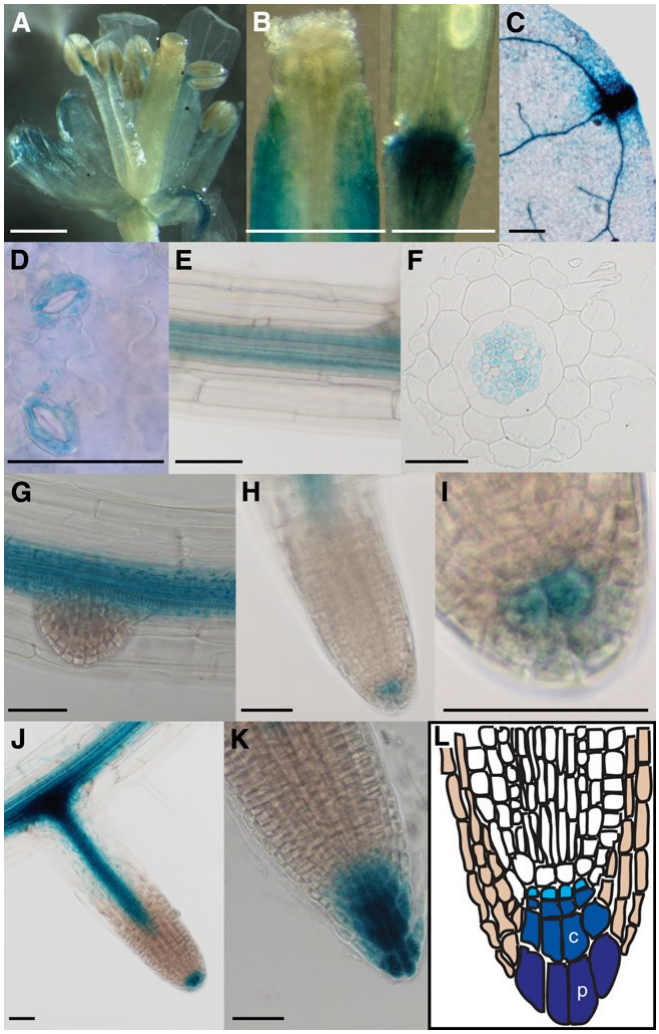

Figure 9. ALA3 Is expressed in a variety of cell types in roots and shoots.
ProALA3:GUS studies were performed on different tissues: flower (A), silique (B), vascular tissue in young leaf (C), stomatal guard cells (D), root vascular tissue ([E] and [F]), emerging side root (G), columella root cap initials ([H] and [I]), and all cells of the columella root cap ([J] and [K]). (L) shows a schematic drawing of the root tip: tan, lateral root cap; light blue, columella initials; darker and darkest blue, columella root cap cells. c, central columella cell; p, peripheral columella cell. Bars ¼ 0.5mm ([A] to [C]) and 50 mm([D] to [K]).
The figure and description were reproduced from Poulsen et al. (2008).

Thus, I searched for phenotypic indications of ALA3 function in the auxin transport process, other than the gravitropic phenotype of *repp12*. A preliminary experiment with root gravitropism in the single *ala3* mutant (outside of the PIN2:PIN1-HA *pin2* model system) hinted at a possible defect in gravitropic responses, wherein the roots sometimes over-bend or under-bend (Figure 10). However, the phenotype is mild and the observation has to be repeated in large samples, and in several available *ala3* alleles. If confirmed, this sensitive phenotype could be an indication of a slight problem with auxin transport in *ala3*.

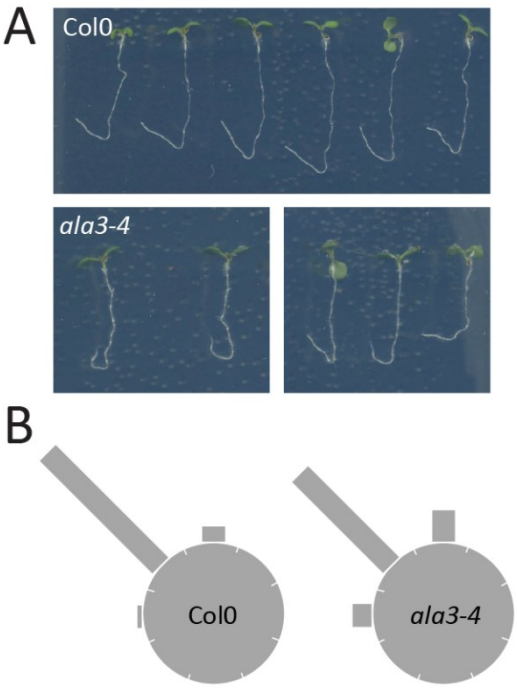

Figure 10. Possible gravitropic defect in single *ala3* mutant
Upon rotation by 135 degrees, the roots of *ala3-4* would sometime over-bend or under-bend (A), as quantified in a circular graph in (B)

Furthermore, I found strong evidence that single *ala3* mutants exhibit a deviation from typical patterns of cotyledon vasculature (Figure 11). The vascular patterns of *ala3* tend to be more complex, with more loops and free ends being generated in a majority of cotyledons. Vasculature develops from cells which in early development formed patterned canals of polar auxin transport. The formation of these canals is described by the auxin canalization hypothesis and is based on group-determination of cell polarities in the tissue, expressed both as auxin transport direction and capacity, and cell morphology (as described in the introduction to this chapter). Therefore, the observed phenotype of more complex vascular patterns could indicate alterations in the auxin canalization process at early stages of cotyledon development. In simplest terms, it could be that in the absence of ALA3, the focused polarization of auxin streams may sometimes not be achieved, producing a network of auxin flow which is more branched than in the wild-type condition.

The identification of *ala3* in gravitropism-based genetic screen presented here, the auxin-related phenotypes of *ala3* mutant, and the pattern of ALA3 expression that corresponds to auxin localization in many plant organs all suggest a possibility that ALA3 may be involved in auxin transport. Regarding the *repp12* phenotype, it may be, for example, that a reduction in auxin transport rates in the root partially alleviates the agravitropic *pin2* phenotype, which is explainable by the inability to remove excess auxin from the root tip.

Further experiments in this direction could include the observation of auxin distribution in *ala3* with auxin-responsive reporters, paying attention to reporter activity levels and alterations in auxin distribution in both root and cotyledon tips. For this purpose, I generated crosses of the auxin response reporter, DR5::GFP, into both *repp12* and the

single *ala3* mutant. Additionally, the pattern of ALA3 expression could be studied in more detail, and compared side-by-side with tissue auxin distributions reported by the DR5::GUS construct. An evidence for alterations of polar auxin transport could come from measurements of transport rates of isotopically labelled auxin in roots or on the whole seedling level.

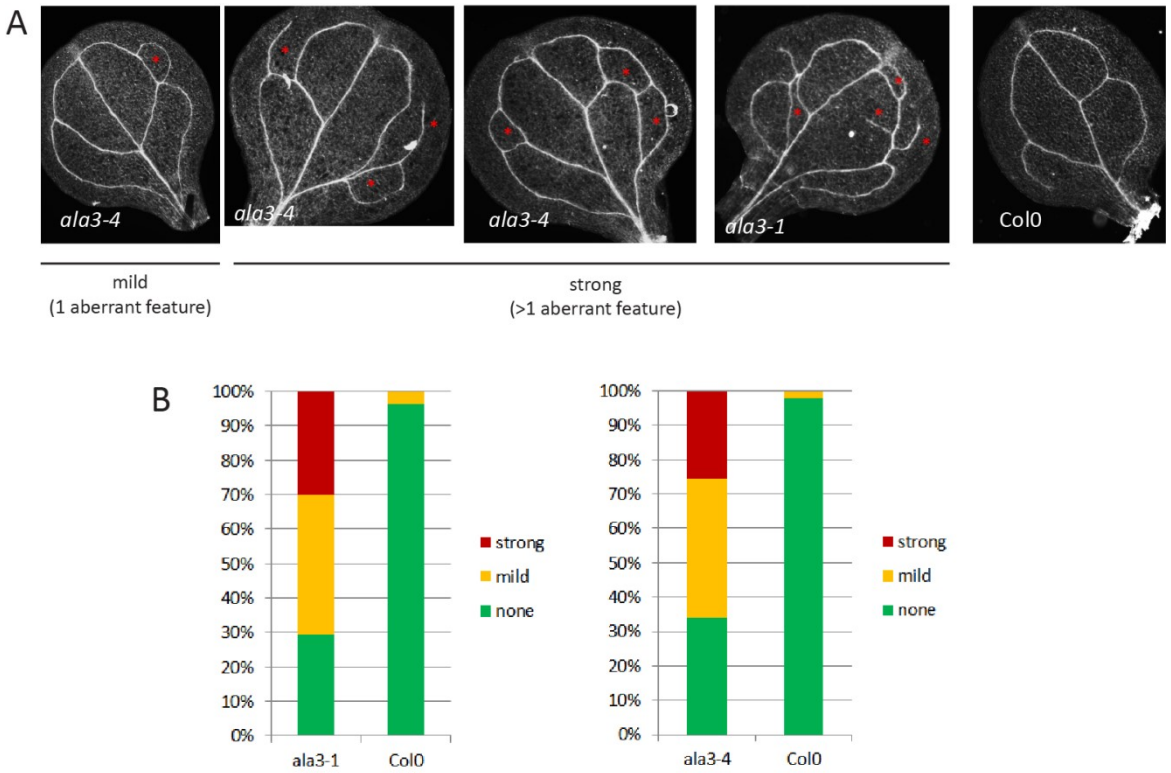

Figure 11. Complex vasculature patterns of *ala3* mutants

(A) *ala3* mutants exhibit more branched vascular patterns, with additional loops and more free ends (both indicated by asterisks). For quantification (B), the phenotype was distinguished between mild (one additional or atypical feature) and severe (more features).

2.2.3.3 Subcellular localization of ALA3

The proposition that ALA3 is involved in polar auxin transport, which takes place at the plasma membrane, does not seem consistent with the reported localization of ALA3 in the Golgi apparatus. In my view, the proposed Golgi localization of ALA3 raises some doubts. First, it has to be noted that for reasons currently unknown, (over)expression of GFP-ALA3 appears to be difficult. Poulsen et al. 2008 shows that 35S::GFP-ALA3 construct rescues *ala3* phenotypes, but apart from faint fluorescence in the root cap, virtually no GFP-ALA3 signals are found in the complemented mutants. In my experiments, I obtained *repp12* lines that were rescued by 35S::GFP-ALA3, and in these lines I was also unable to find normal GFP fluorescence. Perhaps, then, some control mechanism prevents high levels of ALA3

transcripts, or proteins, to be accumulated. In support of this idea, microarray data indicate that ALA3 transcription becomes upregulated when protein translation is inhibited by cycloheximide (3.62 fold change after 3h treatment with 10uM CHX, source: Arabidopsis eFP Browser). Perhaps, following chemical inhibition of translation, ALA3 protein level gradually diminishes due to its degradation, and this is sensed by a putative ALA3 expression-controlling mechanism which leads to transcription upregulation.

With the problem of achieving GFP-ALA3 expression in mind, some doubts can be raised about the proposed localization of ALA3, which was concluded basing on transient expression of GFP-ALA3 constructs in tobacco leaf epidermis. In Poulsen et al 2008., overexpressed GFP-ALA3 is reported to perfectly (pixel-to-pixel) colocalize with ST-YFP (yellow fluorescent protein fused to a targeting domain of sialyltransferase, a Golgi-resident enzyme participating in protein glycosylation). Such perfect colocalization is rarely, if ever, found between any two markers and a technical mistake may be suspected where GFP-ALA3 did not express in this system (as it does not express in *Arabidopsis*) and instead, both channels were capturing the same fluorescent signals of ST-YFP. This appears likely considering that fluorescent proteins with highly overlapping emission spectra (GFP and YFP) were used in this colocalization experiment.

During my work I transiently expressed GFP-ALA3 together with untagged ALIS1 (one of the three homologs of flippase beta-subunit in *Arabidopsis*) in tobacco cells. GFP expression was observed in some cells, and the fluorescent pattern indicated cytosolic, ER, and/or plasma membrane localisation (Figure 12A). No punctate signals that could represent Golgi bodies were found. Furthermore, I generated a GFP-ALA3 expressing construct in the estradiol-induction system (XVE::GFP-ALA3) and transformed it into *Arabidopsis*. When the expression was induced by transferring seedlings to estradiol-containing medium 3 or 4 days after germination, GFP signals of ALA3 could be detected in the root tip epidermis (Figure 12B), although they were weak and scattered. In all cells where GFP signals were detected, ALA3 was found at the plasma membrane, while some cells also showed intracellular signals that may represent components of the endomembrane system. Detection of these very faint signals required high laser power and gain settings, to the extent where autofluorescence of some intracellular components was detected. The autofluorescent background could be distinguished when the GFP signals were specifically bleached by continual application of high laser (Figure 12B, right panels). Thus, for unclear reasons, a pulse of GFP-ALA3 transcription, made possible with an inducible expression system, does lead to expression of GFP-ALA3 protein in *Arabidopsis* seedlings at detectable levels. The observed PM localization is novel and contradicts the published reports. These preliminary findings should be elaborated on and would help to establish the role of ALA3. It should be tested whether co-expression of the flippase beta-subunit ALIS would help achieve better ALA3 expression. For this purpose, I generated an

ALIS1 overexpressing line (35S::ALIS1) and initiated a cross with XVE::GFP-ALA3. To better study the localization of ALA3, an N-terminal fusion of GFP to ALA3 (ALA3-GFP) or internal fusions to ALA3 cytosolic loop could be generated, in case that the stability of ALA3 is obstructed by the C-terminal GFP moiety. Considering the notion that ALA3 expression may be tightly regulated, perhaps it would be interesting to clarify whether the possible regulation of ALA3 expression prevents the accumulation of transcripts, or rather proteins. This could be done by testing GFP-ALA3 transcript levels in overexpressing lines. Also, it may be instructive to look for GFP-ALA3 expression in tissues where the protein should naturally be expressed at high levels, such as the cotyledon tip.

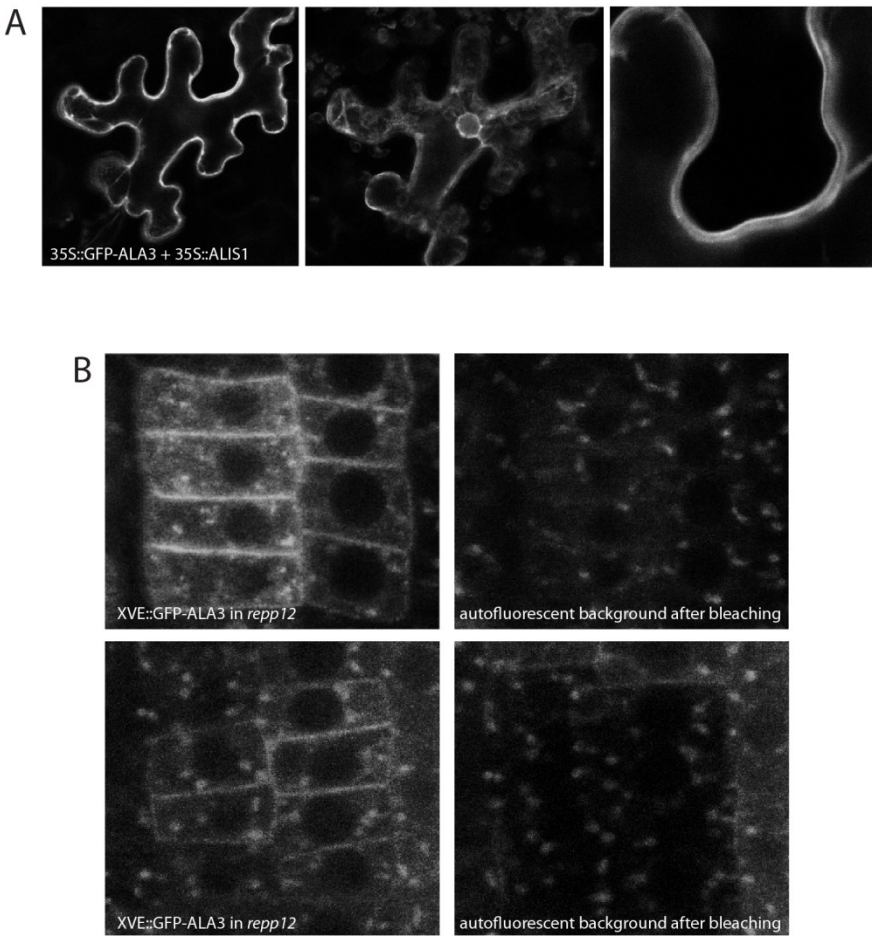

Figure 12. Subcellular localization of GFP-ALA3 fusion

(A) Tobacco epidermis cells coexpressing GFP-ALA3 with untagged ALIS1. The diffuse fluorescent signals are consistent with plasma membrane, cytosolic and/or ER localizations. (B) Inducible expression of GFP-ALA3 in *A.thaliana (repp12* background). GFP was found in some cells of seedling root epidermis, where it localized to the plasma membrane, and sometimes to punctate intracellular bodies (top). Due to very weak signals, high laser power and gain settings had to employed, exposing background autofluorescence in the root cells. The GFP signals were distinguished by selective bleaching with very high laser.

2.2.3.4 ALA family and the mutant material generated

The phenotypes of *ala3* reported in the literature and here, whether or not related to auxin transport, have only limited consequences on plant development. The mutant lines that were used for these investigations: *ala3-1, ala3-2* and *ala3-4,* are all T-DNA insertions in introns of the ALA3 gene (McDowell et al., 2013). The expression levels of ALA3 in these T-DNA lines were not reported. As intron insertions don't directly disrupt the coding sequence, it may be that in these alleles the functional transcript is still produced, but at reduced levels. As a part of investigation into ALA3, it would be instructive to test ALA3 transcript levels in these T-DNA mutant lines. If these mutants are knock-downs, it may be worthwhile to generate artificial microRNA constructs against ALA3 that could be introduced into *ala3* T-DNA backgrounds to further reduce the gene expression. Alternatively, one may attempt to knock-out ALA3 by the CRISPR technology.

As mentioned in the introduction, ALA3 belongs to a family of twelve genes in Arabidopsis, ALA1 – ALA12. ALA3 is most related to a large clade containing ALA4-ALA12 (Pedas et al., 2015). While some of these genes, such as ALA6 and ALA7, are active in pollen development, a majority of them is broadly expressed and could functionally overlap with ALA3. In studies of flippase function, functional redundancy inside the family should be taken into consideration.

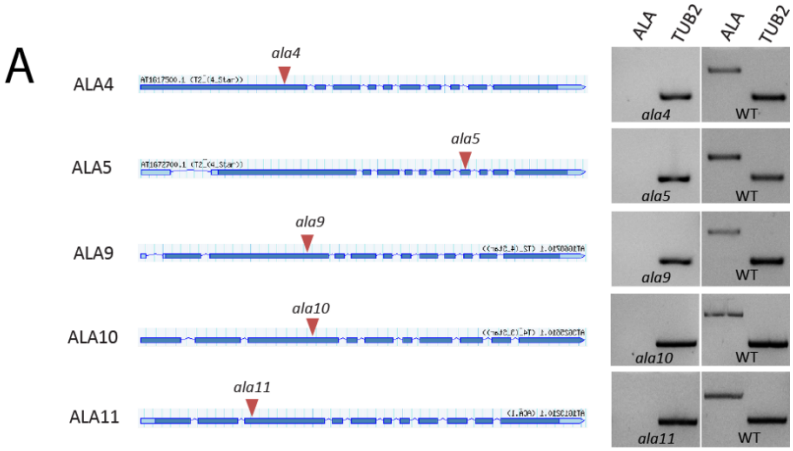

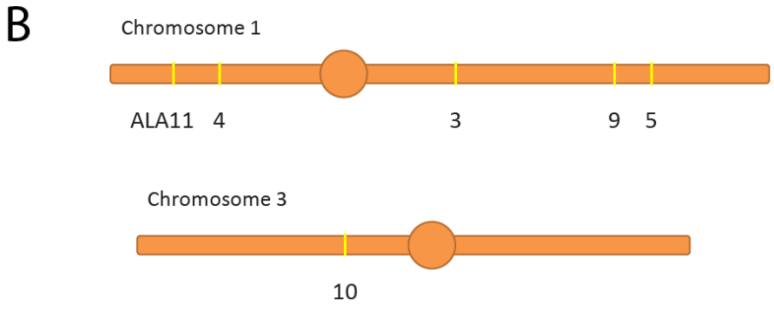

Figure 13. Isolation of ALA family mutants
(A) T-DNA insertions into ALA gene sequences are marked with red arrows. On the right, RT-PCR confirmations of gene knock-out in the homozygous mutants. TUB2 (tubulin subunit) gene was used as reference.
(B) Chromosomal positions of ALA genes from which the multiple mutants were generated.

I isolated a set of mutants in ALA4-ALA12 subclade that are expressed during vegetative development (Figure 13A). These single mutants did not have the reduced root lengths or cotyledon vascular defects observed in *ala3* (results not shown). I proceeded to generating multiple mutant combinations between these genes and ALA3. Five of these genes lie on chromosome 1, causing considerable difficulties in the crossing due to their physical linkage (Figure 13B). The strategy of crossing was aimed at combining most closely linked mutations first, so that they later segregate almost like a single locus. Thus, mutants in pairs of genes lying closest together: ALA4 with ALA11, and ALA5 with ALA9, were crossed, and the F1 generation was immediately crossed to *ala3*. Then, F1 plants from this second cross were genotyped to find a double heterozygote in both *ala4* and *ala11*, or *ala5* and *ala9*. The transmission of both alleles together in one gamete was rare due to the necessity of a crossing-over event taking place between the two neighbouring loci in the first F1 plant. Finding the double heterozygote in the F1 generation after crossing with *ala3* assures that the mutations lie on a common physical chromosome, which simplifies the further crossing procedure. Following this strategy, I finally obtained a triple homozygous *ala3 ala4 ala11* mutant, an *ala3 -/- ala5 +/- ala9 +/-* combination, and additionally a double *ala3 ala10* mutant. During the selection procedure, I observed that the triple *ala3 ala4 ala11* homozygotes were severely dwarfed (to a greater extent that the *ala3* single mutant). Further work on this mutant, as well as obtaining other multiple *ala3* mutants may yield interesting results.

In summary, there are some indications arising from this work that link ALA3 to auxin transport. Potentially valuable plant material was generated and future research directions suggested that could extend our knowledge of flippase function in *Arabidopsis*.

2.2.4 repp10

repp10 is a mutant with a particular root growth phenotype. The gravitropic response appears to be partially restored, but a more interesting and unique feature is the tendency of *repp10* roots to bend in a gradual, smooth fashion, while never creating sharp bends that are typical for wild-type *Arabidopsis* seedling roots (Figure 14A). However, the *repp10* roots are not completely gravitropic. Left to grow without gravitropic stimulations, they may grow in various directions, yet always bending with large, broad curves.

This straight growth mode may indicate a defect in auxin transport, because wild-type seedlings grown in the presence of a moderate dose of an auxin efflux inhibitor, NPA, exhibit a very similar phenotype (Figure 15A). In support of this proposition, the visualization of auxin responses by the DR5::GFP construct suggested that the amount of auxin in the root tip of *repp10* is lower than in the corresponding genetic background, *pin2* PIN2::PIN1-HA (Figure 15B).

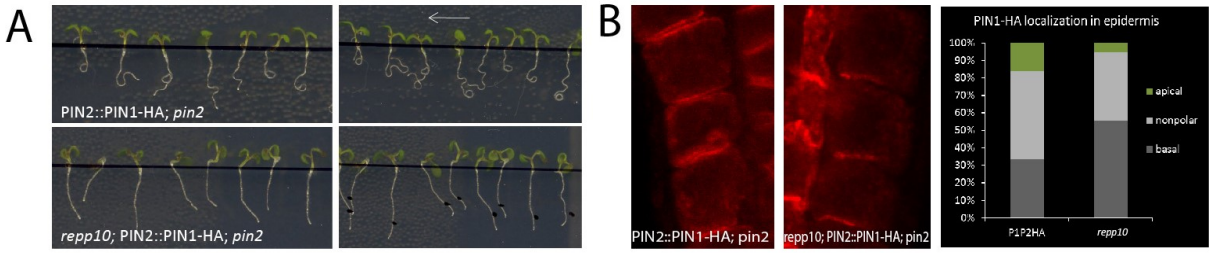

Figure 14. The *repp10* mutant

(A) Gravitropic behaviour of the *repp10* root. The *repp10* roots have a tendency to grow straight, without discernable waving. Upon gravistimulation by rotating the Petri dish, the roots will usually bend in the correct direction, but the direction change is very slow. (B) PIN1-HA was not switched to the apical domain in root epidermis of *repp10*.

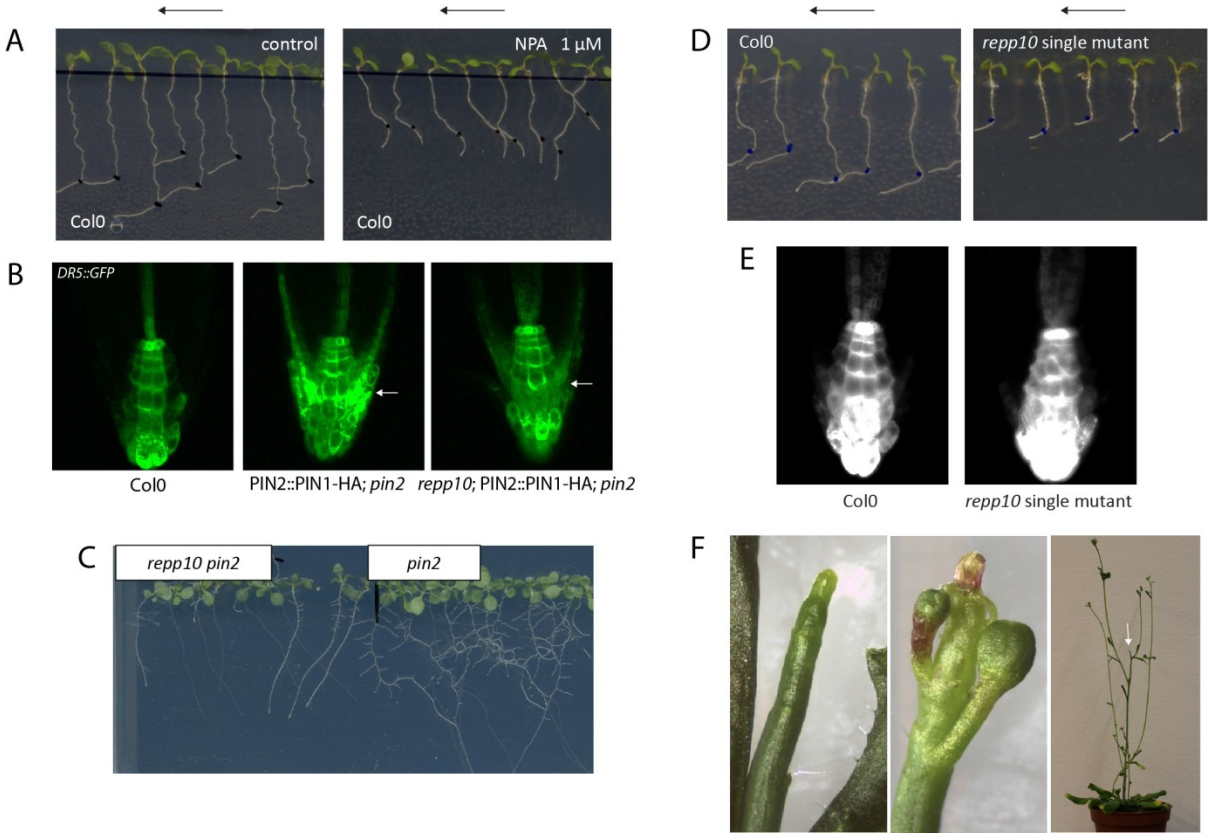

Figure 15. Auxin transport-related phenotypes of *repp10.*

(A) A low dose of auxin transport inhibitor NPA causes in the wild-type a root growth/gravitropism phenotype similar to the *repp10; PIN2::PIN1-HA; pin2* phenotype (compare with Figure 10A). (B) The auxin response, as visualized with DR5::GFP, is diminished in *repp10; PIN2::PIN1-HA; pin2* in comparison to the mutant genetic background *PIN2::PIN1-HA; pin2* (arrows). (C) *repp10 pin2* double mutant without the *PIN2::PIN1-HA* construct retains the straight growth phenotype. (D) *repp10* single mutant exhibits normal gravitropic responses, indicating that the specific root phenotype was a result of a genetic interaction between *repp10* and *pin2*. (E) The auxin response, as visualized with DR5::GFP, appears normal in single *repp10* mutant. (F) Pin-like shoot apical meristems in *repp10.* Left panel shows a pin-like SAM, while middle panel shows a partial loss of meristem function. Right panel shows whole shoot of an adult plant in which a pin-like meristem was formed.

Preliminary immunostaining of PIN1-HA showed that PIN1 apicalization does not take place in this mutant (Figure 14B). After outcrossing the PIN2:PIN1-HA construct to obtain a double mutant (*repp10 pin2*), the specific root growth phenotype was retained, indicating that it is not dependent on the PIN1-HA expression, and thus on its polarity in the epidermis (Figure 15C). However, when a single *repp10* mutant was obtained, the roots exhibited a grossly normal gravitropism - the characteristic persistence of the root growth direction was lost (Figure 15D). Also, the DR5::GFP signal in the single *repp10* mutant appeared normal (Figure 15E). Thus, the NPA-like growth mode, and the reduced DR5::GFP signals that both suggest an auxin transport issue, are a result of a genetic interaction between *repp10* and *pin2.* Still, the seedlings of single *repp10* mutant does not appear completely normal, as its roots are clearly shorter than wild-type (Figure 15D).

An independent phenotype suggesting defects in auxin transport was found in the shoot. I observed that in *repp10* plants, the shoot apical meristem (SAM) was sometimes failing, leading to a phenotype resembling the “naked pin” of the *pin1* mutant (Figure 15F). Although the phenotype was of the same character as *pin1*, it was of a lesser scope: while *pin1* knockouts exhibit whole stems without any SAM-derived organs, *repp10* typically did generate normal shoots, indicating functional meristems, and only sometimes the meristem would suddenly terminate in a pin-like structure.

In summary, there are some indications that *repp10* mutation affects auxin transport through the plant.

The mapping of the *repp10* mutation was based on its root growth phenotype. The seedlings were allowed to grow freely on Petri dishes that were tilted back from the vertical position. These conditions challenge the gravitropic response of the root, and wild-type plants exhibit a characteristic waving, that is, a continuous series of exaggerated gravitropic responses. In my selection procedure, the agravitropism of the *pin2* PIN2::PIN1-HA line was greatly enhanced in these conditions, while the *repp10* mutant was often able to consistently grow straight down, which provided for an effective and easy to spot mutant phenotype.

With a mapping population consisting of 720 individuals displaying the mutant phenotype, selected in the F2 generation of a cross between *repp10 pin2 PIN2:PIN1-HA* and *agr1-1* (*pin2* mutant in Landsberg erecta ecotype), the genetic interval of the *repp10* mutation was confined to a 184 kb stretch of chromosome 1 containing 55 predicted genes. The majority of genes in this interval were subsequently PCR-amplified and sequenced. Some genes were not taken into consideration, based for example on their expression pattern not matching the observed phenotypes (e.g. limited to pollen). Among the sequenced candidate genes, two were found to be mutated (Table 3).

Table 3. Candidate mutations for *repp10*

Gene code	Gene name/description	Old/new codon	Old/new amino acid
AT1G18270	ketose-bisphosphate aldolase class-II family protein	gCa/gTa	Ala/Val
AT1G18500	isopropylmalate synthase 1 (IPMS1)	gGa/gAa	Gly/Glu

AT1G18270 is a single copy gene of uncharacterized function. Bioinformatic analyses identify three distinct enzymatic domains, two of which may be dehydrogenases for unknown substrates, while the third one is an aldolase. The mutation in *repp10* falls into the second dehydrogenase domain. In order to test this mutant candidate, the wild-type cDNA sequence of AT1G18270 was cloned and fused to ubiquitously active promoters of UBQ10 and RPS5A genes. These constructs were then transformed into the *repp10* mutant. Additionally, a T-DNA insertion line in the AT1G18270 gene was isolated and crossed into the PIN2::PIN1-HA *pin2* background.

The second candidate, AT1G18500, encodes IPMS1, one of two *Arabidopsis* paralogues of isopropylmalate synthase (Kraker et al., 2007). The enzyme participates in leucine biosynthetic pathway. Single *ipms1* mutant yielded plants with normal leucine levels, while the level of valine was slightly increased.

The confirmation of these gene candidates was not completed due to the workload related to other projects which were part of this thesis. As the *repp10* mutant exhibits some interesting, auxin-transport related phenotypes, it may be interesting to continue these mapping efforts. Whole genome re-sequencing of the *repp10* mutant could be considered as an alternative approach to search for gene candidates, in the case that some mistakes were made in the gene-by-gene re-sequencing approach undertaken here.

2.2.5 repp13

repp13 exhibited a relatively clear rescue of the gravitropic response (Figure 16A). In a preliminary immunostaining for PIN1-HA, it appeared that the polarity is often switched to apical (Figure 16B). Thus, it may be that *repp13* represents a polarity mutant in the sense that was intended in the design of this genetic screen. The development of the *repp13* mutant is severely affected; the adult plants are stunted in growth and have low fertility.

The mutant was mapped with the whole genome resequencing-based approach, as *repp11* and *repp12*. A mapping population was selected from a cross with the mutant's genetic background PIN2::PIN1-HA *pin2*, and the DNA isolated from the pooled mutant seedlings was subjected to whole-genome sequencing. Similarly to the other mutants, *repp12* seedlings were selected based on root gravitropism.

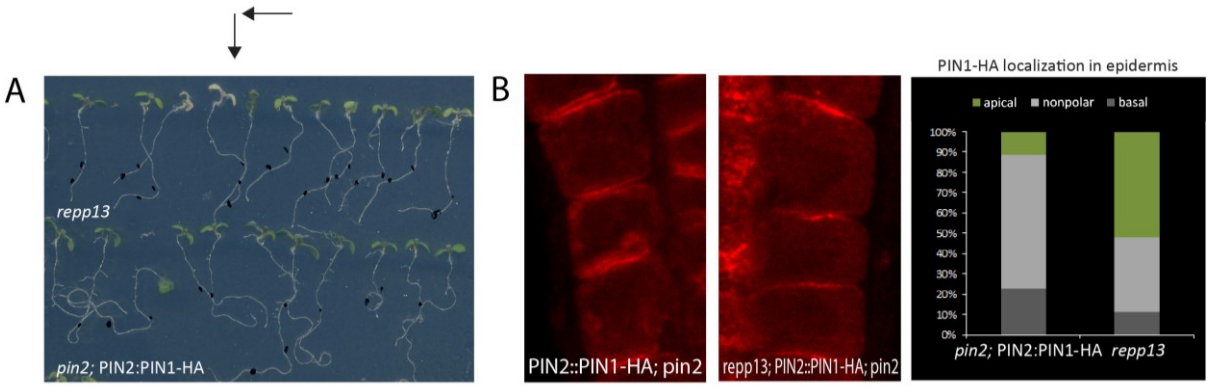

Figure 16. The *repp13* mutant

(A) The gravitropic response of the root is restored in *repp13* mutant as compared to the *PIN2::PIN1-HA; pin2* genetic background. The Petri dish was rotated by 90 degrees twice. Black dots represent the location of root tips before rotation. (B) Increase of apical localization of PIN1-HA in the root epidermis of *repp13.* The number of cells scored were 173 and 67 for the genetic background and *repp13,* respectively.

After whole-genome resequencing, high-frequency SNPs unique to *repp13* were plotted onto a chromosomal map (Figure 17). In contrast to *repp11* and *repp12*, no evident region with large amount of high-frequency SNP rate could be found, and so, a confident selection of a genomic region of interest was not possible. Instead, codon-changing mutations identified with frequency 0.9 or higher in the whole genome were taken under consideration. Four candidates were found with this approach (Table 4). Due to time constraints, the work on this mutant was not continued.

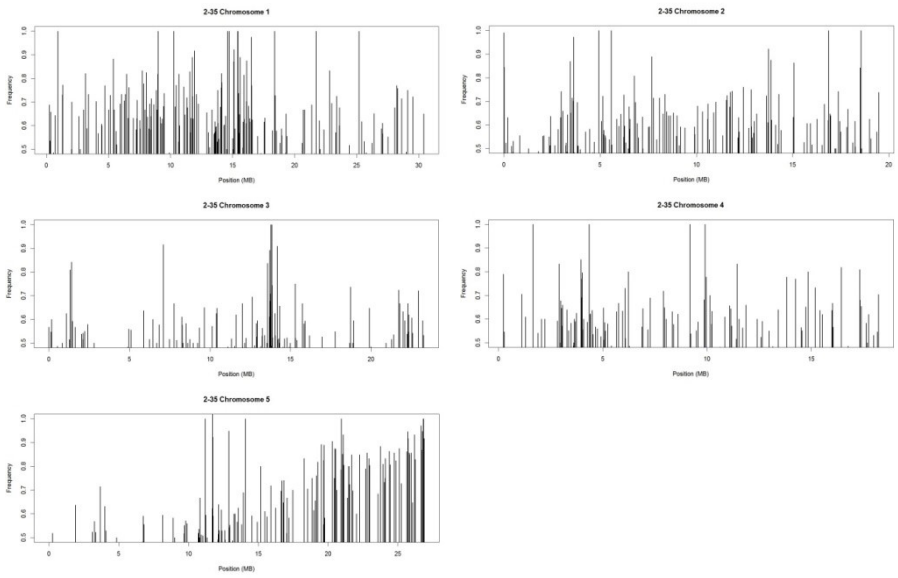

Figure 17. Mapping of *repp13*.

Plots represent chromosomes of *A.thaliana* with *repp13* SNPs co-segregating with the gravitropic phenotype in the F2 generation of *repp13 x PIN2::PIN1-HA; pin2*. Heights of peaks indicate SNP frequency in the sample. No reliable mutant interval could be deduced from these plots.

Table 4. Candidate mutations for *repp13*

Gene code	Gene name/description	Old/new codon	Old/new amino acid
AT5G49910	CHLOROPLAST HEAT SHOCK PROTEIN 70-2	cCt/cTt	Pro/Leu
AT5G64290	DICARBOXYLATE TRANSPORT 2.1	Cct/Tct	Pro/Ser
AT5G66810	Contains C-terminal LisH motif	Gcc/Acc	Ala/Thr
AT5G67030	ZEAXANTHIN EPOXIDASE; ABA DEFICIENT 1	cCg/cTg	Pro/Leu

2.3 Materials and methods

2.3.1 Plant material

The following previously published plant material was used: *ala3-1, ala3-4* (McDowell et al., 2013)*, psl2-3* (Saijo et al., 2009)*, crt3-1* (Li et al., 2009)*, stt3a-2* (Frank et al., 2008)*, os9-t* (Su et al., 2012)*, sdf2-2* (Nekrasov et al., 2009)*, erdj3b-1* (Sun et al., 2014)*, psl4-2* (Lu et al., 2009)*, ebs5-5* (Su et al., 2011)*, PIN2::PIN1-HA; pin2* (Wisniewska et al., 2006), *PIN2::PIN1-HA; pin2; DR5::GFP* (Feraru et al., 2011).

Mutants isolated during this study: *ala4* (WiscDsLox435D3; N855695), *ala5* (SALK_049232 N549232), *ala9* (SALK_128495 N628495), *ala10* (SALK_024877C N669487), *ala11* (SAIL_90_A12 N862389).

The following primers were used for genotyping the mutants:

Mutant	F primer	R primer
ala3-1	GCCAGCAAAGCATGATTTT	CACACAATCATACTGAAATAA
ala3-4	GATCTCTGCCTCTCGCAATC	CTCACAGGACTGCAGGACAA
psl2-3	CTCTCTCCTCAATTTAAGGATG	CACACCACAACCACTCTTGG
crt3-1	GTACTTCCTTTCGCCCACCT	CTTCGTCTGTGTTCCGCATA
stt3a-2	CGTTTCAGGTATTCCGCTTT	AGGCTTCAAGAGGCAAAACA
os9-t	AATCCCTCCCTGGATTTGAG	GCGGGTAACACTGAAAATGG
sdf2-2	GGGCAACAACAAGCTCTCTC	TCTCAGGGAATACAAATGTTGC
erdj3b-1	TGTACACGTAACCCGACCAC	GCAATCTGCACCCTTTAAACA
psl4-2	TCTGGCCAAGTGCTTACAAA	TCAAAACAACGACCATGGAA
ebs5-5	AACTCGCCAAGATGTTCCAT	GCGCATTGGACTGTGATTTA
ala4	TGCTGGATTTGTCCATCTGA	ACCTGTCAGCTCCTTTGCAT
ala5	TCAGAAGGAGGATCCCAAGA	GCGATTACTGGCAATGAGGT
ala9	TTCTTTGACCCCAAAAGAGC	GTCCCGTGTTTCCTCTTCAA
ala10	CCGATTTCGCTTTACGTTTC	CGGAAGCCTTAGCTTCATTG
ala11	CGCTGACTGCTCTCTCTCCT	TTGGAGCTCTGTCTGGATCA

2.3.2 Seedling growth and gravitropism assays

Arabidopsis seedlings were grown on 1/2MS medium with 1% sucrose, at 24 degrees in constant light regime. Gravitropic stimuli were applied by rotating the Petri dishes by 90 degrees (135 degrees for *ala3* single mutant). During the selection of mutant seedlings for mapping populations, three consecutive gravitropic stimulations were employed to reduce the false positive rates. For 'tilted plate' assays of *repp10* mutant, Petri dishes were mounted on special racks which allowed the plate to be tilted back from the vertical position by approximately 15 degrees.

2.3.3 PIN1 polarity measurement

Immunostaining of PIN1-HA was performed with Intavis InsituPro robot according to a previously published protocol (Sauer et al., 2006). Rabbit Anti-PIN1 primary antibody (Paciorek et al., 2005) was used at 1:1000 dilution and Cy3 anti-rabbit secondary antibody (Sigma) was used at 1:600 dilution. Epidermal cell files were imaged by confocal microcopy and the polar localizations of PIN1-HA were evaluated on a single cell basis. 'Apolar' category refers to PIN1-HA being localized in both apical and basal domains the same cell.

2.3.4 Molecular cloning

All constructs were cloned using the Gateway technology. pDONR221 vector containing UGGT was kindly provided by Xu Chen (Friml laboratory). UGGT promoter was cloned with the following primers: attB4-pEBS1-F GGGGACAACTTTGTATAGAAAAGTTGTCAATTGCCCCTTTCAAGAC and attB1r-pEBS1-R GGGGACTGCTTTTTTGTACAAACTTGctttccgcgacggagaa. The UGGT promoter and UGGT coding sequence were then cloned together into pK7m24GW,3 Gateway vector.

35S::GFP-ALA3 expression vector and ALA3/pENTR entry vector were kindly provided by Rosa Lopez-Marques (University of Copenhagen). RPS5A promoter in pDONRP4P1r is a vector of untraceable origin commonly used in the lab. RPS5A::ALA3 was constructed in pK7m24GW,3 expression vector. XVE::GFP-ALA3 was constructed by fusing GFP with ALA3 sequences in pMDCGWm42 expression vector.

ALIS1 coding sequence was cloned from Arabidopsis cDNA with the following primers: attB1-ALIS1-F GGGGACAAGATTGTACAAAAAAGCAGGCTTTATGTCTTCTTCTAACACGCCATC and attB2-ALIS1-R GGGGACCACTTTGTACAAGAAAGCTGGGTTTAACGACCTCCAGGAATTCTG. 35S::ALIS1 construct was made in the pK7WG2 expression vector.

AT1G18270 coding sequence was cloned from Arabidopsis cDNA with the following primers: attB1-AT1G18270-F GGGGACAAGTTTGTACAAAAAAGCAGGCTTTATGAGTGGCGTGGTTGG, attB2-AT1G18270-R

GGGGACCACTTTGTACAAGAAAGCTGGGTTCAAGCTTTTCCGGCAGAG. RPS5A::AT1G18270 was constructed in pK7m24GW,3.

2.3.5 RT-PCR

RNA was isolated from 4d old seedlings with RNeasy kit (Qiagen) and cDNA synthetized with iScript cDNA kit (Biorad). PCR was performed with gene-specific primers flanking the T-DNA insertions, and TUB2 was used as a reference gene.

2.3.6 Cotyledon vasculature

10-day old seedlings were immersed in 70% ethanol overnight, then treated with 4% HCl, 20% Methanol at 65 degrees for min, and then with 7% NaOH, 70% ethanol at room temperature for 15 minutes. The cleared seedlings were then rehydrated by washing for 10 minutes in ethanol solutions of gradually decreasing percentage (70%, 50%, 25%, 10%). Finally, they were washed in 25% glycerol, 5% ethanol, cotyledons were cut off with a razor blade and mounted on microscopy slides in 50% glycerol.

2.4 External contributions

The following work has been performed by Dr. Petra Marhava as part of her doctorate studies:

- The initial screening process leading to the isolation of *repp* mutants
- crosses of *repp9* and *repp10* with *pin2* mutant in Landsberg erecta ecotype, used for the purpose of mapping
- backcrosses of *repp11* and *repp12* with PIN2::PIN1-HA *pin2,* used for the purpose of mapping
- immunostaining of PIN1-HA in *repp10* and *repp13* used in Figures 14 and 16

Next-generation sequencing and bioinformatic of *repp11* and *repp12* were performed at University of Lausanne by Dr. Luca Santuari.

Next-generation sequencing and bioinformatic analyses of *repp13* was performed at Gregor Mendel Institute of Molecular Plant Biology (GMI) in Vienna.

3 Overexpression of auxilin homologs in *Arabidopsis thaliana* inhibits clathrin-mediated endocytosis and suggests homeostatic regulations of endomembrane trafficking

3.1 Introduction

The endomembrane system provides a spatial organization of the plant cell activities. Its compartments, such as the plasma membrane (PM), various endosomal populations, Golgi apparatus, endoplasmic reticulum, and the vacuole perform distinct, specialised functions. At the cell periphery, endocytosis internalises PM-localised proteins, lipids, and extracellular material. To date, the best characterised endocytotic mechanism in plants depends on the coat protein clathrin (Dhonukshe et al., 2007; Kitakura et al., 2011; Wang et al., 2013). During clathrin-mediated endocytosis (CME), a patch of the PM area is shaped into a vesicle and internalized due to scaffolding by a protein cage composed of clathrin, endocytotic adaptor proteins, and other protein factors. Our description of the events that comprise CME in plants is based on the far more advanced studies of CME in animal and yeast systems (reviewed in McMahon and Boucrot, 2011).

The initiation mechanisms of the endocytotic process are still not well understood (reviewed in Godlee and Kaksonen, 2013). Classically, the adaptor protein complex AP2 is considered the master initiator that acts through its interactions with specific PM lipids and signalling motifs of the cargoes, and through clathrin recruitment. More recently, proteins of the FCH domain only (FCHo) family have been proposed as the initial factors for endocytotic pit formation (Henne et al., 2010). However, data questioning the pivotal role in initiation for both AP2 and FCHo have been reported (reviewed in Godlee and Kaksonen, 2013). In plants, two well-characterised candidates for initiation factors are the classical AP2 complex (Di Rubbo et al., 2013; Kim et al., 2013; Yamaoka et al., 2013; Bashline et al., 2013; Fan et al., 2013) and the recently identified TPLATE complex (Gadeyne et al., 2014; Zhang et al., 2015). A large and until now poorly characterised family of monomeric AP180 N-Terminal Homology and Epsin N-Terminal Homology (ANTH/ENTH) adaptors is present in plant genomes as well (reviewed in Zouhar and Sauer, 2014).

The progression of the coated pit formation relies on the recruitment of clathrin hexamers, termed triskelions, that consist of three clathrin light chain (CLC) and three clathrin heavy chain (CHC) subunits. Clathrin assembles into a regularly shaped cage which stabilizes the forming vesicle containing the endocytotic cargoes. The scission of a completed vesicle from the PM is mediated by dynamins, molecular scissors that mechanically constrict the neck between the clathrin-coated vesicle (CCV) and the PM. In the final stage of CME, CCVs are uncoated through the action of DnaJ domain proteins called

auxilins and cyclin G-associated kinases (GAKs). These factors bind to the coat to recruit and activate the molecular chaperone Hsc70. The disassembly of the clathrin coat by Hsc70 represents a canonical chaperone function: Hsc70 dissociates an existing protein complex, the clathrin coat, and binds clathrin to prevent its aberrant aggregation (reviewed in Sousa and Lafer, 2015). The uncoating step releases the vesicle for its subsequent fusion with endosomal compartments and allows recycling of the CME machinery components for further rounds of endocytosis.

Thus far, manipulating endocytosis in plants has been possible by means of clathrin mutants and the dominant negative version of CHC (Kitakura et al., 2011; Dhonukshe et al., 2007), lines downregulating the endocytotic adaptors (Gadeyne et al., 2014, Di Rubbo et al., 2013; Kim et al., 2013; Bashline et al., 2013; Fan et al., 2013), as well as mutants defective in early endosomal components (Tanaka et al., 2013) and the dynamin homologue DRP1A (Collings et al., 2008). These and similar tools allowed the identification of roles of endocytosis in processes such as plant immunity (reviewed in Khaled et al., 2015), establishment of the polar auxin transport through the polarised subcellular localization of PIN-FORMED (PIN) transporters (reviewed in Adamowski and Friml, 2015) and brassinosteroid signalling (Irani et al., 2012; Di Rubbo et al., 2013).

In a broad perspective, endocytosis is just one of the many trafficking processes in the endomembrane system. Trafficking between the different compartments necessarily involves an exchange of membranes of which the compartments themselves are composed. Thus, while the endomembrane system appears as a collection of discrete elements, it might be considered as a single, continuous entity of membrane forming temporary distinct features. From this point of view, the structure of the endomembrane system, understood as the relative contribution of each type of compartment, can be seen as sum of the activities of distinct trafficking processes, as well as of membrane lipid biosynthesis and degradation processes. A question to be asked is, then, how are the rates of these trafficking processes mutually adjusted to maintain the endomembrane system in homeostasis at the whole cell level. For instance, maintenance of PM structure appropriate for the current cell volume presumably requires the coupling of the rate of delivery of new membranes to the PM by secretion and of the competing removal of membranes by endocytosis.

Previously, ideas similar to the membrane trafficking homeostasis problem formulated above have been proposed in the context of PM area changes during the animal cell cycle (reviewed in McCusker and Kellogg, 2012). For example, a “membrane reservoir” resulting from differential mutual rates of endo- and exocytosis has been suggested to account for the changes in PM area during the cell cycle (Boucrot and Kirchhausen, 2007). We consider not only changes in the PM area, related to growth or division, but rather pose

a broader question about mechanisms that maintain all parts of the endomembrane system in homeostasis at any given time.

Here, our aim was to extend the knowledge of protein components that participate in CME in plants. To this end, we screened for physical interactors of CLC with tandem affinity purification. Among the interactors, we found two putative homologs of the vesicle-uncoating factor auxilin, which we designated Auxilin1 and Auxilin2. Overexpression of these auxilin homologs effectively inhibited CME by preventing clathrin recruitment to the initiating endocytotic pits. We realised that by inhibiting endocytosis, we may be able to make inferences about the opposite process of secretion and its relationship to endocytosis. Thus, with this genetic tool, we made observations hinting at possible mechanisms for the homeostatic regulation of endocytosis and exocytosis in plant cells.

3.2 Results

3.2.1 Identification of clathrin machinery components in *Arabidopsis*

To identify additional proteins involved in CME in plants, we carried out tandem affinity purification combined with mass spectrometry (TAP-MS) (Van Leene et al., 2014) in *Arabidopsis thaliana* cell suspension cultures with clathrin light chain1 (CLC1) as bait. Among the isolated CLC-associated proteins (Figure 1A), we identified four proteins with similarity to known classes of endocytotic components: two highly homologous proteins which we designated Auxilin1 and Auxilin2 due to their C-terminal DnaJ domains, found in auxilins and GAKs; an ANTH family monomeric adaptor protein CAP1 (Zouhar and Sauer, 2014), recently reported to interact with the TPLATE adaptor complex (Gadeyne et al., 2014); and the SH3 DOMAIN-CONTAINING PROTEIN2 (SH3P2), the domain composition of which is similar to that of endocytotic factors called endophilins (Renard et al., 2015; Boucrot et al., 2015). Predictably, we also found isoforms of CLC and CHC, on which we did not focus further. Finally, we isolated DHNA-CoA thioesterase2 (DHNAT2), a peroxisome-localised enzyme involved in phylloquinone biosynthesis (Widhalm et al., 2012), which was not included in any experiments as it appears unlikely to be a factor in CME.

Next, we aimed to confirm independently the protein-protein interactions between CLC1 and the proteins isolated with TAP-MS, namely Auxilin1, Auxilin2 (referred to as Auxilins hereafter), CAP1, and SH3P2. To this end, we utilized bimolecular fluorescent complementation (BiFC) (Hu et al., 2002). All four proteins of interest showed robust interactions with CLC1 in tobacco (*Nicotiana benthamiana*) leaves (Figure 1B). In contrast, neither CLC1 nor its four interactors gave positive signals when assayed with phosphatidylinositol 4,5-bisphosphate kinase1 (PIP5K1) (Figure 1B and Supplemental Figure 1A). This control attests the specificity of BiFC interactions, because PIP5K1 is a peripheral

PM-localised protein (Ischebeck et al., 2013; Tejos et al., 2014), making it potentially available for partnership with PM-bound endocytotic components. Furthermore, the BiFC assays revealed interactions between the clathrin-associated proteins, as both SH3P2 and CAP1 interacted with Auxilins (Supplemental Figure 1B). In contrast, SH3P2 and CAP1 did not interact with any combination of the split GFP tag positions (Supplemental Figure 1A), demonstrating that the BiFC assay gave highly specific outputs. In summary, by a TAP-MS approach and its confirmation with BiFC (summarised in Figure 1C), we identified proteins with potential roles in clathrin-mediated processes, including endocytosis.

A

AGI code	Protein name	Isolated with (no. exp.)	
		C-terminal tag	N-terminal tag
AT4G12780 / AT4G12770	Auxilin1 / Auxilin2	2	-
AT4G32285	CAP1	2	-
AT4G34660	SH3P2	1	-
AT5G48950	DHNAT2	2	2
AT3G08530	Clathrin Heavy Chain1	2	2
AT3G11130	Clathrin Heavy Chain2	2	2
AT2G20760	Clathrin Light Chain1	2	2
AT2G40060	Clathrin Light Chain2	2	-

B

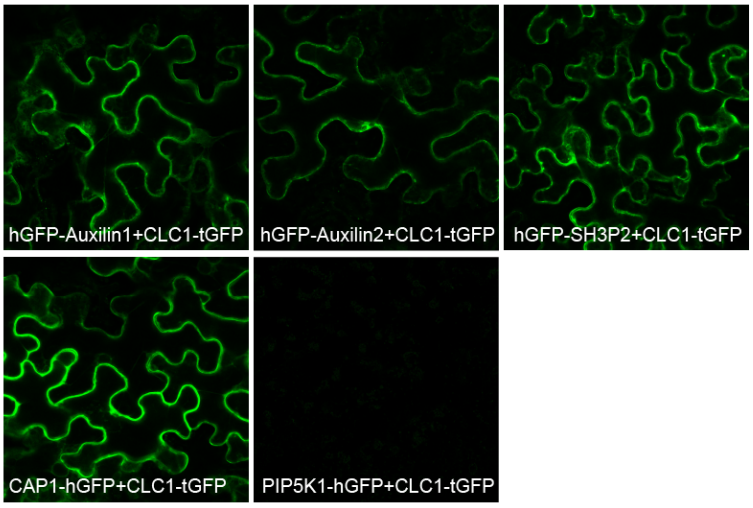

C

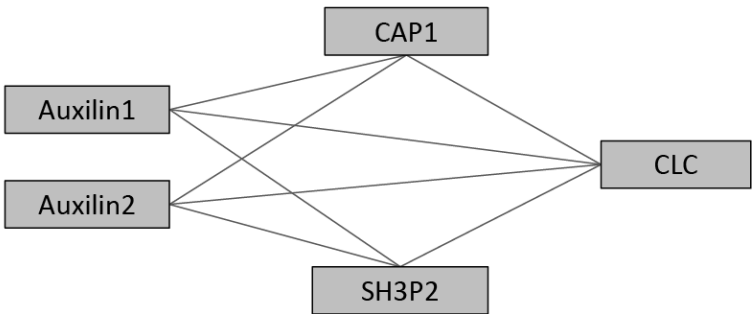

Figure 1. Identification and confirmation of CLC-interacting proteins.
(A) Tandem Affinity Purifi-cation-Mass Spectrometry (TAP-MS) isolation of proteins associated with clathrin. Clathrin light chain 1 (CLC1) was fused with TAP tags at C- and N-termini and two repetitions with each constructs were performed.
(B) BiFC interactions between CLC1 and selected interactors identified with TAP-MS. PIP5K1 was used as negative control.
(C) Schematic representation of all interactions detected with BiFC.

3.2.2 Clathrin-associated proteins localise to the PM and the cell plate

Clathrin localises to multiple subcellular compartments in plant cells. Besides the PM, it is found at the cell plate and endosomal compartments, with a large population at the *trans*-Golgi network/early endosome (TGN/EE) (Ito et al., 2012; Robinson and Pimpl, 2014). To identify the site of action of CAP1, SH3P2, and Auxilins, we analysed their subcellular localizations by live imaging with fluorescent protein fusions. We utilised confocal laser scanning microscopy (CLSM) and variable-angle epifluorescence microscopy (VAEM) (Konopka and Bednarek, 2008), which is a plant-specific modification of total internal reflection fluorescence microscopy (TIRF) that allows imaging of the PMs in spite of the presence of cell walls. CLSM imaging in the epidermal cells of the root apical meristem (RAM) showed SH3P2-GFP (Zhuang et al., 2013) and CAP1-mCherry localising predominantly to the PM and cell plates, with weaker signals in the cytosol and the nucleus (Figure 2A and 2B). The imaging of RFP-Auxilins was difficult due to a relatively low expression levels and patchy expression of the transgenes. In cells expressing the transgenes at very low levels, Auxilins showed a cytosolic localization with some enrichment at the PM and the cell plate (Figure 2C and 2D, left), while in cells with high expression, Auxilins localised to the cytosol and the nucleus and without evident enrichment at the PMs (Figure 2C and 2D, right).

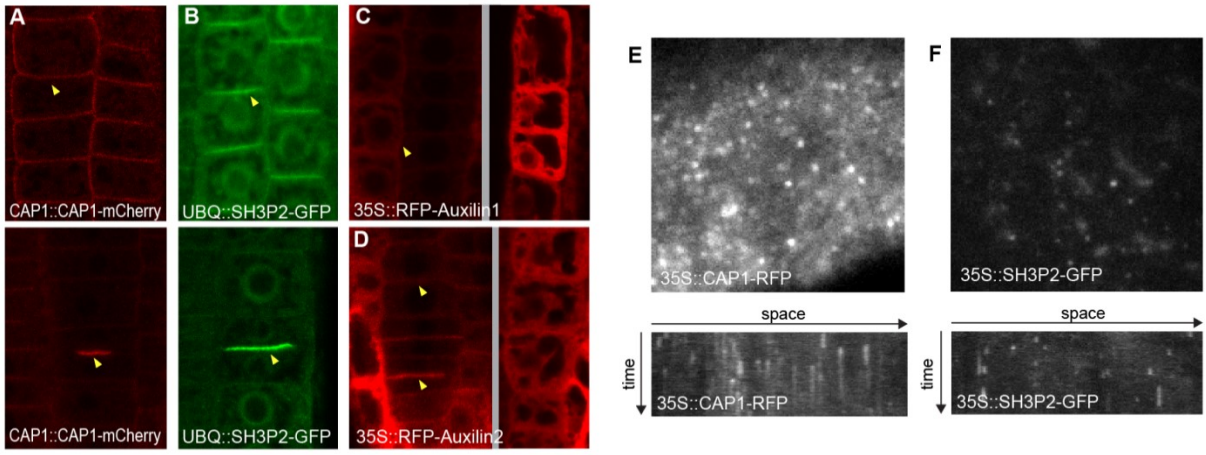

Figure 2. Subcellular localizations of the identified clathrin interactors.

(A) Localisation of CAP1-mCherry to the PM and growing cell plates.

(B) Localisation of SH3P2-GFP to the PM and growing cell plates.

(C) and **(D)** Enrichment of RFP-Auxilin1 and RFP-Auxilin2 at the PM and cell plates in weakly expressing cells (left) and localization to the cytosol and nucleus in strongly expressing cells (right).

(E) and **(F)** CAP1-RFP and SH3P2-GFP forming dynamic foci at the PM reminiscent of known endocytotic proteins. Single VAEM images (top) and kymographs (bottom) are shown.

Arrowheads in **(A)** to **(D)** indicate membrane-associated signals**.**

VAEM imaging in etiolated hypocotyl epidermis revealed that both CAP1 and SH3P2 formed dynamic foci at the PM (Figure 2E and 2F, Supplemental Movie 1 and 2), reminiscent

of endocytotic components such as CLC, DRP1C, AP2, and the TPLATE complex (Konopka et al., 2008; Gadeyne et al., 2014). Occasionally, SH3P2-GFP also formed elongated, intracellular bodies that might have been artefacts resulting from its overexpression (Supplemental Movie 2). We were unable to image RFP-Auxilins in this system due to the low expression of the transgenes. In summary, these subcellular localization data together with the interaction studies suggest that Auxilins, CAP1, and SH3P2 may participate in CME at the PM as well as in CCV formation at the cell plate.

3.2.3 Overexpression of Auxilins leads to defects in cell morphology and to a developmental arrest

Next, we tried to obtain loss-of-function mutants in the four corresponding genes, but failed to isolate true knock-out alleles for any of them from the public collections of T-DNA insertion lines. We also generated transgenic *Arabidopsis* lines overexpressing these genes under the control of the strong constitutive CaMV 35S promoter. Overexpression of SH3P2-GFP or CAP1-RFP did not cause immediately visible defects in seedling development (Supplemental Figure 2A). In contrast, only a few primary (T1) transformants overexpressing RFP-Auxilin1 or RFP-Auxilin2 fusions could be recovered and the T2 generation seeds often failed to germinate even after prolonged stratification and culturing (Supplemental Figure 2B). Rare, germinated RFP-Auxilin seedlings had a stunted growth and the fusion proteins had a weak and patchy expression, as mentioned above (Figure 2C and 2D). The transgene silencing was almost complete after propagation into the T3 generation. As these observations implied a strong selection against high Auxilin expression levels, we focused on the analysis of phenotypes caused by Auxilin overexpression.

To overcome the seed germination arrest caused by constitutive Auxilin overexpression, we generated chemically inducible lines expressing untagged Auxilins under the control of the estradiol induction system (Zuo et al., 2000). As expected, XVE>>Auxilin1 and XVE>>Auxilin2 seeds did not germinate on half-strength Murashige and Skoog (½MS) medium supplemented with β-estradiol (Figure 3A, top), but germinated and developed normally on a control medium (Supplemental Figure 3). Induction of Auxilin expression in young seedlings caused growth arrest (Figure 3A, bottom). These results show that overexpression of Auxilin1 and Auxilin2 interferes with processes necessary for normal growth and development of *Arabidopsis*.

Microscopic examination of root tips in seedlings of XVE>>Auxilin lines induced for 3 days revealed changes in organ and cell morphology. The most prominent feature was a strikingly transparent appearance of the root tips, caused by an apparent loss of the cytosolic compartments and swelling of the vacuoles (Figure 3B). Already 1 day after the onset of Auxilin induction, vacuoles often occupied most of the epidermal cell volume,

whereas the cytosolic volume seemed reduced (Figure 3C). The nucleus was displaced from its central position, often to the inner parts of the cell (Supplemental Movie 3). These observations show that Auxilin overexpression disturbs normal cellular functions.

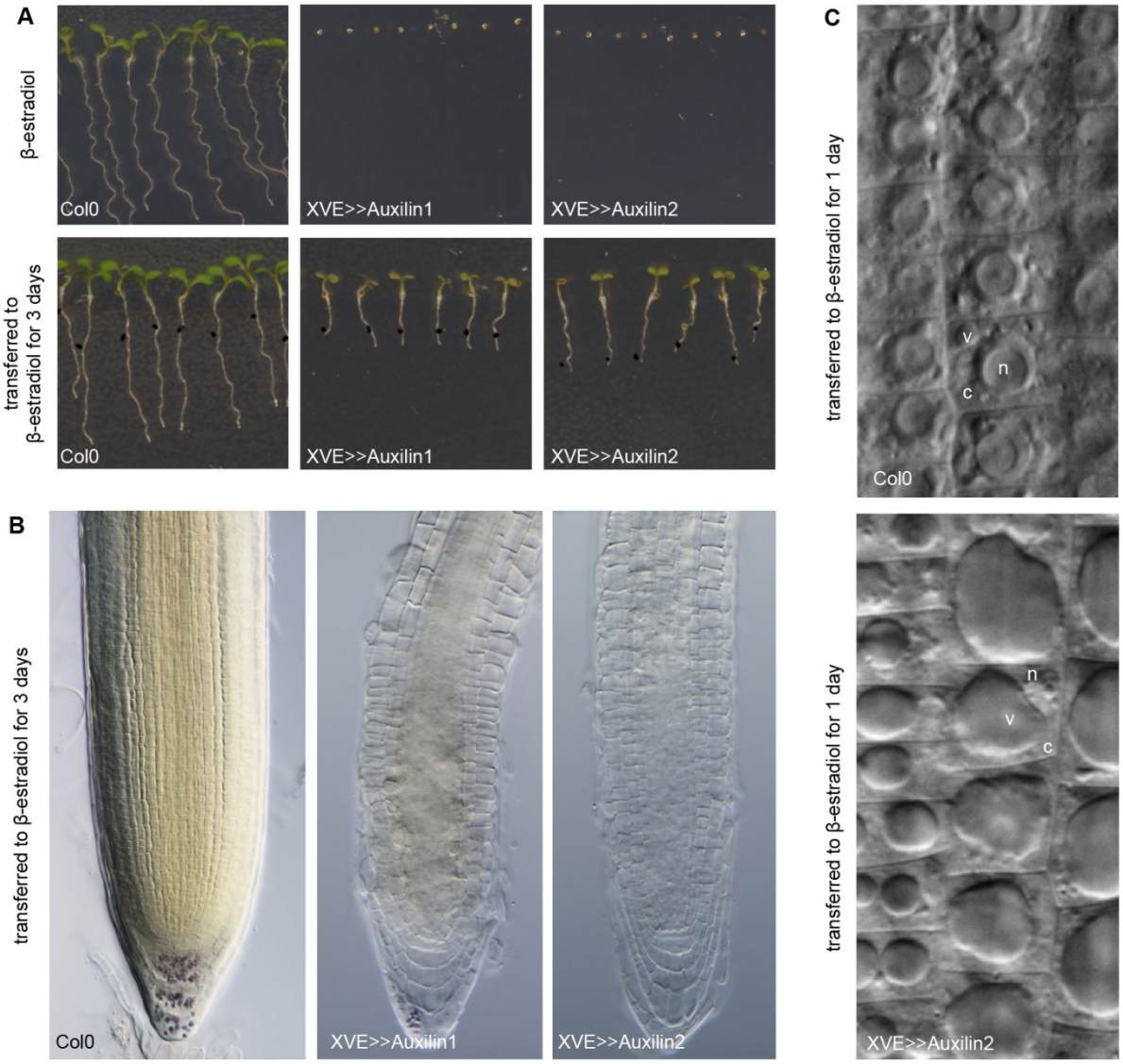

Figure 3. Auxilin overexpression causes an arrest of seed germination and growth and leads to alterations in cell morphology.

(A) Failure of XVE>>Auxilin1 and XVE>>Auxilin2 seeds to germinate after 7 days of culture on β-estradiol-containing media (top). Seedlings induced 3 days after germination terminate growth and development (bottom).

(B) Semi-transparent Lugol-stained roots of XVE>>Auxilin seedlings induced for 3 days displaying shortened RAM.

(C) Light microscopy of XVE>>Auxilin2 roots after 1 day of induction revealing enlarged vacuoles and reduced cytoplasmic volume. V, vacuole; c, cytoplasm; n, nucleus

3.2.4 Auxilin overexpression inhibits CME

Previously, CME inhibition has been reported to interfere with normal plant development (Kitakura et al., 2011; Gadeyne et al., 2014) and auxilin overexpression in HeLa cells was shown to hinder endocytosis (Zhao et al., 2001). Therefore, we suspected that overexpression of Auxilin1 and Auxilin2 in *Arabidopsis* could be similarly affecting CME. As described above, an evident growth arrest and severe morphological changes could be observed 3 days after Auxilin induction, but alterations in cell morphology began to be visible already 1 day after induction (Figure 3C). To assess the cell biological consequences of Auxilin overexpression more specifically, in the following experiments we used 1 day of induction, unless stated otherwise.

First, we applied the endocytotic tracer FM4-64 (Jelinkova et al., 2010) to assess bulk endocytosis rates in XVE>>Auxilin lines. Auxilin overexpression clearly reduced the endocytotic uptake of FM4-64, as evidenced by faint or absent staining of early endosomes (Figure 4A). The enlargement of vacuoles and the simultaneous loss of the endosome-containing cytosolic space (Figure 3C) may have hindered the correct interpretation of these observations. We carefully compared the FM4-64 fluorescence channel with transmitted light images to find areas not occupied by vacuoles in which endosomes were either stained by FM4-64, albeit very weakly, or were not stained at all (Supplemental Figure 4).

Then, we analysed the endocytosis rates of the PM-localised auxin efflux carriers PIN1 and PIN2 (Petrášek et al., 2006) that are CME cargos (Dhonukshe et al., 2007). PIN proteins undergo constitutive cycling between PM and intracellular compartments (reviewed in Adamowski and Friml, 2015); the exocytotic step of this cycling can be pharmacologically inhibited by brefeldin A (BFA) that targets the ADP-ribosylation factor-guanine nucleotide exchange factors (ARF-GEFs). Therefore, BFA causes intracellular trapping of constitutively cycling PIN cargoes in so-called “BFA bodies”, which are agglomerations of endosomal compartments induced by this drug. In the RAMs of Auxilin overexpression lines, very little or no staining of BFA bodies with PIN1 and PIN2 could be observed (Figures 4B and 4C). In a control experiment with CLC2-GFP (Konopka and Bednarek, 2008) as a marker for BFA-sensitive endosomes, BFA bodies could easily be observed in XVE>>Auxilin lines despite the vacuoles taking up most of the cell volumes (Figure 4D). Thus, the lack of detectable intracellular PIN signals after BFA treatment is a result of their inhibited endocytosis.

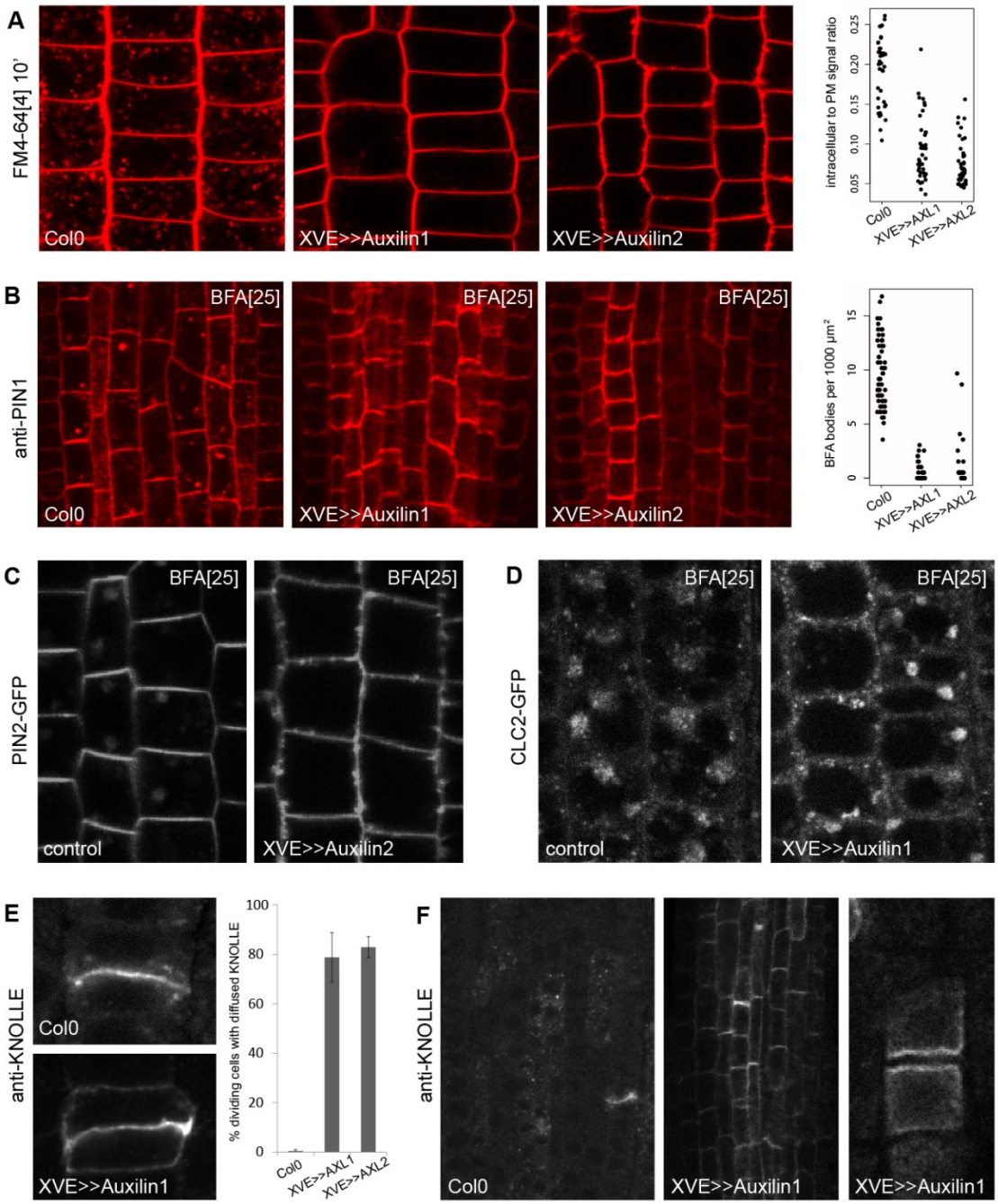

Figure 4. Overexpression of Auxilins leads to inhibition of CME

(A) Reduced uptake of the endocytotic tracer FM4-64 into RAM epidermal cells in XVE>>Auxilin seedlings after 10 minutes of staining.

(B) Immunolocalization of PIN1 after 90 mins of BFA [25 µM] treatment in the RAM central cylinder. The BFA body number is markedly reduced, indicative of inhibition of PIN1 endocytosis.

(C) Lack of PIN2-GFP internalization into BFA bodies in the RAM epidermis after 90 min of BFA [25 µM] treatment in XVE>>Auxilin2 background.

(D) Control experiment with CLC2-GFP shows that after 90 min of BFA [25 µM] treatment, BFA bodies can be easily observed in epidermis of Auxilin overexpressing seedlings despite the enlarged vacuoles.

(E) and **(F)** Immunolocalization of KNOLLE in the RAM of XVE>>Auxilin lines showing diffusion of KNOLLE out of the cell plate and into the PM in late cytokinesis cells **(E)** and KNOLLE signals retained in interphase cells **(F)**, indicating a failure to internalise and degrade the protein. Error bars indicate SD from 3 experiments.

Many auxin-regulated processes in plant development require an auxin transport directed by the polar localization of PIN transporters (reviewed in Adamowski and Friml, 2015). CME, as well as subsequent endosomal trafficking events, are necessary to maintain a polar PIN distribution at the PMs (Kitakura et al., 2011; Kleine-Vehn et al., 2011; Tanaka et al., 2013, 2009). In line with previous reports, endocytosis inhibition in XVE>>Auxilin lines led to depolarisation of the PIN distribution at the PMs (Supplemental Figures 5A-5C) and, consistently, produced altered auxin response patterns in the RAM (Supplemental Figure 5D).

Finally, we analysed the subcellular localization of KNOLLE, a syntaxin specifically expressed during cytokinesis and targeted to the growing cell plate (Lauber et al., 1997). KNOLLE is maintained at the cell plate and blocked from lateral diffusion into the surrounding PM by endocytosis (Boutté et al., 2010). In late cytokinetic cells of the XVE>>Auxilin lines, KNOLLE stained not only the cell plates, but was also distributed in the surrounding PMs (Figure 4E), indicating a failure to internalise the diffusing protein. Furthermore, while interphase cells normally do not express KNOLLE (Lauber et al., 1997), we often found the protein retained at the PMs of interphase cells (Figure 4F), presumably because the protein could not be efficiently internalised and transported to the vacuole for degradation. Taken together, our results imply that overexpression of Auxilin1 or Auxilin2 causes inhibition of CME.

3.2.5 Overexpressed Auxilins interfere with clathrin recruitment to the endocytotic foci at the PM

To characterise the mechanism by which overexpressed Auxilins cause CME inhibition, we investigated the localization of CLC2-GFP(Konopka and Bednarek, 2008)(Konopka and Bednarek, 2008) in RAM epidermis cells by CLSM. In control roots, CLC2 localised to the PM as well as endosomal compartments, as previously reported (Figure 5A). In contrast, in a vast majority of XVE>>Auxilin1 seedling roots, CLC2 was absent from the PMs, while endosomal signals were retained (Figure 5A; see also intracellular CLC2 signals agglomerated into a BFA body in Figure 4D), suggesting that clathrin function is specifically lost from the PM. Next, we characterized the behaviour of CLC2 in more detail by observing the PMs of etiolated hypocotyl epidermis cells with VAEM. With this approach, we were capturing the membrane-associated clathrin foci as well as intracellular (cytoplasmic) signals that are in close proximity to the PM (Konopka and Bednarek, 2008). In control hypocotyls, abundant endocytotic CLC2 foci at the PM were observed as well as clathrin-positive endosomal compartments moving laterally with the cytoplasmic streaming (Figure 5B and Supplemental Movie 4). In the XVE>>Auxilin1 line, only few or no endocytotic foci were present (Figure 5B). Instead, we observed relatively sparse signals of a size larger than

typical membrane foci of clathrin, and often moving laterally, suggesting that they not membrane-bound, but cytosolic (Supplemental Movie 4). As in the root epidermis observed with CLSM, normal endosomal clathrin signals could be still observed. Some cells exhibited abnormally numerous and large intracellular agglomerations of CLC2 (Supplemental Figure 6).

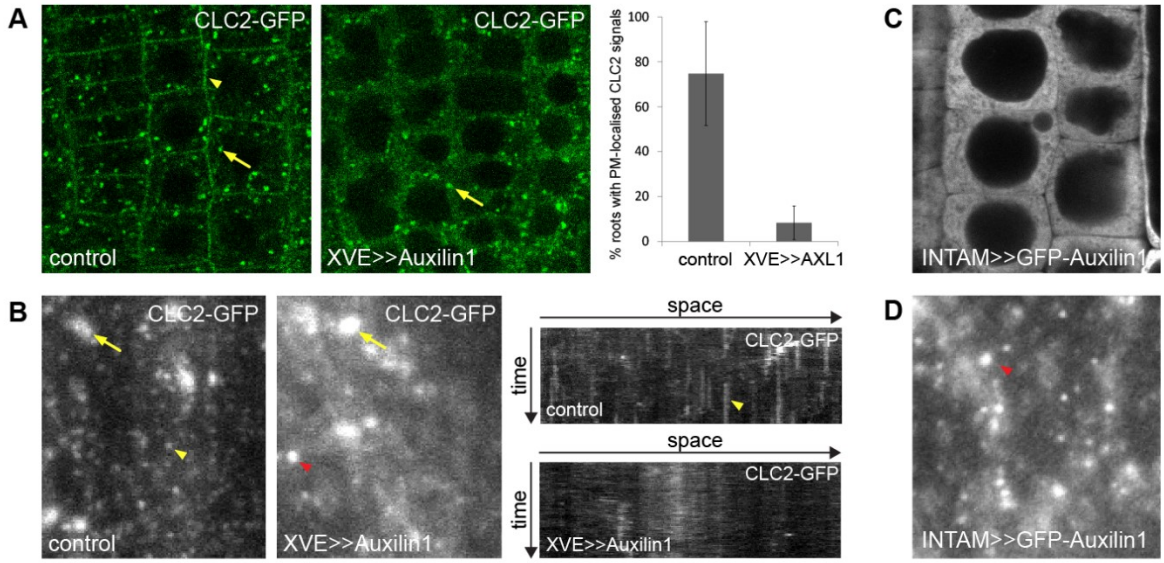

Figure 5. Overexpressed Auxilins interfere with clathrin recruitment to the endocytotic foci at the PM.
(A) CLSM images of CLC2-GFP in the RAM epidermis. Overexpression of Auxilin1 causes a loss of CLC2-GFP from the PMs, but not from the endosomes. Yellow arrowhead and arrows indicate PM and endosomal CLC2-GFP, respectively.
(B) VAEM images (left) and kymographs (right) of CLC2-GFP in hypocotyl epidermis. In XVE>>Auxilin1, endosomal CLC2-GFP signals are retained, while endocytotic foci are not observed. Yellow arrowheads and arrows indicate endocytotic foci and endosomes, respectively. Red arrowhead indicates small, mobile agglomerations of CLC signal.
(C) CLSM imaging in root tip epidermis showing INTAM>>GFP-Auxilin1 localisation to the cytosol.
(D) VAEM imaging in hypocotyl epidermis shows cytosolic GFP-Auxilin1 background together with small mobile agglomerations of signal (red arrowhead).

These observations suggest that Auxilin overexpression causes clathrin to be depleted from the PM. Clathrin formed small, mobile intracellular agglomerations, and it remained bound to, and presumably active at, the endosomes. To better understand the mechanism of this inhibition, we examined the localization of fluorescently tagged, overexpressed Auxilin. As our constitutive overexpression lines (35S::RFP-Auxilin) had a high degree of transgene silencing, we generated an inducible overexpression line of fluorescently tagged Auxilin1 (INTAM>>GFP-Auxilin1) by means of the tamoxifen-driven two-component expression system (Friml et al., 2004). Overexpressed GFP-Auxilin1 localised to the cytosol and caused cell morphological changes seen previously in XVE>>Auxilin lines (Figure 5C and Supplemental Movie 3). With VAEM, we observed a background of cytosolic GFP-Auxilin1 signal, as well as laterally moving intracellular granules (Figure 5D and

Supplemental Movie 5) which were reminiscent of the CLC2-GFP bodies seen in the XVE>>Auxilin1 line (Supplemental Movie 4). Taking into account the interaction between CLC and Auxilins (Figure 1), it is conceivable that these bodies represent inactivated agglomerations of CLC bound to Auxilin, similar to those reported upon auxilin overexpression in HeLa cells (Zhao et al., 2001). In contrast, we did not observe GFP-Auxilin1 at the endosomal compartments, suggesting that overexpressed Auxilin does not bind the endosomal clathrin pool.

Next, we investigated the localization of DRP1C, a dynamin isoform that participates in CME (Konopka et al., 2008). Dynamins are involved in the scission of vesicles from the membrane, and as such, they mark late stages of CME (Merrifield et al., 2002). Similarly to the effect on clathrin, Auxilin1 overexpression caused a decrease in DRP1C-GFP activity at the PM, as there was a marked reduction in, or a complete loss of, PM signals in the root epidermis (Figure 6A), as well as a decreased density of DRP1C-GFP foci at the PM of hypocotyl epidermis (Figure 6B). The partially reduced DRP1C activity at the PM, in contrast to a virtually complete disappearance of CLC2, could be explained by additional, non-clathrin related functions of DRP1C which are insensitive to Auxilin overexpression. Alternatively, variations in XVE>>Auxilin1 expression levels between the two crossed progenies might be the reason for the difference.

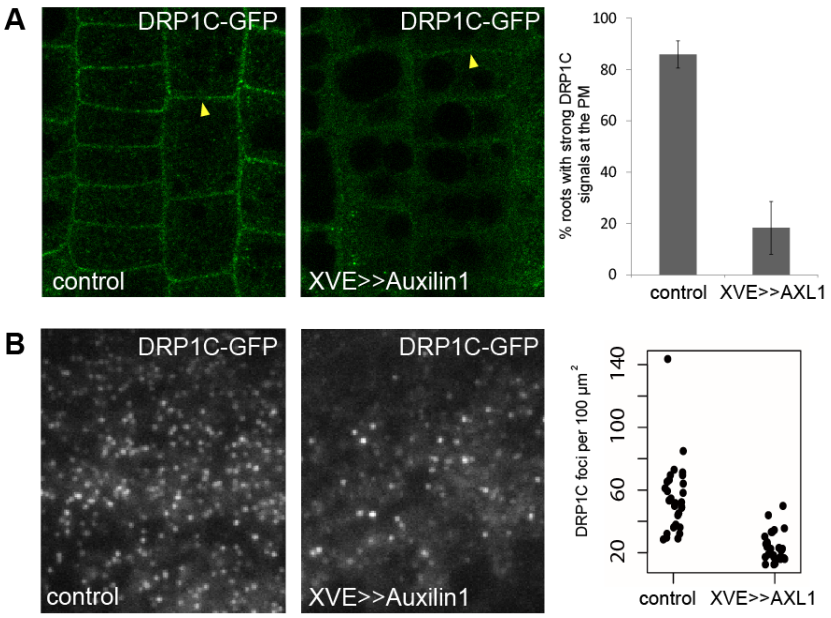

Figure 6. Decreased dynamin activity at the PMs of the XVE>>Auxilin1 line.
(A) CLSM images of DRP1C-GFP in the RAM epidermis. The PM localisation of DRP1C-GFP (arrowheads) was markedly reduced or completely lost in the XVE>>Auxilin1 background.
(B) VAEM images of DRP1C-GFP foci in hypocotyl epidermis showing a reduced foci density upon Auxilin1 overexpression.

In summary, Auxilin overexpression prevented clathrin recruitment to the PM, but probably without a major impact on its function at endosomal compartments. The inability to recruit clathrin to nascent endocytotic foci at the PM hindered the progression of endocytosis through budding and scission of the coated vesicles, marked by dynamin recruitment, providing a plausible mechanism for endocytosis inhibition.

3.2.6 Trafficking imbalance at the PM caused by inhibition of endocytosis

Next, we turned our attention to the issue of membrane trafficking homeostasis maintenance. As discussed in the introduction, one can view the structure of the endomembrane system as resulting from the sum of its transport activities. It appears that a regulation of rates of trafficking processes could be necessary to maintain the endomembrane system in its structural homeostasis. We realised that by inhibiting endocytosis we could study the process of secretion as well, and in particular, we could investigate its relationship with endocytosis. Specifically, we can ask whether a mechanism exists that adjusts the rates of secretion to the current activity of endocytosis. Such a regulatory mechanism could act to block secretion in the XVE>>Auxilin lines as a response to the drastically low, or absent, endocytosis, resulting in a cell where all trafficking to and from the PM is ceased. In the opposite scenario, where exocytosis is not modulated by endocytosis and still occurs when endocytosis is inhibited, an imbalance in the trafficking could result, in which the continued secretion of membranes is not counteracted by their internalization from the PM. One can imagine that in result, the membranes of the endosomal compartments would be gradually lost from the cell interior and deposited at the PM. To investigate these scenarios, we visualised the PMs in XVE>>Auxilin seedling roots by staining with the membrane dye FM4-64, and with the PM-localised transmembrane protein PIN2-GFP. With both these markers, we observed excessive membranous material that accumulated at the periphery of epidermal cells, often forming thick filaments running approximately transversally to the long axis of the cell (Figure 7; see also PM-localised agglomerations in XVE>>Auxilin2 in Figure 4A, Supplemental Figure 4, and Supplemental Figures 5B and 5C). Depending on the particular seed batch used, this phenotype could be observed after 1 or 2 days of induction, presumably reflecting the XVE>>Auxilin construct activity.

Our observations visually demonstrate the process of secretion, which in this imbalanced condition manifests itself as excessive deposition of membranes at the cell surface. It appears, then, that by selectively inhibiting CME we were able to decouple the opposing processes of exo- and endocytosis. This observation suggests that the cell does not adjust the rates of secretion to the current state of endocytosis or, at least, does not do it efficiently. Instead, secretion appears to be taking place independently of endocytosis.

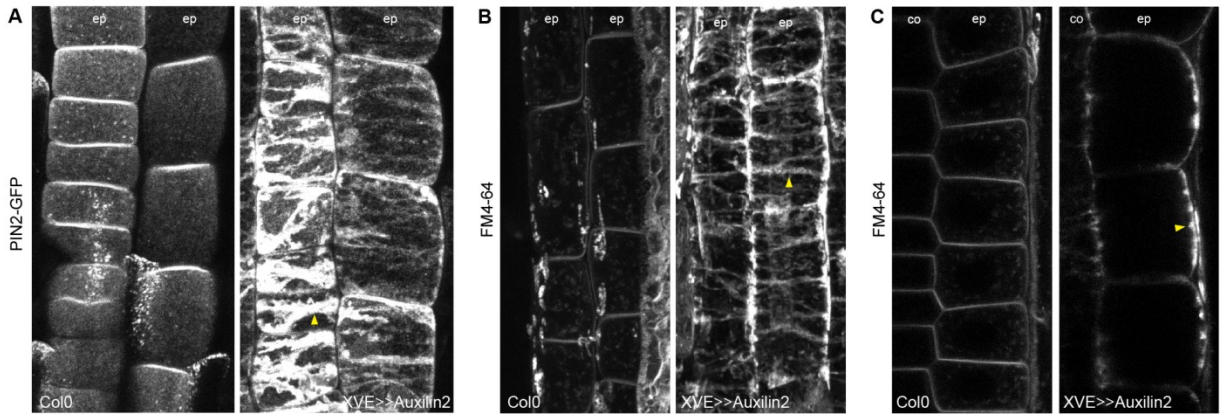

Figure 7. Trafficking imbalance at the PM caused by inhibited endocytosis.

(A) to **(C)** Overexpression of Auxilin2 caused excessive deposition of membrane material at the PM, as visualised with PIN2-GFP **(A)** or FM4-64 staining (**B and C**) in the root epidermis. Arrowheads indicate strands of accumulated membranes in the XVE>>Auxilin2 line.

(A) and **(B)** Maximum intensity projections of *z*-stacks through outer epidermis regions.

(C) Longitudinal cross sections of epidermal cells.

3.2.7 High recruitment of endocytotic adaptor proteins to the PM in secretion-imbalanced cells

We then asked if an opposite regulatory mechanism could exist, in which secretion is the "primary" trafficking process to which the rates of endocytosis are adjusted as a response, so as to maintain homeostasis. Such hypothesis could be tested directly by analysing endocytosis rates in secretory mutants. Nonetheless, our tool for inhibiting endocytosis could give some clues about this process as well. In the XVE>>Auxilin lines, trafficking is highly imbalanced, with an excess of secretion over effective endocytosis. Therefore, any putative mechanism acting to maintain homeostasis by adjusting endocytosis to secretion should be highly active in these conditions.

Auxilin overexpression caused depletion of clathrin and dynamin from the PMs (Figures 5 and 6), suggesting that the endocytotic process is inhibited at the stage of clathrin recruitment to the forming pits. The interaction of Auxilins with CLC (Figure 1) hinted at clathrin as the molecular target of endocytosis inhibition by Auxilin overexpression. However, the adaptor protein complexes AP2 and TPLATE, which initiate endocytotic pits before clathrin recruitment (Fan et al., 2013; Gadeyne et al., 2014) might not be affected by overexpressed Auxilins. Therefore, their behaviour might inform us about potential regulatory mechanisms which adjust the rates of endocytosis to the rates of secretion.

After Auxilin overexpression, in contrast with clathrin and dynamin, both AP2A1-TagRFP and TPLATE-GFP not only were still present at the PMs, but consistently showed a clear increase in signal intensities in root epidermal cells (Figures 8A and 8B). Similarly, with VAEM, increased densities of foci marked by these adaptors were observed at the PMs of

hypocotyl epidermis (Figures 8C and 8D), although the increase in AP2A1-TagRFP binding was not as clear as in the root. Interestingly, time-lapse movies revealed that both TPLATE-GFP and AP2A1-TagRFP stayed at the PM for much shorter times than in control conditions (Figures 8E and 8F and Supplemental Movies 6 and 7). Such short-lived adaptor protein foci probably represent attempts at CCV formation which were aborted due to a failure to recruit clathrin and progress through the budding process.

We think that the increase in adaptor protein binding to the PMs, observed in conditions of excess secretion to the PM, may be a manifestation of a mechanism attempting to increase endocytotic rates. It may be that by regulated recruitment of adaptor proteins, and thus regulated initiation of endocytic foci, plant cells modulate endocytic rates in response to the current demand imposed by secretory activity.

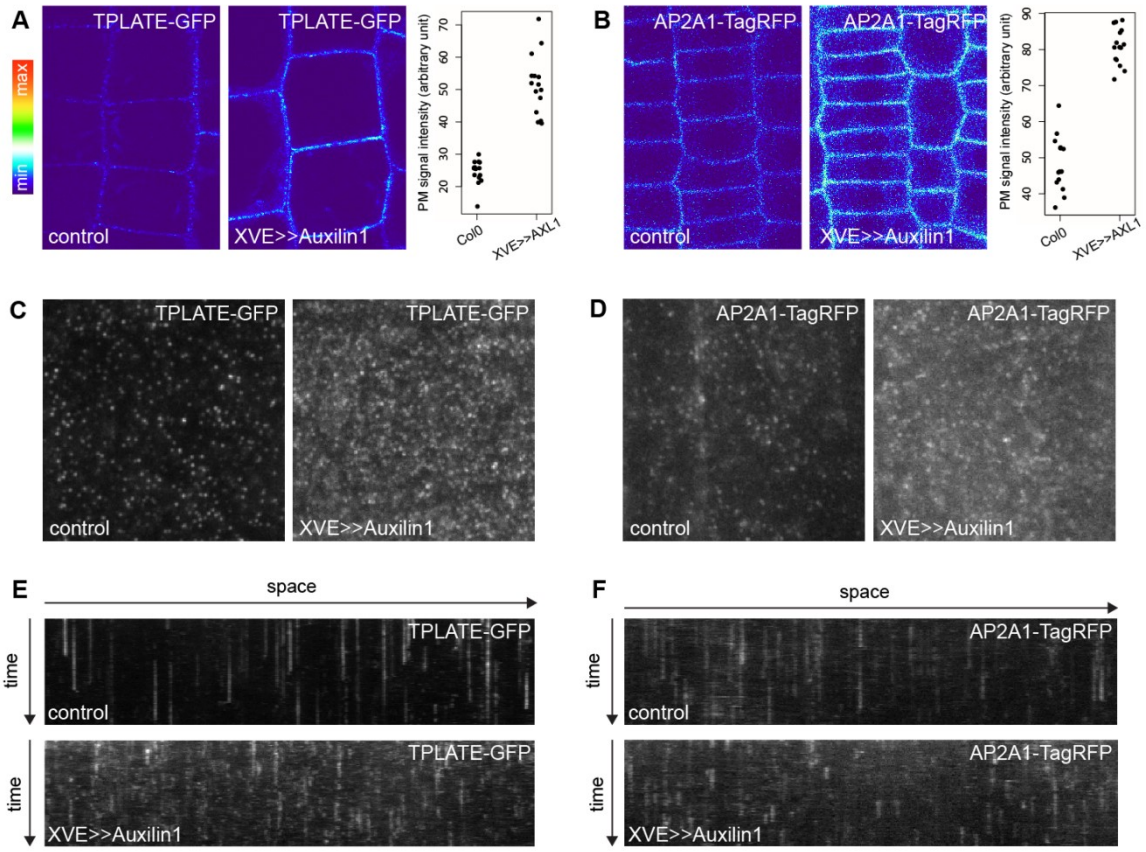

Figure 8. Elevated PM recruitment of endocytotic adaptor proteins in cells imbalanced towards secretion

(A) and **(B)** CLSM images showing an increase in PM binding of TPLATE-GFP **(A)** and AP2A1-TagRFP **(B)** binding to the PMs in the RAM epidermis of the XVE>>Auxilin1 line.

(C) and **(D)** VAEM images of TPLATE-GFP **(C)** and AP2A1-TagRFP **(D)** in the hypocotyl epidermis showing an increased density of nascent endocytotic foci in the XVE>>Auxilin1 line.

(E) and **(F)** Kymographs of VAEM time series indicating that upon Auxilin overexpression, TPLATE-GFP **(E)** and AP2A1-TagRFP **(F)** foci remain at the PM for shorter time periods than in the control.

3.3 Discussion

3.3.1 Identification of clathrin machinery components in *Arabidopsis*

Here, we aimed to extend our knowledge of the molecular machinery of CME (summarised in Zhang et al., 2015) by identifying and characterising protein-protein interactors of CLC (Figure 1). Among the CLC-binding partners, we found the ANTH family adaptor protein CAP1, which interacts with the TPLATE complex as well (Gadeyne et al., 2014). We showed that CAP1 localises to the PM and the cell plate (Figures 2A and 2E; Supplemental Movie 1), similarly to its closest homologue ETA4, which additionally stains the endosomes (Song et al., 2012). We also indentified SH3P2, a BAR and SH3-domain protein that together with its homologues SH3P1 and SH3P3 has been implicated in CME by biochemical approaches (Lam et al., 2001, 2002). Interestingly, SH3P2 has been ascribed an additional role in autophagosome formation (Zhuang et al., 2013). Our interaction data support the previously proposed function of SH3P2 in CME (Figure 1). In our VAEM experiments, SH3P2 formed relatively sparse and short-lived PM foci, suggesting that its role might be specific for a subset of endocytotic events (Figure 2F and Supplemental Movie 2), rather than being a general factor in CME. In animals, proteins with similar domain architecture are called endophilins and, interestingly, have been reported to function in a clathrin-independent endocytotic process (Renard et al., 2015; Boucrot et al., 2015).

Finally, the interaction studies revealed two proteins with C-terminal DnaJ domains that are characteristic of CCV-uncoating factors auxilins, which we therefore named Auxilin1 and Auxilin2, and which are discussed in detail below. With the exception of DHNAT2, a peroxisome-localised enzyme, our TAP experiment identified proteins with features expected of molecular factors mediating endocytosis. However, certain trafficking-related protein families are expanded in plants, such as the auxilin-like family and the ANTH/ENTH/VHS family of monomeric adaptor proteins. Thus, this work contributes to clarifying how proteins involved in trafficking functionally diverged in higher plants.

3.3.2 Auxilin1 and Auxilin2, two putative auxilin homologues in *Arabidopsis*

Our TAP approach identified two proteins with C-terminal DnaJ domain typical for auxilins and GAKs, endocytotic factors mediating the uncoating of CCVs in non-plant systems. The two paralogues share a high degree of homology, with 90% indentity in protein sequence. The corresponding genes, AT4G12780 (Auxilin1) and AT4G12770 (Auxilin2) probably arose through a recent local gene duplication event, because they occupy a common locus on the fourth chromosome of *Arabidopsis* where they are symmetrically oriented around a short promoter sequence. In the *Arabidopsis* genome, a total of seven genes code for auxilin-like proteins with C-terminally located DnaJ domains (Suetsugu et al.,

2005). While most of the genes are uncharacterized, JAC1 acts in chloroplast relocation and its function is likely unrelated to clathrin (Suetsugu et al., 2005). Previously, Auxilin1 had been isolated as an interactor of SH3P1, and its role in CCV uncoating suggested by biochemical approaches (Lam et al., 2001). Our protein-protein interaction, localisation and overexpression data strongly favour a function of Auxilin1 and Auxilin2 in the endocytotic process.

By analysing several endocytotic cargoes, we determined that overexpression of Auxilin1 or Auxilin2 inhibited CME (Figure 4), similarly to the effect of auxilin overexpression in HeLa cells (Zhao et al., 2001). Thorough examination of the endocytotic machinery by CLSM and VAEM imaging revealed a loss of clathrin and dynamin from the PMs (Figures 5 and 6), while the adaptor protein complexes AP2 and TPLATE were not only retained at the PM, but their binding was higher than in wild-type conditions (Figure 8). Thus, overexpressed Auxilins inhibited CME after the initial step of adaptor protein binding, probably by retaining clathrin in inactive cytosolic agglomerations and preventing its recruitment to the initiating endocytotic pits.

Besides acting at the PM, clathrin also localises at the TGN/EE compartment. The trafficking pathways in which TGN/EE-localised clathrin participates are far from being clarified (Robinson and Pimpl, 2014). The TGN/EE compartment in plant cells is a trafficking hub where endocytotic, secretory, and vacuolar trafficking intersects (reviewed in Park and Jürgens, 2012). Theoretically, TGN/EE-localised clathrin could mediate vacuolar and/or secretory trafficking. Few lines of evidence suggest that the activity of Auxilin could be specific for PM pool of clathrin. First, we found that Auxilin1 and Auxilin2 localise to the PM and the cell plates (Figures 2C and 2D) and interact with CAP1 and SH3P2, which are are both PM localised (Figure 1). Second, our microscopic observations of CLC2 show that Auxilin overexpression causes depletion of clathrin from the PM, while endosomal signals are retained (Figures 5A and 5B and Supplemental Movie 4), suggesting that the clathrin activity at the endosomes may be maintained upon Auxilin overexpression. Conceivably, the large, intracellular CLC2 signals observed by CLSM in the XVE>>Auxilin1 line could be representing not normal endosomes stained by CLC, but large agglomerations of clathrin bound and inactivated by Auxilin. However, these intracellular CLC2 signals in the XVE>>Auxilin1 line do become coalesced into BFA-induced bodies in a manner typical for endosomal structures (Figure 4D), indicating that they are not cytosolic protein aggregates. Furthermore, overexpressed GFP-Auxilin1 does not form large bodies reminiscing CLC2-positive endosomes, but only small mobile punctae observable by VAEM (Figures 5C and 5D; Supplemental Movie 5). Finally, it has been reported that interference with the AP-1 complex, which likely functions with clathrin at the endosomes, blocks the delivery of KNOLLE to the cell plate (Park et al., 2013). In contrast, KNOLLE could still reach the cell plate in XVE>>Auxilin lines (Figure 4E). Based on all these premises, we suggest that clathrin-

mediated processes at the TGN/EE are probably not inhibited by Auxilin overexpression. However, at present, we are unable to propose a mechanism by which overexpressed Auxilin could be specifically active towards only a sub-pool of CLC.

The inhibitory activity of overexpressed Auxilins most likely differs from that of the HUB domain, a truncated variant of CHC, the overexpression of which also blocks endocytosis (Kitakura et al., 2011). Unlike Auxilins, RFP-HUB appears to localise to endosomal compartments (Figure 1K in Kitakura et al., 2011), indicating that expression of the CHC HUB domain has an inhibitory effect also on clathrin-mediated processes at the TGN/EE. Furthermore, our thorough characterization of the endocytotic machinery upon Auxilin overexpression hints at inhibition after the adaptor protein recruitment step, distinguishing our lines from genetic tools depleting the adaptors themselves (Gadeyne et al., 2014, Di Rubbo et al., 2013; Kim et al., 2013; Bashline et al., 2013; Fan et al., 2013). Finally, the use of Tyrphostin A23 as a specific chemical inhibitor of AP2-mediated endocytosis in plant cells has been questioned (Dejonghe et al., 2016). Thus, the Auxilin-overexpressing lines presented here are well-characterised and efficient tools for endocytosis inhibition in *Arabidopsis* boasting unique characteristics.

This work was focused on characterising the effects of Auxilin overexpression and it does not provide evidence for a possible activity of these Auxilins in CCV uncoating. Considering the available data, we carefully interpret the endocytosis inhibition phenotype resulting from Auxilin overexpression as a useful artefact that results from cytosolic binding of CLC by Auxilin, rather than a phenomenon related to uncoating of clathrin. In considerations of the molecular role of Auxilin1 and Auxilin2, it is also imporant to note that the sequence similarity of these proteins to known uncoating factors is limited only to a small C-terminal stretch of the polypeptide where the HSC70-activating DnaJ domain is located. The majority of Auxilin1 and Auxilin2 sequences are not similar to known auxilin/GAK proteins from other kingdoms. Interestingly, yeast auxilin also shows very little homology to mammalian auxilins (Eisenberg and Greene, 2007). In summary, while our work strongy ties Auxilin1 and Auxilin2 to the endocytotic process, the exact molecular function of these proteins remains an open question.

3.3.3 Homeostatic regulatory mechanisms in the plant endomembrane system

Plant cells possess an intracellular trafficking system consisting of a multitude of compartments that continuously exchange membranes. The flow of membranes occurs through vesicle transport as well as maturation of compartments (e.g. Scheuring et al., 2011). In a sense, trafficking processes can be seen as “producing” the particular compartments. The various trafficking activities, which often counteract one another, seem

to operate in a perfect balance, that is, the amount of membrane building each compartment at any time is maintained at a correct level. This raises questions about potential regulatory mechanisms which, by regulating the rates of particular trafficking activities, would assure structural homeostasis of the endomembrane system at the whole cell level.

The generation and thorough characterization of Auxilin overexpressing lines, in terms of both trafficking processes and endocytotic components, allowed us preliminary insights into this issue. In particular, we were interested in potential mechanisms regulating the relative rates of secretion and endocytosis. As a consequence of endocytosis inhibition, we conditionally created an imbalance in the trafficking to and from the PM, manifested indirectly by excessive membrane accumulation at the cell periphery (Figure 7). This observation suggests that the cell does not adjust secretion to the current rate of endocytosis. Such regulation could conceivably be achieved by probing and responding to the arrival of endocytotic vesicles at the early endosomal compartments. However, with the limited available data, we do not reject the possibility that a certain level of such adjustment of secretion does exist.

On the other hand, our observations suggest an opposite regulatory process that takes place at the PM, in which the cell modulates endocytosis, seen as a “secondary” process, in order to meet the requirements imposed by secretion, a “primary” process. In XVE>>Auxilin lines, in which the endomembrane system is highly imbalanced toward secretion and in demand for endocytosis, such regulation reveals itself as elevated PM recruitment of the endocytotic adaptor proteins TPLATE and AP2 (Figure 8), which in normal conditions would lead to an upregulation of endocytic rates.

It is conceivable that such a regulatory process could be mediated by the endocytotic cargoes themselves. A change in the endo- to exocytosis ratio would result in differences in cargo accumulation at the PM, and therefore, by adaptor-cargo binding, could modulate the recruitment of endocytotic adaptors. However, this concept has to be treated with caution, as the ability of cargos to initiate endocytosis is a matter of debate (reviewed in Godlee and Kaksonen, 2013). For instance, overexpression of a classical CME cargo, the transferrin receptor, did not increase the membrane recruitment of clathrin and AP2 (Loerke et al., 2009). On the other hand, experimentally induced clustering of the receptor (distinct from its pure concentration in the PM) could promote coated pit initiation (Liu et al., 2010). Furthermore, imaging of physiological cargoes together with clathrin machinery in mammalian and yeast cells showed that cargoes, rather than initiating endocytotic sites, are recruited to pre-existing sites that originate without cargoes (Ehrlich et al., 2004; Toshima et al., 2006). The molecular mechanisms of endocytosis initiation are even less clear in plants. Very few examples of interactions between cargo and adaptor proteins have been reported so far (reviewed in Zhang et al., 2015). Therefore, mechanisms other than cargo binding

could mediate the regulation of adaptor recruitment to the PM and its coupling to secretion rates.

While our proposition regarding the control of endocytosis rates focuses on the regulation of the adaptor protein activity, further regulation of this kind could be mediated by clathrin and other associated factors. Recent in vitro experiments on unilamellar vesicles exposed to various osmotic conditions show that membrane tension can modulate clathrin polymerization and coated vesicle budding (Saleem et al., 2015). Similarly, cell biological experiments in *Arabidopsis* demonstrate that transient hyperosmotic stress causes an increase in endocytosis, while hypoosmotic conditions downregulate the process (Zwiewka et al., 2015). Conceivably, an imbalance between exocytosis and endocytosis could cause changes in the PM tension because of changing amount of the membrane. For example, insufficient endocytosis would increase the amount of membrane material at the PM, reducing tension of the lipid bilayer and thus facilitating CCV budding, leading back to homeostasis.

In addition to the morphological and molecular changes at the PM, another prominent cellular phenotype observed in Auxilin-overexpressing cells is an apparent enlargement of vacuoles in meristematic epidermal cells of the root (Figures 3B, 3C, and 5C). A change in tonoplast area could be indicative of an imbalance in the trafficking between the vacuole and earlier compartments, in analogy to the observations at the PM. While superficially the vacuole enlarges, its transition from a complex, convoluted architecture typical for the wild type (e.g. Nováková et al., 2014) into a more rounded shape with a lower surface-to-volume ratio (Figures 3C and 5C) makes it challenging to evaluate how the surface area (i.e., the amount of membrane) actually changes. Nevertheless, as discussed above, there are indications that Auxilin overexpression does not interfere with endosomal clathrin activity which is probably responsible for vacuolar trafficking. In summary, we are unable to propose an interpretation of the observed vacuole morphology in terms of alterations in endomembrane trafficking processes.

In summary, this work extends our knowledge of the endocytotic machinery in *Arabidopsis* and provides a powerful and well-characterised tool for inhibition of endocytosis. With the observations made in Auxilin-overexpressing lines, we point out the idea of homeostatic control of endomembrane trafficking processes and propose initial models of regulation acting between endo- and exocytosis. Future work, in independent experimental systems, is necessary to evaluate these hypotheses and to broaden our understanding of how the endomembrane system maintains its structural and functional integrity. With these concepts, we wish to underline that trafficking processes do not act separately but are all interrelated, and thus highlight the need for a holistic view on the endomembrane system in future studies.

3.4 Materials and methods

3.4.1 Plant material

The previously published lines were used: UBQ10::SH3P2-GFP (Zhuang et al., 2013), PIN2::PIN2-GFP (Abas et al., 2006), CLC2::CLC2-GFP, DRP1C::DRP1C-GFP (Konopka and Bednarek, 2008), pINTAM::GAL4 (Friml et al., 2004), DR5::GFP (Benková et al., 2003), and TPLATE-GFP x AP2A1-TagRFP (Gadeyne et al., 2014). The lines generated and used in this study: XVE>>Auxilin1, XVE>>Auxilin2, XVE>>Auxilin1×CLC2::CLC2-GFP, XVE>>Auxilin1×DRP1C::DRP1C-GFP, XVE>>Auxilin1×TPLATE-GFP, XVE>>Auxilin1×AP2A1-TagRFP, XVE>>Auxilin2×PIN2::PIN2-GFP, XVE>>Auxilin1×DR5::GFP, XVE>>Auxilin2×DR5::GFP, CAP1::CAP1-mCherry, 35S::CAP1-RFP, 35S::SH3P2-GFP, 35S::RFP-Auxilin1, 35S::RFP-Auxilin2, and INTAM>>GFP-Auxilin1. UAS::GFP-Auxilin1 is also available on request. We regret to inform that seeds of 35S::RFP-Auxilin lines are not available due to low yields and high degree of silencing, but expression vectors for plant transformation can be provided instead.

3.4.2 Seedling growth conditions

Seedlings of *Arabidopsis thaliana* (L.) Heynh. were grown on ½MS medium with 1% (w/v) sucrose at 21°C in a 16-h/8-h day/night cycle, or in darkness for imaging of hypocotyls. Estradiol induction of the XVE>>Auxilin lines was done by transferring 3-day-old seedlings to media containing 2.5 µg/ml β-estradiol (Sigma-Aldrich) or solvent (ethanol) as a control. Induction of the INTAM>>GFP-Auxilin1 line was done analogously on media supplemented with 5 µM tamoxifen (Sigma-Aldrich).

3.4.3 Seedling morphology

For light microscopy of the XVE>>Auxilin seedling roots, seedlings were stained in Lugol's solution for approximately 1 min, washed, and mounted on slides in chloral hydrate solution.

3.4.4 Molecular cloning

All constructs used for TAP, for generation of stable *Arabidopsis* transgenic lines, and for BiFC assays were cloned with the Gateway system. The following Gateway entry clones were generated in this study: CLC1/pDONR221, Auxilin1/pENTR/D-TOPO, Auxilin2/pENTR/D-TOPO, CAP1/pENTR/D-TOPO, SH3P2/pENTR/D-TOPO (all in variants with and without stop codons), PIP5K1/pDONR221, Auxilin1/pDONRP2rP3, pCAP1/pDONRP4P1r. Auxilin2/pDONRP2rP3 was also generated, but not used, and is available on request. Coding sequences of CLC1, Auxilin1, Auxilin2, and CAP1 were cloned from *Arabidopsis* (accession

Columbia 0) cDNA, whereas those of SH3P2 and the CAP1 promoter from the *Arabidopsis* Col0 genomic DNA with the following primers:

construct	F primer	R primer (with stop)	R primer (without stop)
Auxilin1/pENTR	CACCATGGATGATTTCACAGGATTGTT	TCAGAAGAGTTCTTCTGAGTTAAAC	GAAGAGTTCTTCTGAGTTAAACTTG
Auxilin2/pENTR	CACCATGGATGATTTCACAGGATTGTT	TCAAAAGAGTTCCTCTGAGTTGAAT	AAAGAGTTCCTCTGAGTTGAATTTG
CAP1/pENTR	CACCATGGCGCTAAGCATGCGA	TCAGTAAGGGTTGTTGTAGTAATAACC	GTAAGGGTTGTTGTAGTAATAACC
SH3P2/pENTR	CACCATGGATGCAATTAGAAAACAAGC	TCAGAAAACTTCGGACACTTTG	GAAAACTTCGGACACTTTGCTA
Auxilin1/pDONRP2rP3	GGGGACAGCTTTCTTGTACAAAGTGGCCATGGATGATTTCACAGGATTGTT	GGGGACAACTTTGTATAATAAAGTTGGTCAGAAGAGTTCTTCTGAGTTAAAC	–
Auxilin2/pDONRP2rP3	GGGGACAGCTTTCTTGTACAAAGTGGCCATGGATGATTTCACAGGATTGTT	GGGGACAACTTTGTATAATAAAGTTGGTCAAAAGAGTTCCTCTGAGTTGAAT	–
CLC1/pDONR221	GGGGACAAGTTTGTACAAAAAAGCAGGCTCGATGGCGACTTTTGATGATGGAG	GGGGACCACTTTGTACAAGAAAGCTGGGTTTCACTCCGCCTTGGTTCCCTCGGCC	GGGGACCACTTTGTACAAGAAAGCTGGGTTCTCCGCCTTGGTTCCCTCGGCC
PIP5K1/pDONR221	GGGGACAAGTTTGTACAAAAAAGCAGGCTATGAGTGATTCAGAAGAAGA	–	GGGGACCACTTTGTACAAGAAAGCTGGGTGCCCTCTTCAATGAAGA
pCAP1/pDONRP4P1r	GGGGACAACTTTGTATAGAAAAGTTGggataggcgttcaaatcgg	GGGGACTGCTTTTTTGTACAAACTTGgattccactactacttaaggattcgaa	

The expression vectors generated were cloned with previously published Gateway vectors (Karimi et al., 2002; Barbez et al., 2012; Van Leene et al., 2014). Constructs for TAP were generated by fusing CLC1 with TAP tags and with 35S promoter sequences in pKCTAP and pKNTAP destination vectors to obtain C- and N-terminal fusions of CLC1 with the tag. The following vectors were cloned and used for stable transformation of *Arabidopsis*: XVE>>Auxilin1 (pMDC7B(UBQ10)), XVE>>Auxilin2 (pMDC7B(UBQ10)), 35S::RFP-Auxilin1 (pK7WGR2), 35S::RFP-Auxilin2 (pK7WGR2), 35S::SH3P2-GFP (pH7FWG2), 35S::CAP1-RFP (pK7RWG2), pUAS::GFP-Auxilin1 (pK7m34GW), and CAP1::CAP1-mCherry (pK7m34GW). The constructs used for BiFC assays were cloned in p*7m34GW and p*7m24GW backbones (where * indicates various resistance cassettes not relevant for these constructs) and

consisted of fusions of N- and C-terminal parts of EGFP fused to CLC1, Auxilin1, Auxilin2, CAP1, SH3P2, and PIP5K1 and under the control of the 35S promoter.

3.4.5 Tandem Affinity Purification

TAP with CLC1 as bait was carried out as described previously (Van Leene et al., 2014) with *Arabidopsis* cell cultures. The cloning procedure for TAP constructs is described above.

3.4.6 Fluorescent imaging

CLSM imaging was done with a Zeiss LSM700 confocal microscope with Plan-Apochromat 20x/0.8 and Plan-Apochromat 40x/1.2 lenses. VAEM imaging was carried out with an Olympus IX83 inverted microscope equipped with a Cell^TIRF module and UAPON OTIRF 100× lens.

3.4.7 Immunostaining

An Intavis InsituPro VSi robot was used for immunostaining according to the previously published protocol (Sauer et al., 2006). The following antibodies were used: anti-PIN1, anti-PIN2, anti-KNOLLE, and Anti Rabbit-Cy3 (Sigma-Aldrich).

3.4.8 BiFC assays

For BiFC assays, leaves of *Nicotiana benthamiana* were used and transiently transformed with *Agrobacterium tumefaciens.* The *Agrobacterium* strains carrying the BiFC constructs were grown to OD=1, spun down, and resuspended in an infiltration buffer (10 mM $MgCl_2$, 10 mM MES, 100 µM acetosyringone) to OD=1.5. The suspensions were incubated at room temperature on a shaker for 2 h. Strains carrying the two assayed constructs were mixed and injected into the bottom side of leaves. Leaves were imaged by CLSM 3-4 days after injection.

3.4.9 BFA treatments

Seedlings were incubated in liquid ½MS medium with 1% (w/v) sucrose and containing Brefeldin A (Sigma-Aldrich) at a final concentration of 25 µM. The solvent (DMSO) was added to controls.

3.4.10 FM4-64 staining

Seedlings were stained in liquid ½MS medium with 1% (w/v) sucrose supplemented with 2 µM FM 4-64 dye (ThermoFisher) for 5 min, in the dark and on ice. Excess dye was washed out in ½MS medium and seedlings mounted on microscopy slides at room temperature, marking the start of the internalization time measurement.

3.4.11 Accession numbers

The *Arabidopsis* genes mentioned in this paper are: Auxilin1 (AT4G12780), Auxilin2 (AT4G12770), CAP1 (AT4G32285), SH3P2 (AT4G34660), CLC1 (At2g20760), CLC2 (At2g40060), DRP1C (AT1G14830), KNOLLE (AT1G08560), PIN1 (AT1G73590), PIN2 (AT5G57090), TPLATE (AT3G01780), AP2A1 (At5G22770), and PIP5K1 (AT1G21980).

3.5 Supplementary figures

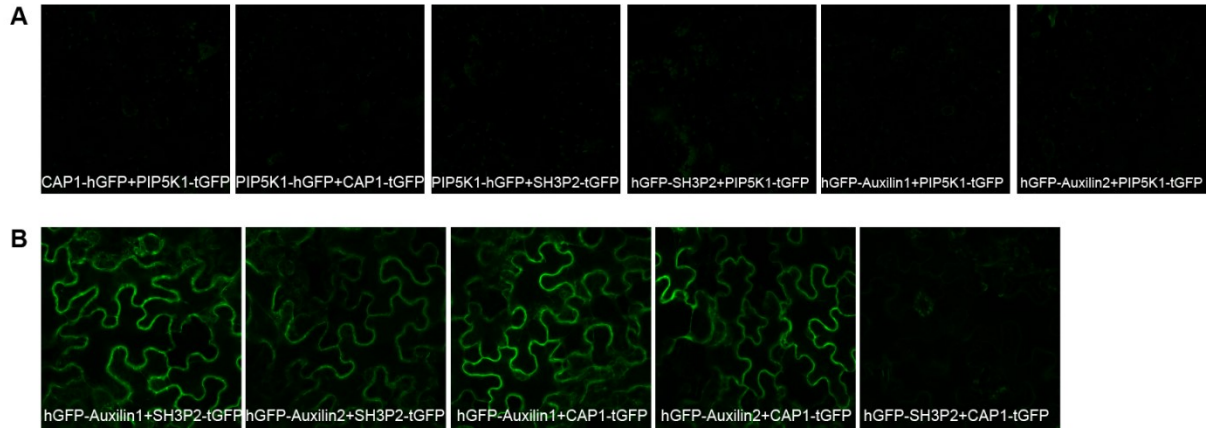

Supplementary Figure 1. Additional BiFC interactions.

(A) Lack of GFP fluorescence upon coexpression of any CLC1 interactor with PIPK51.

(B) BiFC interactions among selected CLC1 interactors. No interaction was detected between SH3P2 and CAP1 (rightmost panel).

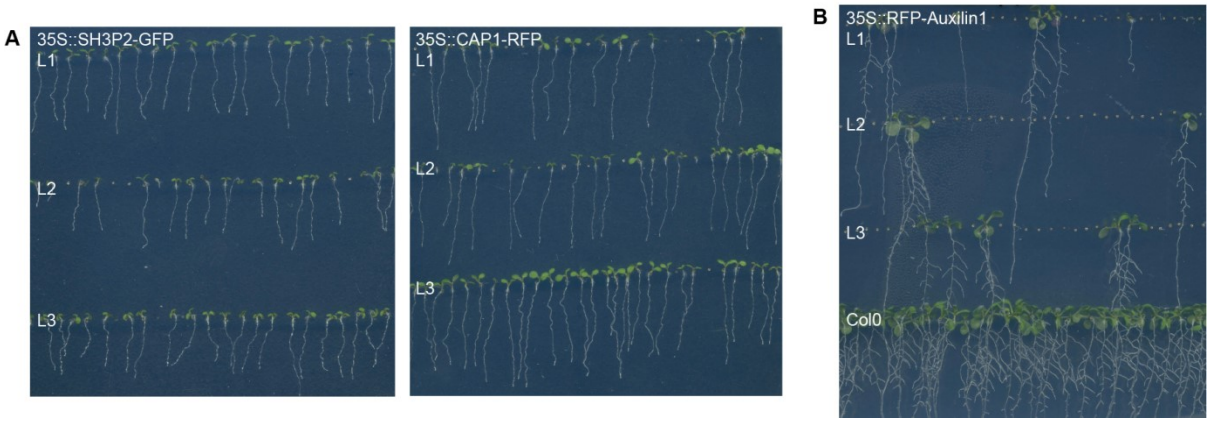

Supplementary Figure 2. Growth and development in lines constitutively overexpressing Auxilin1, SH3P2, and CAP1.

(A) Normal seed germination and growth in 35S::SH3P2-GFP and 35S::CAP1-RFP lines.

(B) Germination arrest in segregating T2 populations of 35S::RFP-Auxilin1 lines.

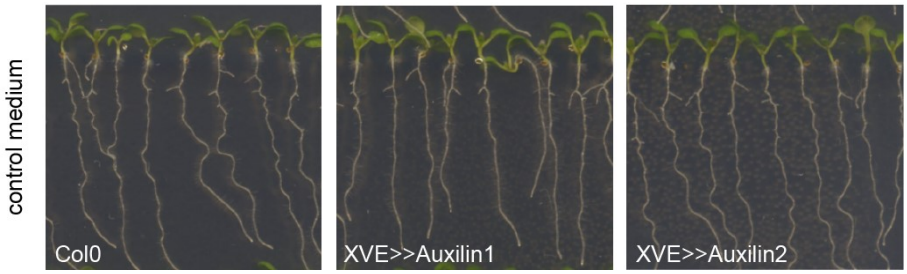

Supplementary Figure 3. Noninduced controls for seed germination experiments with XVE>>Auxilin lines.
Normal germination of XVE>>Auxilin seedlings on control medium.

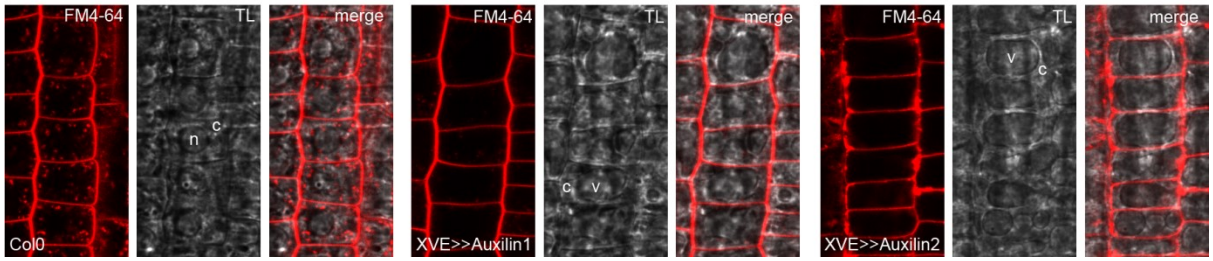

Supplementary Figure 4. FM4-64 uptake into XVE>>Auxilin root epidermis.
Comparison of FM4-64 fluorescence and transmitted light channel showing areas of cytosol with faint or absent staining of endosomes in the Auxilin-overexpressing lines. V, vacuole; n, nucleus; c, cytoplasm.

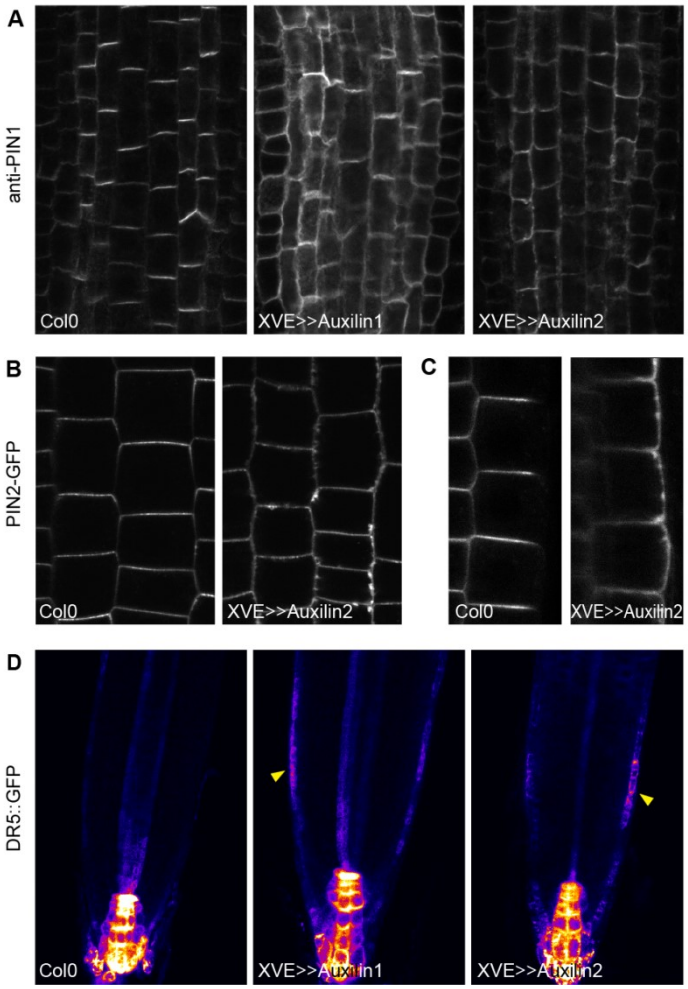

Supplementary Figure 5. Inhibition of endocytosis by Auxilin overexpression affecting PIN protein polarity and auxin transport in the RAM.
(A) Immunolocalisation of PIN1 in the central cylinder showing depolarization of PIN1 in the XVE>>Auxilin lines.
(B) and (C) Depolarisation of PIN2-GFP in the epidermis in the XVE>>Auxilin2 background. Longitudinal sections showing lateral (B) and inner-outer (C) cell sides.
(D) Auxin response maxima visualised with DR5::GFP. Arrowheads indicate additional DR5::GFP signals in lateral root caps of XVE>>Auxilin seedlings.

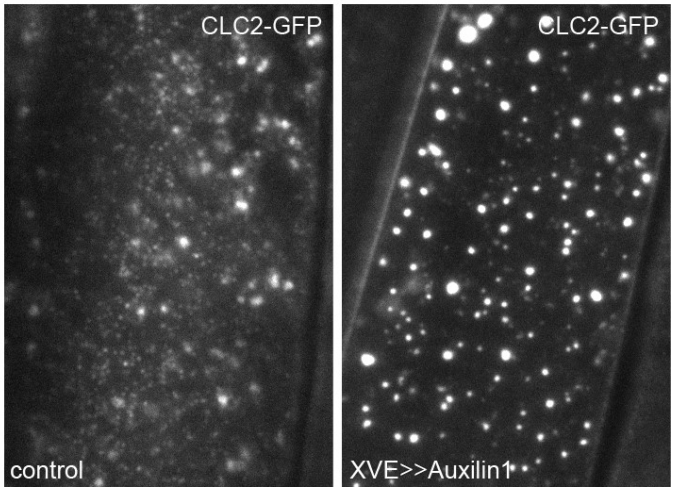

Supplementary Figure 6. Numerous, large intracellular CLC2 agglomerations rarely observed in the XVE>>Auxilin1 hypocotyl epidermis.
VAEM images show numerous large agglomerations of CLC2-GFP signals which were rarely observed in the hypocotyl epidermis upon Auxilin1 overexpression.

3.6 External contributions

The Tandem Affinity Purification experiment has been performed by Dr Urszula Kania in collaboration with the lab of Prof. Geert De Jaeger at Plant Systems Biology Department of VIB in Ghent.

Split GFP constructs for PIP5K1 were cloned by Anna Mueller.

4 Cortical microtubule arrays reorient in response to growth, and not auxin signaling, in the *Arabidopsis* hypocotyl epidermis

4.1 Introduction

In interphase plant cells, microtubules are localized just underneath the cell membrane where they are organized into well-aligned arrays. In elongating epidermal cells, such as those in roots, hypocotyls or coleoptiles, cortical microtubule arrays under the outer plasma membrane have an ability to reorient in relation to the long cell axis. These reorientations have been linked to cell growth rates: growing cells typically exhibit microtubules transverse to the long cell axis, and cells that ceased growth exhibit longitudinally oriented microtubules (Fischer and Schopfer, 1997). With the advent of long-term live imaging, greater complexity of array orientations has been revealed: in light-grown hypocotyls, microtubule arrays are only stably transverse in cells growing at high rates, while slower growth corresponds to slow, rotary movement of the arrays (Chan et al., 2007, 2011; Chan, 2012).

Growth-regulating internal and external signals, such as light and certain hormones, chief among them auxin, have been suggested to mediate these microtubule reorientations (summarized in Fischer and Schopfer, 1997). Because of the commonly observed correlation between growth states and microtubule orientations, early on a hypothesis was put forward where the reorientation of microtubules was part of the mechanism of growth activation and inhibition. This hypothesis has been rejected by a majority of subsequent studies (Shibaoka, 1994). Instead, a broadly accepted model proposes that the function of ordered cortical microtubule arrays is in defining growth directionality (anisotropy) rather than growth rate (Baskin, 2001). The so-called “alignment hypothesis” states that microtubules help define the trajectory of CESA complexes, thus being instructive for the alignment of cellulose microfibrils (Paredez et al, 2006). Cellulose microfibrils, as rigid structural elements aligned transversely to the cell axis would prevent isotropic swelling of the cell in response to non-directionally acting turgor pressure, while allowing cell elongation along its long axis. This microtubule-cellulose relationship is possible due to the physical linkage between microtubules and cellulose synthase (CESA) complexes docked in the plasma membrane, which is mediated by CSI1 (Li et al., 2012; Lei et al., 2012; Bringmann et al., 2012)

Under this model, where the reorientation of microtubule arrays is a phenomenon coexisting with growth for the purpose of controlling cell wall architecture and growth anisotropy in the long term, it becomes interesting to scrutinize the commonly held view that growth-regulating factors like light or auxin regulate microtubule array reorientations. Since those factors regulate both growth and CMT orientation, a simpler solution can be

considered wherein growth is the only process controlled by these signaling factors, while the changes in CMT orientation are merely responses to the growth itself instead of being specific downstream effects of light or hormonal signaling. Such considerations have been put to test with experiments in various model systems such as maize coleoptiles, azuki bean epicotyls or sunflower cotyledons, which often used tropic responses, or mechanical bending of plant organs as experimental cases of differential growth. Fisher and Schopfer (1998) studied CMT orientation in gravi- or photostimulated maize coleoptiles which were forcibly bent in a direction opposite to that imposed by the tropic stimulus. The authors asked whether CMTs on upper and lower sides of the coleoptile in fact respond to the tropic stimuli (and implicitly, differential auxin concentrations), or rather to the cell deformation that results from organ bending. In their experiments, CMTs aligned according to the imposed deformation, and not to the opposite tropic stimulus, indicating that it is the actual change of cell shape that determines CMT orientation, and not the sensing of tropic stimuli or sensing of auxin. A similar experiment was performed on azuki bean epicotyls with comparable results (Ikushima and Shimmen 2005). Burian and Hejnowicz attempted to observe such cell deformation-dependent CMT reorientations in epidermal peels isolated from sunflower hypocotyls that were stretched by external forces, but unsuccessfully (Burian and Hejnowicz 2010) unless fusicoccin, a growth-activating drug acting similarly to auxin, was additionally applied (Burian and Hejnowicz 2011).

Therefore, there is evidence that reorientation of microtubules in elongating cells, such as those on the extending side of a tropically bending organ, is in fact a secondary result of cell elongation, rather than a process primarily controlled by auxin accumulation and signaling. However, Himmelspach and Nick (2001) report that a transverse-to-longitudinal CMT reorientation can be observed on the upper side of a gravistimulated maize coleoptile that is mechanically prevented from bending, indicating a CMT reorientation mechanism independent of growth and instead related to perception of tropic stimuli, presumably related to auxin concentration. Furthermore, azuki bean epicotyl segments placed under anaerobic conditions, where their growth is inhibited, still exhibit transverse CMTs when treated with auxin, demonstrating the ability of auxin to cause CMT reorientation independently of growth (Takesue and Shibaoka 1999).

Thus, the relationship between auxin, the activation or inhibition of growth, and the reorientation of cortical microtubule arrays has been a matter of much debate. We revisit this problem with a set of experiments in the modern-day experimental system of choice for plant biologists, *Arabidopsis thaliana*. We study the processes taking place in the elongating cells of the hypocotyl, where auxin causes promotion of growth and reorientation of microtubules towards transverse arrays.

4.2 Results

4.2.1 Auxin-induced reorientation of cortical microtubules in isolated hypocotyls of *Arabidopsis*

Throughout this study, we used 3 day old, dark-grown hypocotyls of *A.thaliana*. These hypocotyls were separated from the apical part of the seedling and the root (Figure 1A; Takahashi et al., 2012; Fendrych et al., 2016). Upon separation from the apical auxin source, the hypocotyls become depleted from endogenous auxin and cease growth within approximately 30 minutes. Consequently, growth can be experimentally controlled by external application of auxin.

We first tested the applicability of isolated hypocotyls for studies of the auxin- and growth-related microtubule reorientations. Cortical microtubule arrays were visualized with GFP-MAP4 microtubule marker line (Marc et al., 1998) using CLSM (confocal laser scanning microscopy). We imaged MTs in the outer domain of epidermis of the subapical region of the hypocotyl that undergoes rapid growth in 3 day old hypocotyls (red rectangle in Figure 1A). In all experiments, microtubule arrays were categorized, on a single-cell basis, into longitudinal, oblique and transverse, based on the predominant orientation of the microtubules in relation to the long cell axis (see Supplementary Figure 1 for examples). Cells in which microtubules were disordered, or in which multiple orientations could be observed with similar contribution, belong to the fourth category of random arrays. All microscopic pictures captured in an experiment were put together and randomized before scoring array orientations in order to reduce experimenter's bias.

In agreement with similar experiments performed in other plant species, in auxin-depleted, non-growing hypocotyls, cortical microtubules were predominantly longitudinal (Figure 1B). Application of auxin (indole-3-acetic acid, IAA) triggered growth and lead to a gradual reorganization of microtubules into oblique and transverse arrays over a course of 1 hour (Figure 1B). A relatively high dose of 10 µM IAA was used in order to elicit robust, clear growth and microtubule reorientation responses. In conclusion, our experimental system allows a precise control over auxin signaling and growth and offers clear-cut cortical microtubule array reorientations.

Interference with auxin signaling by expressing a dominant-negative variant of an auxin signaling component AXR3 (HS::*axr3-1)* or by blocking protein translation with cycloheximide (CHX) abolished the auxin-induced MT reorientation (Figure 2A and B). Thus, both growth (Fendrych et al., 2016) and the associated MT reorientation in the hypocotyl epidermis rely on the TIR-dependent auxin signaling pathway.

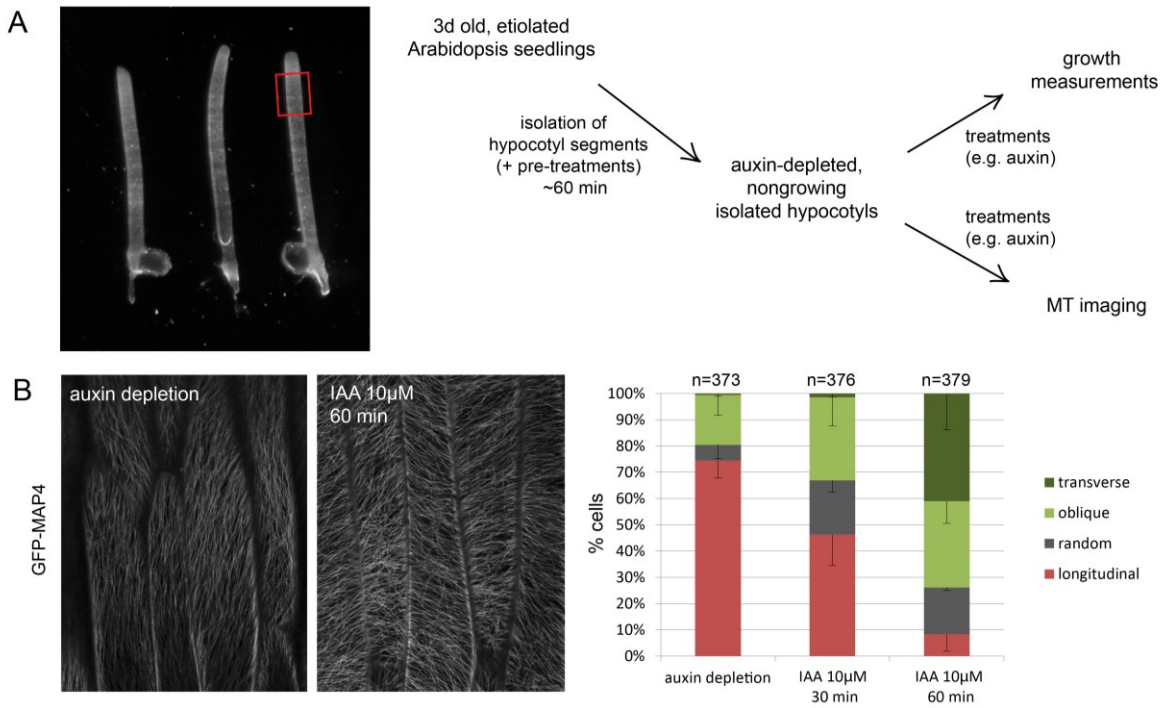

Figure 1. Auxin-induced reorientation of cortical microtubules in isolated hypocotyls of Arabidopsis

(A) An overview of the experimental setup used throughout this study. Hypocotyls were isolated from 3d old, etiolated Arabidopsis seedlings. Depletion of endogenous auxin and resulting cessation of growth was allowed within following time of approx. 1 hour. If necessary, chemical pre-treatments were applied during this period. Hypocotyls were then transferred to treatment media (e.g. containing auxin) and imaged by CLSM, typically after 1 hour of treatments, or placed in a flatbed scanner for growth measurements. Isolated hypocotyls are shown on the left, with a red rectangle depicting the subapical region that actively grows in 3d old hypocotyls, where orientations of MTs were scored.

(B) Auxin (IAA, 10 µM) causes efficient reorientation of cortical MTs from longitudinal into oblique and transverse arrays in the outer faces of hypocotyl epidermis in isolated hypocotyls. Cells were scored into four categories based on the prevalent type of MT array observed. Average percentage from three experiments is shown. Error bars indicate standard deviation of cell percentages between three experiments.

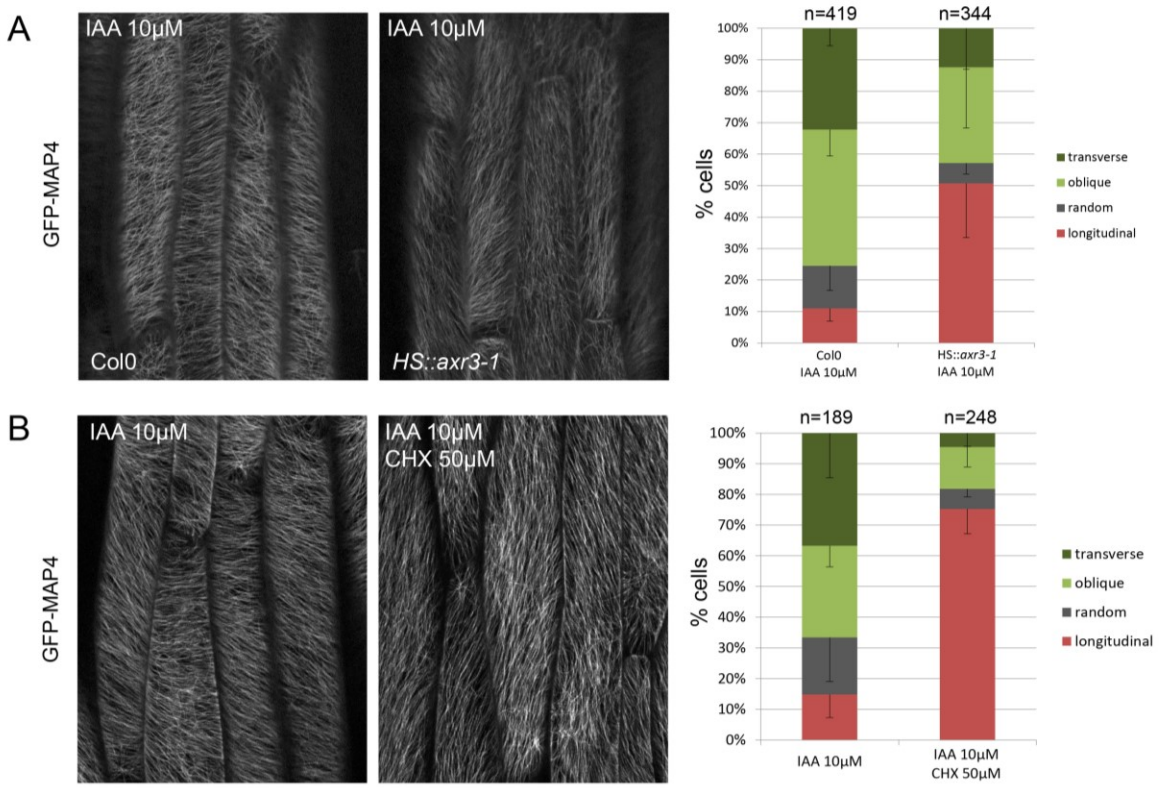

Figure 2. MT reorientation in hypocotyl epidermis depends on the nuclear auxin signaling pathway.
Inhibition of nuclear auxin signaling by a conditional expression of a dominant-negative mutant of AXR3 (HS::axr3-1) (A), or by blocking protein translation with cycloheximide (CHX, 50μM) (B) prevents auxin-induced reorientation of cortical MTs. The average % of cells with different array categories from three experiments are shown. Error bars indicate standard deviation of percentages between three experiments.

4.2.2 Considered scenarios for the relationship between auxin signaling, cell growth, and cortical microtubule orientations in elongating hypocotyl cells

We initially considered three scenarios for the relationship between auxin, the promotion of growth, and the reorientation of cortical microtubules. In the first scenario, auxin signaling triggers the reorientation of microtubules into transverse arrays, and this reorientation, by an unknown mechanism, leads to a downstream activation of growth (Figure 3A, referred to as model A). As discussed in the introduction, mechanisms in which auxin regulates growth rates through its effect on microtubule array orientation were considered and rejected by majority of studies, but we still included this possibility in an effort to provide a comprehensive and clear study of the problem. In the second scenario, auxin simultaneously triggers two distinct and independent signaling pathways leading to two separable outcomes: first, the activation of cell growth, and second, the reorientation of microtubules into transverse arrays (Figure 3B, referred to as model B). This scenario, although not necessarily formulated in these precise terms, is equivalent to that assumed by

workers who propose the ability of auxin to reorient microtubules, while recognizing the auxin effect on growth explained by mechanisms unrelated to microtubules, in particular by the acid growth theory encompassing, as drivers of growth, the acidification and loosening of cell walls on the one hand, and the action of turgor pressure on the other. Finally, the third scenario poses that the only direct outcome of auxin signaling under consideration is the activation of cell growth, while the reorientation of cortical microtubules into transverse arrays is not controlled by auxin signaling *per se*, but is a downstream consequence of the highly anisotropic growth (elongation) of the epidermal cells (Figure 3C, referred to as model C). In this scenario, in contrast to the previous two, it can be said that auxin does not reorient microtubules. The reorientation of microtubules under model C is mediated by signals associated with growth, whose nature could be, for example, mechanical.

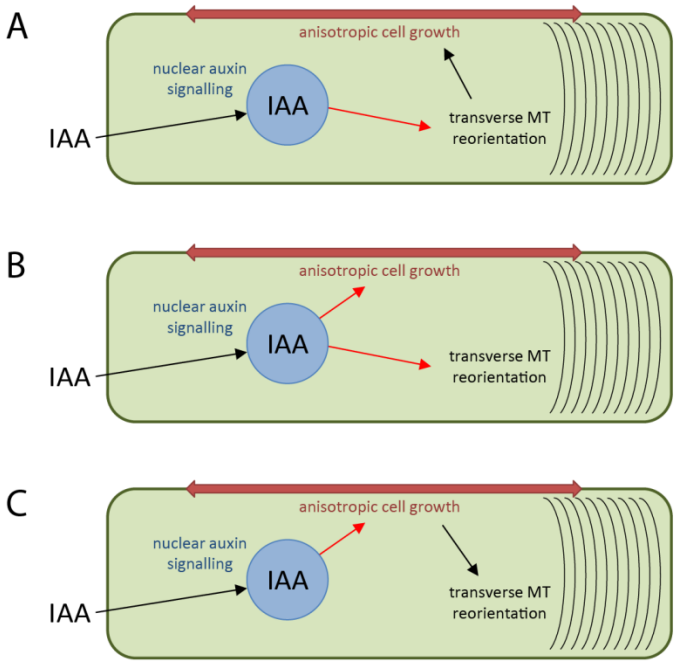

Figure 3. Considered scenarios for the relationship between auxin, cell growth, and cortical microtubule orientations in elongating hypocotyl cells
(A) Auxin triggers reorientation of MTs into transverse arrays; this reorientation is a necessary part of a mechanism activating growth
(B) Auxin triggers cell growth and the reorientation of MTs by two distinct signaling pathways; both these pathways are active in elongating cells of the hypocotyl
(C) Auxin solely triggers cell growth; the reorientation of MTs into transverse arrays is not caused by auxin signaling, but is a downstream consequence of the anisotropic growth of hypocotyl epidermal cells

4.2.3 Microtubules are not required for auxin-mediated activation of hypocotyl growth

First, we addressed the scenario in which auxin signaling triggers the reorientation of microtubules towards transverse arrays, and by doing so, activates growth (model A). A prediction of this scenario is that upon disruption of microtubules, auxin will be unable to trigger hypocotyl growth. In contrast, the remaining scenarios predict that auxin will be able to trigger growth in the absence of functional microtubules, since in these cases the reorientation of microtubules is either independent from (model B), or downstream of, growth (model C). We treated the hypocotyls with the microtubule-disrupting drug oryzalin and subsequently applied auxin in an attempt to trigger growth. Oryzalin was applied at a

high dose (100 µM) during a 1-hour pre-treatment to assure an efficient depolymerisation of microtubules (Figure 4A) before auxin is applied. We found that disruption of microtubules did not interfere with auxin-triggered growth of hypocotyls after 1 h of auxin treatment (Figure 4B), leading to the conclusion that microtubules are not necessary for the promotion of growth by auxin.

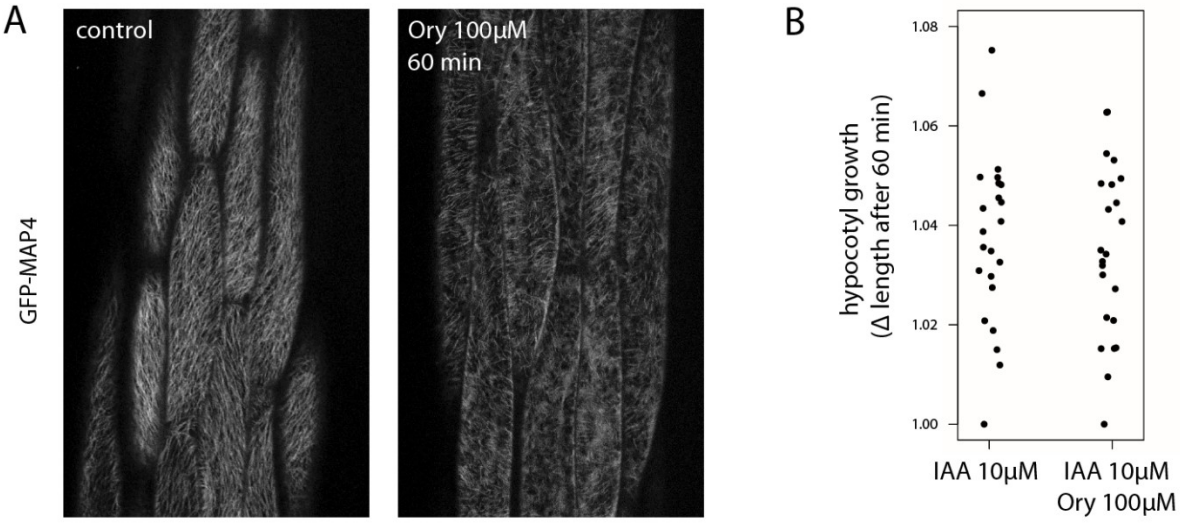

Figure 4. Microtubules are not necessary for the promotion of hypocotyl growth by auxin

(A) Confirmation of oryzalin effectivity on Arabidopsis hypocotyl segments. A majority of microtubules are disrupted after 60 mintues of oryzalin (100 µM) treatment throughout the hypocotyl length.

(B) Measurement of elongation of isolated hypocotyls after 1 hour of auxin treatment (IAA, 10µM) upon disruption of microtubules by oryzalin (100 µM). Disruption of microtubules did not interfere with auxin-induced growth. Oryzalin was applied as a pre-treatment for 60 min as well as during subsequent auxin-induced growth. The graph shows collated growth measurements from three experiments, each data point representing one hypocotyl.

4.2.4 Microtubule array reorientation triggered by auxin depends on the presence of growth

The result above supports the long-standing notion that microtubules are not a crucial part of the mechanism by which auxin regulates cell growth. The reorientation of microtubules by auxin is rather an accompanying phenomenon, necessary not for the activation of growth, but rather for the regulation of growth directionality in the long term due to the influence on the cell wall structure. However, a more interesting question can be asked next: is auxin at all responsible for the reorientation of microtubules towards transverse arrays in elongating cells, as is commonly believed? Or is auxin signaling responsible solely for activating cell growth, while the reorientation of microtubules is just a consequence of the growth, and not a “prescribed” auxin response? To address these

questions, we attempted to limit or inhibit the auxin-induced growth of hypocotyls, while maintaining auxin signaling, and observe whether microtubules still reorient efficiently. Under model B, where auxin causes reorientation of microtubules as a dedicated, separate signaling pathway distinct from that which triggers growth, microtubules will still be reoriented. In contrast, under model C, microtubules will not reorient as efficiently when auxin-induced growth is limited, because the reorientation is not due to auxin signaling, but due to the growth itself.

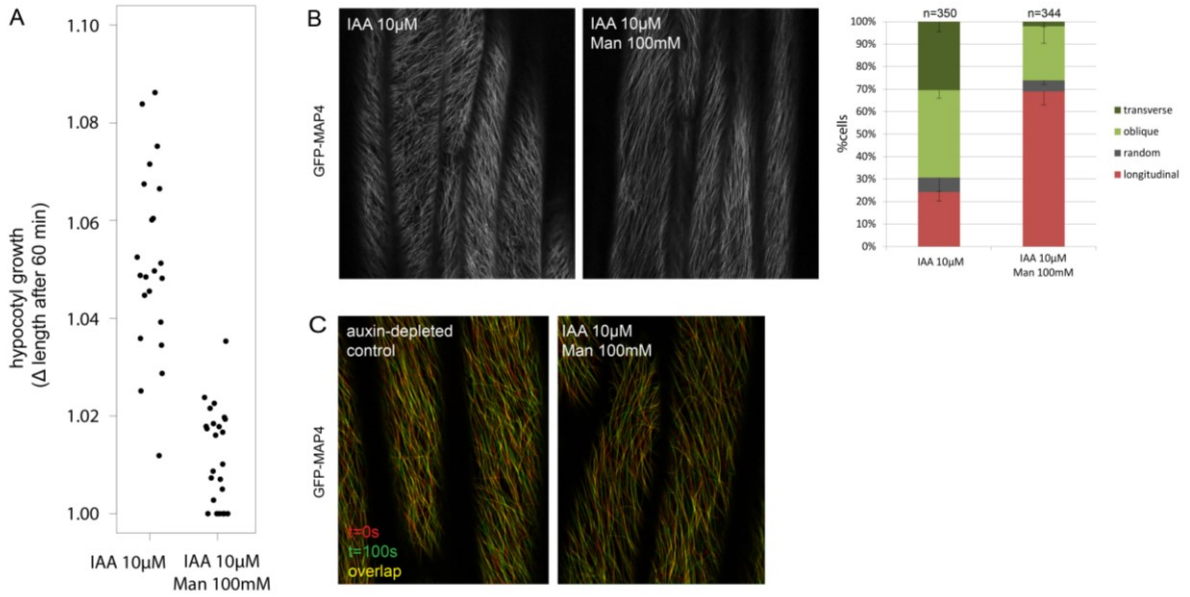

Figure 5. MT reorientation triggered by auxin depends on growth

(A) Inhibition of auxin-induced growth of hypocotyl segments. Increased osmolarity brought about by addition of 100mM mannitol (Man) to the medium lead to a reduction of growth rates of hypocotyl segments. The graph shows collated growth measurements from three experiments, each data point representing one hypocotyl.

(B) Auxin-induced reorientation of MTs into transverse arrays depends on growth. In auxin-treated hypocotyls which are prevented from growing by mannitol, MTs do not efficiently reorient towards transverse arrays, demonstrating that the reorientation of MTs is not directly caused by auxin signaling, but is rather a consequence of growth triggered by auxin. The average percentages of cells with different MT array categories from three experiments are shown. Error bars indicate standard deviation of cell percentages between three experiments.

(C) Mannitol does not interfere with the dynamic behaviour of MTs. Two frames, 100 seconds apart, are shown by red and green colours. See also Supplementary Movie 1.

In the acid theory of plant cell growth, growth happens as a result of internal hydrostatic pressure of the vacuole and cytoplasm overcoming the mechanical resistance of the cell wall. In an attempt to reduce growth, we employed a mild increase in osmotic conditions by the addition of 100 mM mannitol to the medium in order to counteract the uptake of water and the build-up of turgor. Indeed, hypocotyls placed on mannitol-

supplemented medium showed a clear reduction of growth (Figure 5A). We observed that in these hypocotyls, microtubules did not reorient into transverse arrays as efficiently as in rapidly growing controls, but instead retained mostly longitudinal orientations (Figure 5B). This result clearly shows that the reorientation of microtubules by auxin is not a distinct auxin response that is still active when growth is limited, but instead, is a phenomenon depending on the presence of growth. Thus, this result argues for model C, and against model B. In a control experiment, we assured that under the mannitol treatment, the longitudinally oriented microtubules retain their normal dynamics (Figure 5C), demonstrating that those microtubule arrays are fully capable of reorientation, but are only lacking the trigger to do so.

4.2.5 Growth without auxin signaling is sufficient to reorient microtubules into transverse arrays

The results above strongly argue for the scenario where the reorientation of microtubules is a downstream consequence of the growth triggered by auxin (model C), and not an independent auxin response. To confirm that this growth-associated reorientation of microtubules indeed does not require auxin signaling, we aimed to trigger hypocotyl growth in the absence of auxin and observe whether microtubules reorient. We utilized fusicoccin (FC), a fungal toxin that causes hyperactivation of PM-ATPases and triggers auxin-like growth, but without the activation of auxin signaling (Fendrych et al., 2016). FC caused rapid elongation of hypocotyls, as previously described (Figure 6A). In these growing hypocotyls, after 1 h of FC treatment, microtubules were reoriented to transverse and oblique arrays (Figure 6B), demonstrating directly that growth without auxin signaling leads to the reorientation of microtubules. This finally confirms model C, in which the action of auxin in growing hypocotyls is to activate growth, while the reorientation of MTs is an indirect effect (Figure 3C).

From this it can be inferred that the experimental inhibition of auxin signaling (Figure 2A and B) prevented MT reorientation indirectly, due to the lack of auxin-induced growth. In contrast, MT reorientation was achieved in CHX-treated and HS::*axr3-1* hypocotyls that were successfully triggered to grow by FC (Figure 6C, Supplementary Figure 2; see Fendrych et al. 2016 for relevant growth charts). The observation that growth-induced MT reorientation was not prevented by CHX (Figure 6C) additionally informs that the growth-associated signal for MT reorientation does not involve the synthesis of new proteins but relies on already existing protein factors.

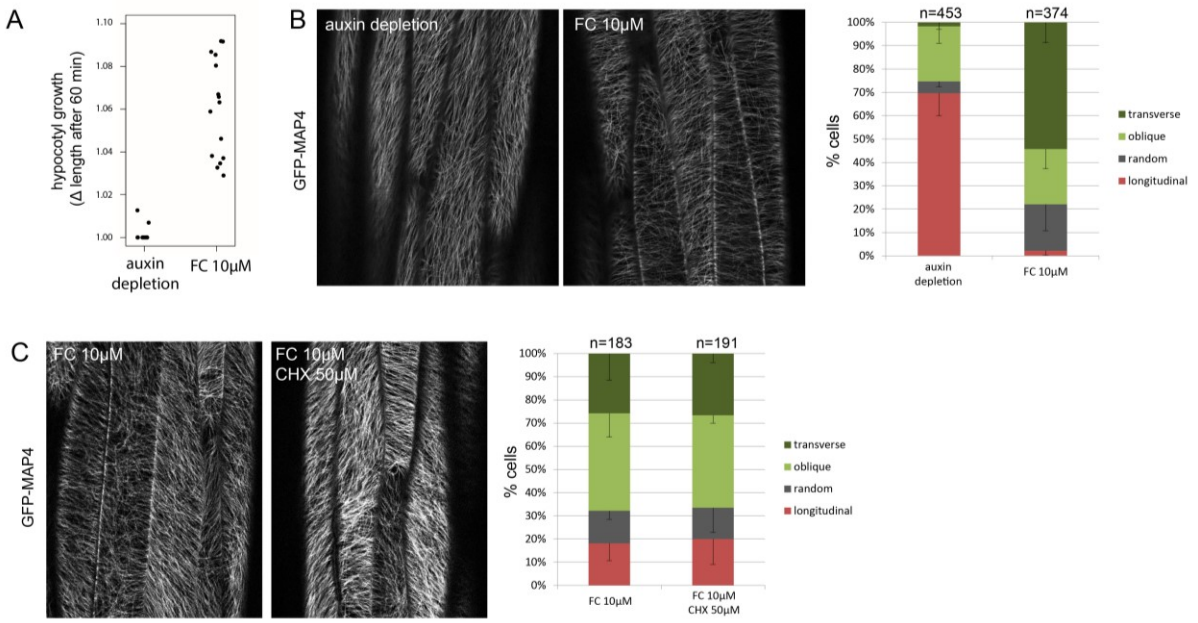

Figure 6. Anisotropic cell growth triggers MT reorientation without auxin signaling

(A) Fusicoccin (FC; 10 µM) triggers growth of hypocotyl segments, as previously reported. The graph shows collated growth measurements from two experiments, each data point representing one hypocotyl.

(B) Cell elongation triggered by FC leads to reorientation of MTs into transverse arrays, demonstrating that reorientation of MTs in anisotropically growing cells is a consequence of growth, and not hormonal signaling.

(C) Inhibition of protein synthesis by cycloheximide (CHX, 50µM) does not prevent MT reorientation, demonstrating that the reorientation process relies on pre-existing protein components.

In (B) and (C), the average percentages of cells with different MT array categories from three experiments are shown. Error bars indicate standard deviation of cell percentages between three experiments.

4.3 Discussion

Our work investigates the causes of CMT reorientation in the outer face of epidermis in growing hypocotyls. By selectively manipulating auxin signaling and growth, two phenomena that normally coexist in growing hypocotyls, we show that auxin signaling without growth is not sufficient for CMT reorientation, while growth in the absence of auxin signaling is sufficient to trigger CMT reorientation. Therefore, we conclude that in intact hypocotyls of growing seedlings, microtubule orientation is not controlled by auxin signaling directly, but is rather related to the growth status of the cells, which in turn is controlled by auxin, among other factors. These conclusions are consistent with the model previously proposed based on experiments with maize coleoptiles undergoing tropic responses (Fisher and Schopfer, 1998).

Although our study demonstrates that the microtubule-reorienting signal is associated with cell growth, its exact nature remains unknown. It is likely that the reorienting trigger is not simply the change of cell length. Fisher and Schopfer (1997) analyze CMT reorientations in excised maize coleoptiles under conditions of mechanical

bending. These excised organs are depleted of auxin, and these authors find that on the extended side, CMTs will not reorient into transverse arrays unless the coleoptile segments are supplied with auxin. It appears, then, that the change of cell length, here caused by mechanical bending, is in itself not sufficient for CMT reorientation. Instead, a physiological growth-related phenomenon, perhaps cell wall acidification and relaxation, and/or turgor increase, are also necessary to effect the reorientation.

Apart from regulation by auxin and other signaling inputs, it has been proposed that the orientation of microtubule arrays may be regulated by mechanical forces acting in the cell wall. Cell walls, as load-bearing elements of the cell, experience tensile stress resulting from turgor pressure of the cytoplasm. Due to specific cell and tissue geometry, these stresses may be anisotropic, that is, act predominantly along particular directions. Mechanisms for microtubule orientation instructed by predominant cell wall tensions have been proposed in the epidermis of shoot apical meristems and leaves (Hamant et al., 2008; Sampathkumar et al., 2014). It is conceivable that a similar mechanism guides microtubule orientation in elongating epidermal cells of hypocotyls or roots. If this is the case, then the activation of growth would have to cause changes in the predominant tensile stresses in the cell walls from axial into transverse direction. Thus far, scarce experimental evidence, as well as theoretical considerations, suggest that the predominant stress in the stem is in fact, axial (Baskin and Jensen, 2013). It remains unclear whether the orientation of MTs in epidermis of elongating organs is driven by directional cell wall tensions.

In summary, this work serves to simplify the existing views on CMT reorientation in elongating cells by clarifying that the role of auxin in this process is indirect. It appears that future efforts aimed at elucidating the exact mechanisms of CMT orientation in elongating cells should focus on researching growth-related and mechanical phenomena, rather than on hormonal signaling pathways.

4.4 Materials and methods

4.4.1 Plant material

The following previously published lines were used in this study: GFP-MAP4 (Marc et al., 1998), HS::*axr3-1* (Knox et al., 2003). Experiments in HS::*axr3-1* background were performed in the F1 generation of a cross with GFP-MAP4.

4.4.2 Seedling growth and handling

Seedlings of Arabidopsis thaliana (L.) Heynh. were grown on ½MS medium with 1% (w/v) sucrose at 21°C in darkness, after an initial period of light exposure to promote seed germination. Hypocotyls were cut from the seedlings by razor blades. Cuts were made at the

apical hook and at the root-shoot junction. During the course of experiments seedlings were kept on solid ½MS medium with 1% (w/v) sucrose, which was supplemented with necessary chemicals for treatments. The following chemicals were used as treatments: IAA, mannitol, fusicoccin, cycloheximide. HS::*axr3-1* was induced by a 40-minute incubation at 37^{o}C together with GFP-MAP4 controls, approximately 3 hours prior to cutting the seedlings.

For experiments involving cycloheximide, "depletion medium" (Takahashi et al., 2012) was used instead of ½MS medium with 1% (w/v) sucrose. This is due to the fact that the inhibitory effect of cycloheximide on growth, which on the depletion medium is slight and present only after more than 1 h (observed when growth is triggered by fusicoccin; Fendrych et al., 2016), was more pronounced on the ½MS medium. In the case of IAA+CHX co-treatment, the use of ½MS medium would make it impossible to distinguish the inhibitory effect of cycloheximide on transcriptional auxin signaling from its inhibitory effect on growth itself.

4.4.3 Imaging and scoring of cortical microtubule arrays

GFP-MAP4 hypocotyls were imaged using Zeiss LSM700 confocal microscope with 20X lens. At least three repetitions of each experiment were performed, with approx. 8-16 hypocotyls, corresponding to 50-100 cells scored per sample, in each experiment. Microscopic pictures from each experiment were collected together, randomized and scored blindly to avoid experimenter's bias.

4.4.4 Growth measurements

Growth of hypocotyl segments was captured using a flatbed scanner. Growth assays were performed on solid ½MS medium with 1% (w/v) sucrose with supplements as indicated. Hypocotyl length before and after a 1h growth period was measured using ImageJ.

4.5 Supplementary Figures

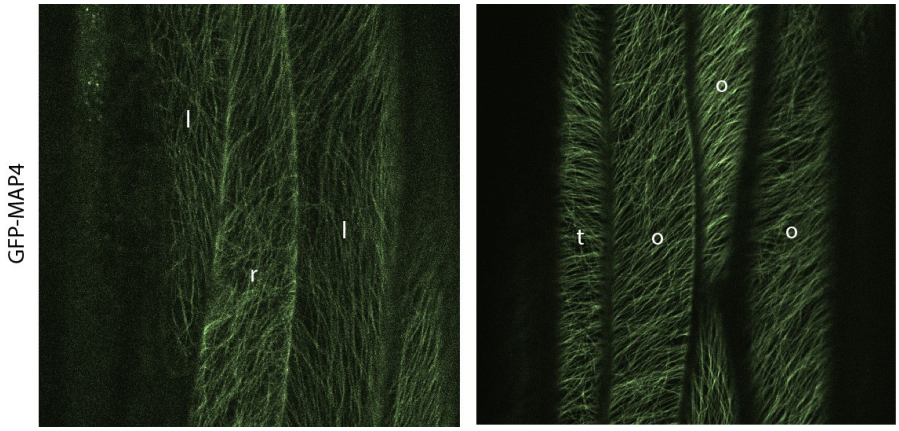

Supplementary Figure 1. Examples of microtubule array orientation classes

Figures show examples of longitudinal (l), oblique (o), transverse (t) and random (r) microtubule arrays.

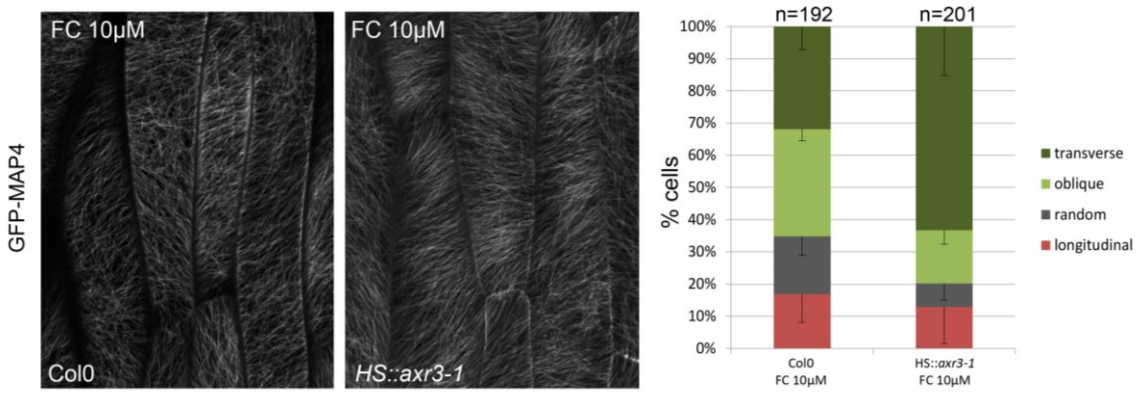

Supplementary Figure 2. MTs reorient into transverse arrays when growth is triggered by FC in the *HS::axr3-1* mutant background.

The average percentages of cells with different MT array categories from three experiments are shown. Error bars indicate standard deviation of cell percentages between three experiments.

4.6 External contributions

All experiments presented in this chapter were performed by the thesis author.

5 Summary and future prospects

The thesis contains several contributions to the field of plant cell and developmental biology. Chapter 2 offers significant steps towards indentifying novel genes involved in polar targeting of PIN proteins, or otherwise participating in auxin transport. At present, this work unraveled the role of UGGT in polar PIN targeting, but the mechanism of this regulation remains unclear. Future identification of *repp13* causal mutation may provide novel insights, as this mutant manifested significant relocalisation of PIN1 to the apical polar domain. In turn, *repp10* and *repp11* mutants did not cause PIN1 apicalization, but both REPP10 and ALA3 gene may be involved in auxin transport.

Chapter 3 characterizes putative homologs of clathrin uncoating factors auxilins in *Arabidopsis.* While the protein-protein interaction data, as well as the endocytic inhibition resulting from Auxilin overexpression both indicate the involvement of Auxilin1 and Auxilin2 in CME, their exact role in the process remains obscure. The in-depth characterization of Auxilin overexpressing lines presented here should establish them as future tools used for manipulating endocytosis in *Arabidopsis* research. Future work in this project will include the characterization of loss-of-function mutants generated by the CRISPR technology.

Chapter 4 adressess a problem of a very fundamental nature, demonstrating that the reorientations of cortical microtubule arrays observed in hypocotyl epidermis are not directly linked to auxin signaling, but are in fact regulated by cell growth. This finding sheds a new light on microtubule research, since it suggests that the mechanism of CMT reorientation should be sought in physiological and/or physical phenomena related to growth, rather than in hormonal signaling pathways.

6 References

1. Abas, L., Benjamins, R., Malenica, N., Paciorek, T., Wiśniewska, J., Moulinier-Anzola, J.C., Sieberer, T., Friml, J., and Luschnig, C. (2006). Intracellular trafficking and proteolysis of the Arabidopsis auxin-efflux facilitator PIN2 are involved in root gravitropism. Nat. Cell Biol. 8: 249–256.
2. Adamowski, M. and Friml, J. (2015). PIN-Dependent Auxin Transport: Action, Regulation, and Evolution. Plant Cell Online : 1–14.
3. Balla, J., Kalousek, P., Reinöhl, V., Friml, J., and Procházka, S. (2011). Competitive canalization of PIN-dependent auxin flow from axillary buds controls pea bud outgrowth: Competitive canalization of auxin flow. The Plant Journal 65: 571–577.
4. Band L.R., Wells D.M., Larrieu A., Sun J., Middleton A.M., French A.P., Brunoud G., Sato E.M., Wilson M.H., Péret B., Oliva M., Swarup R., Sairanen I., Parry G., Ljung K., Beeckman T., Garibaldi J.M., Estelle M., Owen M.R., Vissenberg K., Hodgman T.C., Pridmore T.P., King J.R., Vernoux T., and Bennett M.J. (2012). Root gravitropism is regulated by a transient lateral auxin gradient controlled by a tipping-point mechanism. Proceedings of the National Academy of Sciences 109: 4668–4673.
5. Barbez, E. et al. (2012). A novel putative auxin carrier family regulates intracellular auxin homeostasis in plants. Nature 485: 119–122.
6. Barbez, E., Kubeš, M., Rolčík, J., Béziat, C., Pěnčík, A., Wang, B., Ruiz Rosquete, M., Zhu, J., Dobrev, P.I., Yuree Lee, Y., Zažímalovà, E., Petrášek, J., Geisler, M., Friml, J., and Kleine-Vehn., J. (2012). A novel putative auxin carrier family regulates intracellular auxin homeostasis in plants. Nature 485: 119–122.
7. Barbez, E., Laňková, M., Pařezová, M., Maizel, A., Zažímalová, E., Petrášek, J., Friml, J., and Kleine-Vehn, J. (2013). Single-cell-based system to monitor carrier driven cellular auxin homeostasis. BMC plant biology 13: 20.
8. Barbosa, I.C.R., Zourelidou, M., Willige, B.C., Weller, B., and Schwechheimer, C. (2014). D6 PROTEIN KINASE Activates Auxin Transport-Dependent Growth and PIN-FORMED Phosphorylation at the Plasma Membrane. Developmental Cell 29: 674–685.
9. Bashline, L., Li, S., Anderson, C.T., Lei, L., and Gu, Y. (2013). The endocytosis of cellulose synthase in Arabidopsis is dependent on μ2, a clathrin-mediated endocytosis adaptin. Plant Physiol. 163: 150–160.
10. Baskin, T.I. (2001). On the alignment of cellulose microfibrils by cortical microtubules: A review and a model. Protoplasma 215: 150–171.
11. Baskin, T.I. and Jensen, O.E. (2013). On the role of stress anisotropy in the growth of stems. J. Exp. Bot. 64: 4697–4707.

12. Baster, P., Robert, S., Kleine-Vehn, J., Vanneste, S., Kania, U., Grunewald, W., De Rybel, B., Beeckman, T., and Friml, J. (2013). SCFTIR1/AFB-auxin signalling regulates PIN vacuolar trafficking and auxin fluxes during root gravitropism. The EMBO journal 32: 260–274.
13. Bender, R.L., Fekete, M.L., Klinkenberg, P.M., Hampton, M., Bauer, B., Malecha, M., Lindgren, K., A. Maki, J., Perera, M.A.D.N., Nikolau, B.J., and Carter, C.J. (2013). PIN6 is required for nectary auxin response and short stamen development. The Plant Journal 74: 893–904.
14. Benjamins, R., Quint, A.B., Weijers, D., Hooykaas, P., and Offringa, R. (2001). The PINOID protein kinase regulates organ development in Arabidopsis by enhancing polar auxin transport. Development 128: 4057–4067.
15. Benková, E., Michniewicz, M., Sauer, M., Teichmann, T., Seifertová, D., Jürgens, G., and Friml, J. (2003). Local, Efflux-Dependent Auxin Gradients as a Common Module for Plant Organ Formation. Cell 115: 591–602.
16. Bennett, S.R., Alvarez, J., Bossinger, G., and Smyth, D.R. (1995). Morphogenesis in pinoid mutants of Arabidopsis thaliana. The Plant Journal 8: 505–520.
17. Bennett, T.A., Liu, M.M., Aoyama, T., Bierfreund, N.M., Braun, M., Coudert, Y., Dennis, R.J., O'Connor, D., Wang, X.Y., White, C.D., Decker, E.L., Reski, R., and Harrison, C.J. (2014). Plasma Membrane-Targeted PIN Proteins Drive Shoot Development in a Moss. Current Biology, in press
18. Bilsborough, G.D., Runions, A., Barkoulas, M., Jenkins, H.W., Hasson, A., Galinha, C., Laufs, P., Hay, A., Prusinkiewicz, P., and Tsiantis, M. (2011). Model for the regulation of Arabidopsis thaliana leaf margin development. Proceedings of the National Academy of Sciences 108: 3424–3429.
19. Bishopp, A., Benková, E., and Helariutta, Y. (2011). Sending mixed messages: auxin-cytokinin crosstalk in roots. Current Opinion in Plant Biology 14: 10–16.
20. Blanco-Herrera, F., Moreno, A.A., Tapia, R., Reyes, F., Araya, M., Alessio, C.D., Parodi, A., and Orellana, A. (2015). The UDP-glucose : glycoprotein glucosyltransferase (UGGT), a key enzyme in ER quality control , plays a significant role in plant growth as well as biotic and abiotic stress in Arabidopsis thaliana. BMC Plant Biol.: 1–12.
21. Blilou, I., Xu, J., Wildwater, M., Willemsen, V., Paponov, I., Friml, J., Heidstra, R., Aida, M., Palme, K., and Scheres, B. (2005). The PIN auxin efflux facilitator network controls growth and patterning in Arabidopsis roots. Nature 433: 39–44.
22. Botella, C., Sautron, E., Boudiere, L., Michaud, M., Dubots, E., Yamaryo-botté, Y., Albrieux, C., Marechal, E., Block, M.A., and Jouhet, J. (2016). Desaturation of Phosphatidylcholine in the ER and Affects Chloroplast Lipid Composition in. 170: 1300–1314.

23. Boucrot, E. and Kirchhausen, T. (2007). Endosomal recycling controls plasma membrane area during mitosis. Proc. Natl. Acad. Sci. U. S. A. 104: 7939–7944.
24. Boucrot, E., Ferreira, A.P.A., Almeida-Souza, L., Debard, S., Vallis, Y., Howard, G., Bertot, L., Sauvonnet, N., and McMahon, H.T. (2015). Endophilin marks and controls a clathrin-independent endocytic pathway. Nature 517: 460–5.
25. Boutté, Y., Frescatada-Rosa, M., Men, S., Chow, C.-M., Ebine, K., Gustavsson, A., Johansson, L., Ueda, T., Moore, I., Jürgens, G., and Grebe, M. (2010). Endocytosis restricts Arabidopsis KNOLLE syntaxin to the cell division plane during late cytokinesis. EMBO J. 29: 546–558.
26. Bringmann, M., Landrein, B., Schudoma, C., Hamant, O., Hauser, M.T., and Persson, S. (2012). Cracking the elusive alignment hypothesis: The microtubule-cellulose synthase nexus unraveled. Trends Plant Sci. 17: 666–674.
27. Brunoud, G., Wells, D.M., Oliva, M., Larrieu, A., Mirabet, V., Burrow, A.H., Beeckman, T., Kepinski, S., Traas, J., Bennett, M.J., and Vernoux, T. (2012). A novel sensor to map auxin response and distribution at high spatio-temporal resolution. Nature 482: 103–106.
28. Buchberger, A., Bukau, B., and Sommer, T. (2010). Protein Quality Control in the Cytosol and the Endoplasmic Reticulum: Brothers in Arms. Mol. Cell 40: 238–252.
29. Cazzonelli C.I., Vanstraelen M., Simon S., Yin K., Carron-Arthur A., Nisar N., Tarle G., Cuttriss A.J., Searle I.R., Benkova E., Mathesius U., Masle J., Friml J., and Pogson B.J. (2013). Role of the Arabidopsis PIN6 Auxin Transporter in Auxin Homeostasis and Auxin-Mediated Development. PLoS ONE 8: e70069.
30. Chan, J. (2012). Microtubule and cellulose microfibril orientation during plant cell and organ growth. J. Microsc. 247: 23–32.
31. Chan, J., Calder, G., Fox, S., and Lloyd, C. (2007). Cortical microtubule arrays undergo rotary movements in Arabidopsis hypocotyl epidermal cells. Nat. Cell Biol. 9: 171–175.
32. Chan, J., Eder, M., Crowell, E.F., Hampson, J., Calder, G., and Lloyd, C. (2011). Microtubules and CESA tracks at the inner epidermal wall align independently of those on the outer wall of light-grown Arabidopsis hypocotyls. J. Cell Sci. 124: 1088–1094.
33. Chen R., Hilson P., Sedbrook J., Rosen E., Caspar T., and Masson P.H. (1998). The arabidopsis thaliana AGRAVITROPIC 1 gene encodes a component of the polar-auxin-transport efflux carrier. Proceedings of the National Academy of Sciences 95: 15112-15117.
34. Chen, R., Rosen, E., and Masson, P.H. (1999). Gravitropism in higher plants. Plant Physiology 120: 343–350.
35. Christensen, S.K., Dagenais, N., Chory, J., and Weigel, D. (2000). Regulation of auxin response by the protein kinase PINOID. Cell 100: 469–478.
36. Collings, D.A., Gebbie, L.K., Howles, P.A., Hurley, U.A., Birch, R.J., Cork, A.H., Hocart, C.H., Arioli, T., and Williamson, R.E. (2008). Arabidopsis dynamin-like protein DRP1A: A null

mutant with widespread defects in endocytosis, cellulose synthesis, cytokinesis, and cell expansion. J. Exp. Bot. 59: 361–376.

37. Dal Bosco C., Dovzhenko A., Liu X., Woerner N., Rensch T., Eismann M., Eimer S., Hegermann J., Paponov I.A., Ruperti B., Heberle-Bors E., Touraev A., Cohen J.D., and Palme K. (2012). The endoplasmic reticulum localized PIN8 is a pollen-specific auxin carrier involved in intracellular auxin homeostasis. The Plant Journal 71: 860–870.
38. Dello Ioio R., Nakamura K., Moubayidin L., Perilli S., Taniguchi M., Morita M.T., Aoyama T., Costantino P., and Sabatini S. (2008). A genetic framework for the control of cell division and differentiation in the root meristem. Science 322: 1380–1384.
39. Dhonukshe, P., Aniento, F., Hwang, I., Robinson, D.G., Mravec, J., Stierhof, Y.D., and Friml, J. (2007). Clathrin-Mediated Constitutive Endocytosis of PIN Auxin Efflux Carriers in Arabidopsis. Curr. Biol. 17: 520–527.
40. Di Rubbo, S. et al. (2013). The clathrin adaptor complex AP-2 mediates endocytosis of brassinosteroid insensitive1 in Arabidopsis. Plant Cell 25: 2986–97.
41. Ding Z., Wang B., Moreno I., Dupláková N., Simon S., Carraro N., Reemmer J., Pěnčík A., Chen X., Tejos R., Skůpa P., Pollmann S., Mravec J., Petrášek J., Zažímalová E., Honys D., Rolčík J., Murphy A., Orellana A., Geisler M., and Friml J. (2012). ER-localized auxin transporter PIN8 regulates auxin homeostasis and male gametophyte development in Arabidopsis. Nature Communications 3: 941.
42. Ding, Z., Galván-Ampudia, C.S., Demarsy, E., Łangowski, Ł., Kleine-Vehn, J., Fan, Y., Morita, M.T., Tasaka, M., Fankhauser, C., Offringa, R., and Friml, J. (2011). Light-mediated polarization of the PIN3 auxin transporter for the phototropic response in Arabidopsis. Nature Cell Biology 13: 447–452.
43. Du, Y., Tejos, R., Beck, M., Himschoot, E., Li, H., Robatzek, S., Vanneste, S., and Friml, J. (2013). Salicylic acid interferes with clathrin-mediated endocytic protein trafficking. Proceedings of the National Academy of Sciences 110: 7946–7951.
44. Dubrovsky, J.G., Sauer, M., Napsucialy-Mendivil, S., Ivanchenko, M.G., Friml, J., Shishkova, S., Celenza, J., and Benková, E. (2008). Auxin acts as a local morphogenetic trigger to specify lateral root founder cells. Proceedings of the National Academy of Sciences 105: 8790–8794.
45. Ehrlich, M., Boll, W., Van Oijen, A., Hariharan, R., Chandran, K., Nibert, M.L., and Kirchhausen, T. (2004). Endocytosis by random initiation and stabilization of clathrin-coated pits. Cell 118: 591–605.
46. Eisenberg, E. and Greene, L.E. (2007). Multiple roles of auxilin and Hsc70 in clathrin-mediated endocytosis. Traffic 8: 640–646.
47. Fan, L., Hao, H., Xue, Y., Zhang, L., Song, K., Ding, Z., Botella, M. a, Wang, H., and Lin, J. (2013). Dynamic analysis of Arabidopsis AP2 σ subunit reveals a key role in clathrin-mediated endocytosis and plant development. Development 140: 3826–37.

48. Fendrych, M., Leung, J and Friml, J. (2016). TIR1/AFB-Aux/IAA auxin perception mediates rapid cell wall acidification and growth of Arabidopsis hypocotyls. eLife 2016;5:e19048
49. Feraru, E., Feraru, M.I., Asaoka, R., Paciorek, T., De Rycke, R., Tanaka, H., Nakano, A., and Friml, J. (2012). BEX5/RabA1b Regulates trans-Golgi Network-to-Plasma Membrane Protein Trafficking in Arabidopsis. The Plant Cell 24: 3074–3086.
50. Feraru, E., Feraru, M.I., Kleine-Vehn, J., Martinière, A., Mouille, G., Vanneste, S., Vernhettes, S., Runions, J., and Friml, J. (2011). PIN Polarity Maintenance by the Cell Wall in Arabidopsis. Current Biology 21: 338–343.
51. Feraru, E., Paciorek, T., Feraru, M.I., Zwiewka, M., De Groodt, R., De Rycke, R., Kleine-Vehn, J., and Friml, J. (2010). The AP-3 Adaptin Mediates the Biogenesis and Function of Lytic Vacuoles in Arabidopsis. The Plant Cell 22: 2812–2824.
52. Fischer, K. and Schopfer, P. (1997). Interaction of auxin, light, and mechanical stress in orienting microtubules in relation to tropic curvature in the epidermis of maize coleoptiles. Protoplasma 196: 108–116.
53. Frank, J., Kaulfürst-Soboll, H., Rips, S., Koiwa, H., and von Schaewen, A. (2008). Comparative analyses of Arabidopsis complex glycan1 mutants and genetic interaction with staurosporin and temperature sensitive3a. Plant Physiol. 148: 1354–1367.
54. Friml J., Yang X., Michniewicz M., Weijers D., Quint A., Tietz O., Benjamins R., Ouwerkerk P.B., Ljung K., Sandberg G., Hooykaas P.J., Palme K., and Offringa R.. (2004). A PINOID-Dependent Binary Switch in Apical-Basal PIN Polar Targeting Directs Auxin Efflux. Science 306: 862–865.
55. Friml, J. et al. (2004). A PINOID-dependent binary switch in apical-basal PIN polar targeting directs auxin efflux. Science 306: 862–865.
56. Friml, J., Benková, E., Blilou, I., Wisniewska, J., Hamann, T., Ljung, K., Woody, S., Sandberg, G., Scheres, B., Jürgens, G., and Palme K. (2002a). AtPIN4 Mediates Sink-Driven Auxin Gradients and Root Patterning in Arabidopsis. Cell 108: 661–673.
57. Friml, J., Vieten, A., Sauer, M., Weijers, D., Schwarz, H., Hamann, T., Offringa, R., and Jürgens, G. (2003). Efflux-dependent auxin gradients establish the apical–basal axis of Arabidopsis. Nature 426: 147–153.
58. Friml, J., Wiśniewska, J., Benková, E., Mendgen, K., and Palme, K. (2002b). Lateral relocation of auxin efflux regulator PIN3 mediates tropism in Arabidopsis. Nature 415: 806–809.
59. Fujita, T., Sakaguchi, H., Hiwatashi, Y., Wagstaff, S.J., Ito, M., Deguchi, H., Sato, T., and Hasebe, M. (2008). Convergent evolution of shoots in land plants: lack of auxin polar transport in moss shoots. Evolution & development 10: 176–186.
60. Gadeyne, A. et al. (2014). The TPLATE adaptor complex drives clathrin-mediated endocytosis in plants. Cell 156: 691–704.

61. Galvan-Ampudia, C.S., Julkowska, M.M., Darwish, E., Gandullo, J., Korver, R.A., Brunoud, G., Haring, M.A., Munnik, T., Vernoux, T., and Testerink, C. (2013). Halotropism Is a Response of Plant Roots to Avoid a Saline Environment. Current Biology 23: 2044–2050.
62. Gälweiler L., Guan C., Müller A., Wisman E., Mendgen K., Yephremov A., and Palme K. (1998). Regulation of Polar Auxin Transport by AtPIN1 in Arabidopsis Vascular Tissue. Science 282: 2226–2230.
63. Ganguly, A., Park, M., Kesawat, M.S., and Cho, H.-T. (2014). Functional Analysis of the Hydrophilic Loop in Intracellular Trafficking of Arabidopsis PIN-FORMED Proteins. The Plant Cell 26: 1570–1585.
64. Gao, C., Luo, M., Zhao, Q., Yang, R., Cui, Y., Zeng, Y., Xia, J., and Jiang, L. (2014). A Unique Plant ESCRT Component, FREE1, Regulates Multivesicular Body Protein Sorting and Plant Growth. Current Biology 24: 2556–2563.
65. Gao, Y., Zhang, Y., Zhang, D., Dai, X., Estelle, M., and Zhao, Y. (2015). Auxin binding protein 1 (ABP1) is not required for either auxin signaling or Arabidopsis development. 1.
66. Garbers, C., DeLong, A., Deruere, J., Bernasconi, P., and Söll, D. (1996). A mutation in protein phosphatase 2A regulatory subunit A affects auxin transport in Arabidopsis. The EMBO journal 15: 2115.
67. Geldner N., Friml J., Stierhof Y.D., Jürgens G., and Palme K. (2001). Auxin transport inhibitors block PIN1 cycling and vesicle trafficking. Nature 413: 425-428
68. Geldner, N., Anders, N., Wolters, H., Keicher, J., Kornberger, W., Muller, P., Delbarre, A., Ueda, T., Nakano, A., and Jürgens, G. (2003). The Arabidopsis GNOM ARF-GEF Mediates Endosomal Recycling, Auxin Transport, and Auxin-Dependent Plant Growth. Cell 112: 219–230.
69. Godlee, C. and Kaksonen, M. (2013). From uncertain beginnings: Initiation mechanisms of clathrin-mediated endocytosis. J. Cell Biol. 203: 717–725.
70. Goldsmith, M.H.M. (1977). The polar transport of auxin. Annual Review of Plant Physiology 28: 439–478.
71. Gomès, E., Jakobsen, M.K., Axelsen, K.B., Geisler, M., and Palmgren, M.G. (2000). Chilling tolerance in Arabidopsis involves ALA1, a member of a new family of putative aminophospholipid translocases. Plant Cell 12: 2441–2454.
72. Hamant, O., Heisler, M.G., Jönsson, H., Krupinski, P., Uyttewaal, M., Bokov, P., Corson, F., Sahlin, P., Boudaoud, A., Meyerowitz, E.M., Couder, Y., and Traas, J. (2008). Developmental patterning by mechanical signals in Arabidopsis. Science 322: 1650–1655.
73. Hay A., Barkoulas M., and Tsiantis M. (2006). ASYMMETRIC LEAVES1 and auxin activities converge to repress BREVIPEDICELLUS expression and promote leaf development in Arabidopsis. Development 133: 3955–3961.

74. Heisler, M.G., Ohno, C., Das, P., Sieber, P., Reddy, G.V., Long, J.A., and Meyerowitz, E.M. (2005). Patterns of Auxin Transport and Gene Expression during Primordium Development Revealed by Live Imaging of the Arabidopsis Inflorescence Meristem. Current Biology 15: 1899–1911.
75. Henne, W.M., Boucrot, E., Meinecke, M., Evergren, E., Vallis, Y., Mittal, R., and McMahon, H.T. (2010). FCHo proteins are nucleators of clathrin-mediated endocytosis. Science 328: 1281–4.
76. Hong, Z., Jin, H., Fitchette, A.-C., Xia, Y., Monk, A.M., Faye, L., and Li, J. (2009). Mutations of an alpha1,6 mannosyltransferase inhibit endoplasmic reticulum-associated degradation of defective brassinosteroid receptors in Arabidopsis. Plant Cell 21: 3792–3802.
77. Hong, Z., Kajiura, H., Su, W., Jin, H., Kimura, a., Fujiyama, K., and Li, J. (2012). Evolutionarily conserved glycan signal to degrade aberrant brassinosteroid receptors in Arabidopsis. Proc. Natl. Acad. Sci. 109: 11437–11442.
78. Hu, C., Chinenov, Y., Kerppola, T.K., Hughes, H., and Arbor, A. (2002). Visualization of Interactions among bZIP and Rel Family Proteins in Living Cells Using Bimolecular Fluorescence Complementation. 9: 789–798.
79. Huang, F., Kemel Zago, M., Abas, L., van Marion, A., Galvan-Ampudia, C.S., and Offringa, R. (2010). Phosphorylation of Conserved PIN Motifs Directs Arabidopsis PIN1 Polarity and Auxin Transport. The Plant Cell 22: 1129–1142.
80. Irani, N.G. et al. (2012). Fluorescent castasterone reveals BRI1 signaling from the plasma membrane. Nat. Chem. Biol. 8: 583–589.
81. Ischebeck T., Werner S., Krishnamoorthy P., Lerche J., Meijón M., Stenzel I., Löfke C., Wiessner T., Im Y.J., Perera I.Y., Iven T., Feussner I., Busch W., Boss W.F., Teichmann T., Hause B., Persson S., and Heilmann I. (2013). Phosphatidylinositol 4,5-Bisphosphate Influences PIN Polarization by Controlling Clathrin-Mediated Membrane Trafficking in Arabidopsis. The Plant Cell 25: 4894–4911.
82. Ischebeck, T. et al. (2013). Phosphatidylinositol 4,5-bisphosphate influences PIN polarization by controlling clathrin-mediated membrane trafficking in Arabidopsis. Plant Cell 25: 4894–911.
83. Ito, E., Fujimoto, M., Ebine, K., Uemura, T., Ueda, T., and Nakano, A. (2012). Dynamic behavior of clathrin in Arabidopsis thaliana unveiled by live imaging. Plant J. 69: 204–216.
84. Jang, G. and Dolan, L. (2011). Auxin promotes the transition from chloronema to caulonema in moss protonema by positively regulating PpRSL1and PpRSL2 in Physcomitrella patens. New Phytologist 192: 319–327.
85. Jelinkova, A., Petra, J., and Kubes, M. (2010). Probing plant membranes with FM dyes : tracking , dragging or blocking ? 64: 883–892.

86. Jin, H., Hong, Z., Su, W., and Li, J. (2009). A plant-specific calreticulin is a key retention factor for a defective brassinosteroid receptor in the endoplasmic reticulum. Proc. Natl. Acad. Sci. U. S. A. 106: 13612–13617.
87. Jin, H., Yan, Z., Nam, K.H., and Li, J. (2007). Article Allele-Specific Suppression of a Defective Brassinosteroid Receptor Reveals a Physiological Role of UGGT in ER Quality Control.: 821–830.
88. Kania, U., Fendrych, M., and Friml, J. (2014). Polar delivery in plants; commonalities and differences to animal epithelial cells. Open Biology 4: 140017–140017.
89. Karimi, M., Inzé, D., and Depicker, A. (2002). GATEWAYTM vectors for Agrobacterium-mediated plant transformation. Trends Plant Sci. 7: 193–195.
90. Keuskamp, D.H., Pollmann, S., Voesenek, L.A.C.J., Peeters, A.J.M., and Pierik, R. (2010). Auxin transport through PIN-FORMED 3 (PIN3) controls shade avoidance and fitness during competition. Proceedings of the National Academy of Sciences 107: 22740–22744.
91. Khaled, S. Ben, Postma, J., and Robatzek, S. (2015). A Moving View: Subcellular Trafficking Processes in Pattern Recognition Receptor– Triggered Plant Immunity. Annu. Rev. Phytopathol 53: 379–402.
92. Kim, S.Y., Xu, Z.-Y., Song, K., Kim, D.H., Kang, H., Reichardt, I., Sohn, E.J., Friml, J., Juergens, G., and Hwang, I. (2013). Adaptor protein complex 2-mediated endocytosis is crucial for male reproductive organ development in Arabidopsis. Plant Cell 25: 2970–85.
93. Kitakura, S., Vanneste, S., Robert, S., Lofke, C., Teichmann, T., Tanaka, H., and Friml, J. (2011). Clathrin Mediates Endocytosis and Polar Distribution of PIN Auxin Transporters in Arabidopsis. The Plant Cell 23: 1920–1931.
94. Kleine-Vehn J., Wabnik K., Martinière A., Łangowski Ł., Willig K., Naramoto S., Leitner J., Tanaka H., Jakobs S., Robert S., Luschnig C., Govaerts W., Hell S.W., Runions J., and Friml J. (2011). Recycling, clustering, and endocytosis jointly maintain PIN auxin carrier polarity at the plasma membrane. Molecular Systems Biology 7: 540.
95. Kleine-Vehn, J., Dhonukshe, P., Sauer, M., Brewer, P.B., Wiśniewska, J., Paciorek, T., Benková, E., and Friml, J. (2008a). ARF GEF-Dependent Transcytosis and Polar Delivery of PIN Auxin Carriers in Arabidopsis. Current Biology 18: 526–531.
96. Kleine-Vehn, J., Ding, Z., Jones, A.R., Tasaka, M., Morita, M.T., and Friml, J. (2010). Gravity-induced PIN transcytosis for polarization of auxin fluxes in gravity-sensing root cells. Proceedings of the National Academy of Sciences 107: 22344–22349.
97. Kleine-Vehn, J., Leitner, J., Zwiewka, M., Sauer, M., Abas, L., Luschnig, C., and Friml, J. (2008b). Differential degradation of PIN2 auxin efflux carrier by retromer-dependent vacuolar targeting. Proceedings of the National Academy of Sciences 105: 17812–17817.
98. Knox, K., Grierson, C.S., and Leyser, O. (2003). AXR3 and SHY2 interact to regulate root hair development. Development 130: 5769–5777.

99. Konopka, C. a, Backues, S.K., and Bednarek, S.Y. (2008). Dynamics of Arabidopsis dynamin-related protein 1C and a clathrin light chain at the plasma membrane. Plant Cell 20: 1363–1380.
100. Konopka, C. a. and Bednarek, S.Y. (2008). Variable-angle epifluorescence microscopy: A new way to look at protein dynamics in the plant cell cortex. Plant J. 53: 186–196.
101. Kraker, J. De, Luck, K., Textor, S., Tokuhisa, J.G., Gershenzon, J., Planck, M., Ecology, C., Campus, B., and Jena, D. (2007). Two Arabidopsis Genes (IPMS1 and IPMS2) Encode Isopropylmalate Synthase , the Branchpoint Step in the. 143: 970–986.
102. Lam, B.C., Sage, T.L., Bianchi, F., and Blumwald, E. (2001). Role of SH3 domain-containing proteins in clathrin-mediated vesicle trafficking in Arabidopsis. Plant Cell 13: 2499–2512.
103. Lam, B.C.H., Sage, T.L., Bianchi, F., and Blumwald, E. (2002). Regulation of ADL6 activity by its associated molecular network. Plant J. 31: 565–576.
104. Lauber, M.H., Waizenegger, I., Steinmann, T., Schwarz, H., Mayer, U., Hwang, I., Lukowitz, W., and Jürgens, G. (1997). The Arabidopsis KNOLLE protein is a cytokinesis-specific syntaxin. J. Cell Biol. 139: 1485–1493.
105. Lei, L., Li, S., Gu, Y., Lei, L., Li, S., and Gu, Y. (2017). mediates the intimate relationship between cellulose microfibrils and cortical microtubules Cellulose synthase interactive protein 1 (CSI1) mediates the intimate relationship between cellulose microfibrils and cortical microtubules. 2324.
106. Leitner, J., Petrasek, J., Tomanov, K., Retzer, K., Parezova, M., Korbei, B., Bachmair, A., Zazimalova, E., and Luschnig, C. (2012). Lysine63-linked ubiquitylation of PIN2 auxin carrier protein governs hormonally controlled adaptation of Arabidopsis root growth. Proceedings of the National Academy of Sciences 109: 8322–8327.
107. Li, J., Zhao-Hui, C., Batoux, M., Nekrasov, V., Roux, M., Chinchilla, D., Zipfel, C., and Jones, J.D.G. (2009). Specific ER quality control components required for biogenesis of the plant innate immune receptor EFR. Proc. Natl. Acad. Sci. U. S. A. 106: 15973–15978.
108. Li, S., Lei, L., Somerville, C.R., and Gu, Y. (2012). Cellulose synthase interactive protein 1 (CSI1) links microtubules and cellulose synthase complexes. 109: 185–190.
109. Liu, A.P., Aguet, F., Danuser, G., and Schmid, S.L. (2010). Local clustering of transferrin receptors promotes clathrin-coated pit initiation. J. Cell Biol. 191: 1381–1393.
110. Loerke, D., Mettlen, M., Yarar, D., Jaqaman, K., Jaqaman, H., Danuser, G., and Schmid, S.L. (2009). Cargo and Dynamin Regulate Clathrin-Coated Pit Maturation. PLoS Biol. 7.
111. Löfke, C., Zwiewka, M., Heilmann, I., Van Montagu, M.C.E., Teichmann, T., and Friml, J. (2013). Asymmetric gibberellin signaling regulates vacuolar trafficking of PIN auxin transporters during root gravitropism. Proceedings of the National Academy of Sciences 110: 3627–3632.

112. Lu, X., Tintor, N., Mentzel, T., Kombrink, E., Boller, T., Robatzek, S., Schulze-Lefert, P., and Saijo, Y. (2009). Uncoupling of sustained MAMP receptor signaling from early outputs in an Arabidopsis endoplasmic reticulum glucosidase II allele. Proc. Natl. Acad. Sci. U. S. A. 106: 22522–22527.

113. Luschnig, C., Gaxiola, R.A., Grisafi, P., and Fink, G.R. (1998). EIR1, a root-specific protein involved in auxin transport, is required for gravitropism inArabidopsis thaliana. Genes & development 12: 2175–2187.

114. Marc, J., Granger, C., Brincat, J., Fisher, D., Kao, T., McCubbin, A., and Cyr, R. (1998). A GFP-MAP4 reporter gene for visualizing cortical microtubule rearrangements in living epidermal cells. Plant Cell 10: 1927–1940.

115. Marhavý, P., Bielach, A., Abas, L., Abuzeineh, A., Duclercq, J., Tanaka, H., Pařezová, M., Petrášek, J., Friml, J., Kleine-Vehn, J., and Benková, E. (2011). Cytokinin Modulates Endocytic Trafficking of PIN1 Auxin Efflux Carrier to Control Plant Organogenesis. Developmental Cell 21: 796–804.

116. Marhavý, P., Duclercq, J., Weller, B., Feraru, E., Bielach, A., Offringa, R., Friml, J., Schwechheimer, C., Murphy, A., and Benková, E. (2014). Cytokinin Controls Polarity of PIN1-Dependent Auxin Transport during Lateral Root Organogenesis. Current Biology 24: 1031–1037.

117. Martinière A., Lavagi I., Nageswaran G., Rolfe D.J., Maneta-Peyret L., Luu D.T., Botchway S.W., Webb S.E., Mongrand S., Maurel C., Martin-Fernandez M.L., Kleine-Vehn J., Friml J., Moreau P., and Runions J. (2012). Cell wall constrains lateral diffusion of plant plasma-membrane proteins. Proceedings of the National Academy of Sciences 109: 12805–12810.

118. Mattsson, J., Sung, Z.R., and Berleth, T. (1999). Responses of plant vascular systems to auxin transport inhibition. Development 126: 2979–2991.

119. Mayer, U., Torres-Ruiz R.A., Berleth, T., Miséra, S., and Jürgens, G. (1991). Mutations affecting body organization in the Arabidopsis embryo. Nature 353: 402-407

120. McCusker, D. and Kellogg, D.R. (2012). Plasma membrane growth during the cell cycle: Unsolved mysteries and recent progress. Curr. Opin. Cell Biol. 24: 845–851.

121. McDowell, S.C., López-Marqués, R.L., Poulsen, L.R., Palmgren, M.G., and Harper, J.F. (2013). Loss of the Arabidopsis thaliana P4-ATPase ALA3 Reduces Adaptability to Temperature Stresses and Impairs Vegetative, Pollen, and Ovule Development. PLoS One 8: e62577.

122. McLoughlin, F., Arisz, S.A., Dekker, H.L., Kramer, G., de Koster, C.G., Haring, M.A., Munnik, T., and Testerink, C. (2013). Identification of novel candidate phosphatidic acid-binding proteins involved in the salt-stress response of Arabidopsis thaliana roots. Biochemical Journal 450: 573–581.

123. Mcmahon, H.T. and Boucrot, E. (2011). Molecular mechanism and physiological functions of clathrin-mediated endocytosis. Nat. Publ. Gr. 12: 517–533.
124. Merrifield, C.J., Feldman, M.E., Wan, L., and Almers, W. (2002). Imaging actin and dynamin recruitment during invagination of single clathrin-coated pits. Nat. Cell Biol. 4: 691–698.
125. Michniewicz M., Zago M.K., Abas L., Weijers D., Schweighofer A., Meskiene I., Heisler M.G., Ohno C., Zhang J., Huang F., Schwab R., Weigel D., Meyerowitz E.M., Luschnig C., Offringa R., and Friml J. (2007). Antagonistic Regulation of PIN Phosphorylation by PP2A and PINOID Directs Auxin Flux. Cell 130: 1044–1056.
126. Mravec J., Skůpa P., Bailly A., Hoyerová K., Krecek P., Bielach A., Petrásek J., Zhang J., Gaykova V., Stierhof Y.D., Dobrev P.I., Schwarzerová K., Rolcík J., Seifertová D., Luschnig C., Benková E., Zazímalová E., Geisler M., and Friml J. (2009). Subcellular homeostasis of phytohormone auxin is mediated by the ER-localized PIN5 transporter. Nature 459: 1136–1140.
127. Müller, A., Guan, C., Gälweiler, L., Tänzler, P., Huijser, P., Marchant, A., Parry, G., Bennett, M., Wisman, E., and Palme, K. (1998). AtPIN2 defines a locus of Arabidopsis for root gravitropism control. The EMBO Journal 17: 6903–6911.
128. Muthusamy, B.P., Natarajan, P., Zhou, X., and Graham, T.R. (2009). Linking phospholipid flippases to vesicle-mediated protein transport. Biochim. Biophys. Acta - Mol. Cell Biol. Lipids 1791: 612–619.
129. Naramoto, S., Kleine-Vehn, J., Robert, S., Fujimoto, M., Dainobu, T., Paciorek, T., Ueda, T., Nakano, A., Van Montagu, M.C.E., Fukuda, H., and Friml, J. (2010). ADP-ribosylation factor machinery mediates endocytosis in plant cells. Proceedings of the National Academy of Sciences 107: 21890–21895.
130. Naramoto, S., Otegui, M.S., Kutsuna, N., de Rycke, R., Dainobu, T., Karampelias, M., Fujimoto, M., Feraru, E., Miki, D., Fukuda, H., Nakano, A., and Friml, J. (2014). Insights into the Localization and Function of the Membrane Trafficking Regulator GNOM ARF-GEF at the Golgi Apparatus in Arabidopsis. The Plant Cell 26: 3062–3076.
131. Nekrasov, V. et al. (2009). Control of the pattern-recognition receptor EFR by an ER protein complex in plant immunity. EMBO J. 28: 3428–3438.
132. Nodzyński, T., Feraru, M.I., Hirsch, S., De Rycke, R., Niculaes, C., Boerjan, W., Van Leene, J., De Jaeger, G., Vanneste, S., and Friml, J. (2013). Retromer Subunits VPS35A and VPS29 Mediate Prevacuolar Compartment (PVC) Function in Arabidopsis. Molecular Plant 6: 1849–1862.
133. Nováková, P. et al. (2014). SAC phosphoinositide phosphatases at the tonoplast mediate vacuolar function in Arabidopsis. Proc. Natl. Acad. Sci. U. S. A. 111: 2818–23.

134. Okada, K., Ueda, J., Komaki, M.K., Bell, C.J., and Shimura, Y. (1991). Requirement of the auxin polar transport system in early stages of Arabidopsis floral bud formation. The Plant Cell 3: 677–684.

135. Paciorek, T., Zažímalová, E., Ruthardt, N., Petrášek, J., Stierhof, Y.-D., Kleine-Vehn, J., Morris, D.A., Emans, N., Jürgens, G., Geldner, N., and Friml, J. (2005). Auxin inhibits endocytosis and promotes its own efflux from cells. Nature 435: 1251–1256.

136. Paredez, A.R. (2006). Visualization of Cellulose Synthase with Microtubules. 1491.

137. Park, M. and Jürgens, G. (2012). Membrane Traffic and Fusion at Post-Golgi Compartments. Front. Plant Sci. 2: 1–15.

138. Park, M., Song, K., Reichardt, I., Kim, H., Mayer, U., Stierhof, Y.-D., Hwang, I., and Jürgens, G. (2013). Arabidopsis μ-adaptin subunit AP1M of adaptor protein complex 1 mediates late secretory and vacuolar traffic and is required for growth. Proc. Natl. Acad. Sci. U. S. A. 110: 10318–23.

139. Pedas, P.R., Mcdowell, S.C., Brown, E., Poulsen, L.R., Lo, R.L., Kunze, R., Harper, J.F., Pomorski, T.G., and Palmgren, M. (2015). A phospholipid uptake system in the model plant Arabidopsis thaliana.

140. Petrásek J., Mravec J., Bouchard R., Blakeslee J.J., Abas M., Seifertová D., Wisniewska J., Tadele Z., Kubes M., Covanová M., Dhonukshe P., Skupa P., Benková E., Perry L., Krecek P., Lee O.R., Fink G.R., Geisler M., Murphy A.S., Luschnig C., Zazímalová E., and Friml J. (2006). PIN Proteins Perform a Rate-Limiting Function in Cellular Auxin Efflux. Science 312: 914–918.

141. Petrásek, J. et al. (2006). PIN proteins perform a rate-limiting function in cellular auxin efflux. Science 312: 914–918.

142. Poulsen, L.R., López-Marqués, R.L., McDowell, S.C., Okkeri, J., Licht, D., Schulz, A., Pomorski, T., Harper, J.F., and Palmgren, M.G. (2008). The Arabidopsis P4-ATPase ALA3 localizes to the golgi and requires a beta-subunit to function in lipid translocation and secretory vesicle formation. Plant Cell 20: 658–676.

143. Prigge, M.J., Lavy, M., Ashton, N.W., and Estelle, M. (2010). Physcomitrella patens Auxin-Resistant Mutants Affect Conserved Elements of an Auxin-Signaling Pathway. Current Biology 20: 1907–1912.

144. Rakusová, H., Gallego-Bartolomé, J., Vanstraelen, M., Robert, H.S., Alabadí, D., Blázquez, M.A., Benková, E., and Friml, J. (2011). Polarization of PIN3-dependent auxin transport for hypocotyl gravitropic response in Arabidopsis thaliana. The Plant Journal 67: 817–826.

145. Rakusová, H., Wabnik, K., Sauer, M., Grones, P., Barbez, E., Kaufmann, W.A., De Rycke, R., Chen, X., Simon, S., Robert, H.S., Van Montagu, M., Kleine-Vehn, J., and Friml, J. (2014). AUXIN-BINDING PROTEIN 1 mediates coordination of cell and tissue polarities in Arabidopsis thaliana, accepted for publication

146. Rashotte, A.M., DeLong, A., and Muday, G.K. (2001). Genetic and chemical reductions in protein phosphatase activity alter auxin transport, gravity response, and lateral root growth. The Plant Cell 13: 1683–1697.

147. Reinhardt, D., Pesce, E.-R., Stieger, P., Mandel, T., Baltensperger, K., Bennett, M., Traas, J., Friml, J., and Kuhlemeier, C. (2003). Regulation of phyllotaxis by polar auxin transport. Nature 426: 255–260.

148. Renard, H.-F. et al. (2015). Endophilin-A2 functions in membrane scission in clathrin-independent endocytosis. Nature 517: 493–6.

149. Robert S., Kleine-Vehn J., Barbez E., Sauer M., Paciorek T., Baster P., Vanneste S., Zhang J., Simon S., Čovanová M., Hayashi K., Dhonukshe P., Yang Z., Bednarek S.Y., Jones A.M., Luschnig C., Aniento F., Zažímalová E., and Friml J. (2010). ABP1 Mediates Auxin Inhibition of Clathrin-Dependent Endocytosis in Arabidopsis. Cell 143: 111–121.

150. Robert, H.S., Grones, P., Stepanova, A.N., Robles, L.M., Lokerse, A.S., Alonso, J.M., Weijers, D., and Friml, J. (2013). Local Auxin Sources Orient the Apical-Basal Axis in Arabidopsis Embryos. Current Biology 23: 2506–2512.

151. Robinson, D.G. and Pimpl, P. (2014). Clathrin and post-Golgi trafficking: A very complicated issue. Trends Plant Sci. 19: 134–139.

152. Růžička, K., Šimášková, M., Duclercq, J., Petrášek, J., Zažímalová, E., Simon, S., Friml, J., Van Montagu, M.C., and Benková, E. (2009). Cytokinin regulates root meristem activity via modulation of the polar auxin transport. Proceedings of the National Academy of Sciences 106: 4284–4289.

153. Sabatini, S., Beis, D., Wolkenfelt, H., Murfett, J., Guilfoyle, T., Malamy, J., Benfey, P., Leyser, O., Bechtold, N., Weisbeek, P., and Scheres, B. (1999). An Auxin-Dependent Distal Organizer of Pattern and Polarity in the Arabidopsis Root. Cell 99: 463–472.

154. Sachs, T. (1991). Cell polarity and tissue patterning in plants. Development 113: 83–93.

155. Saijo, Y., Tintor, N., Lu, X., Rauf, P., Pajerowska-Mukhtar, K., Häweker, H., Dong, X., Robatzek, S., and Schulze-Lefert, P. (2009). Receptor quality control in the endoplasmic reticulum for plant innate immunity. EMBO J. 28: 3439–3449.

156. Saleem, M., Morlot, S., Hohendahl, A., Manzi, J., Lenz, M., and Roux, A. (2015). A balance between membrane elasticity and polymerization energy sets the shape of spherical clathrin coats. Nat. Commun. 6: 6249.

157. Sampathkumar, A., Krupinski, P., Wightman, R., Milani, P., Berquand, A., Boudaoud, A., Hamant, O., Jönsson, H., and Meyerowitz, E.M. (2014). Subcellular and supracellular mechanical stress prescribes cytoskeleton behavior in Arabidopsis cotyledon pavement cells. Elife 3: e01967.

158. Sauer, M., Balla, J., Luschnig, C., Wisniewska, J., Reinohl, V., Friml, J., and Benkova, E. (2006). Canalization of auxin flow by Aux/IAA-ARF-dependent feedback regulation of PIN polarity. Genes & Development 20: 2902–2911.

159. Sauer, M., Paciorek, T., Benková, E., and Friml, J. (2006). Immunocytochemical techniques for whole-mount in situ protein localization in plants. Nat. Protoc. 1: 98–103.

160. Sawchuk, M.G., Edgar, A., and Scarpella, E. (2013). Patterning of Leaf Vein Networks by Convergent Auxin Transport Pathways. PLoS Genetics 9: e1003294.

161. Scarpella E., Marcos D., Friml J., and Berleth T. (2006). Control of leaf vascular patterning by polar auxin transport. Genes & Development 20: 1015–1027.

162. Scheuring, D., Viotti, C., Krüger, F., Künzl, F., Sturm, S., Bubeck, J., Hillmer, S., Frigerio, L., Robinson, D.G., Pimpl, P., and Schumacher, K. (2011). Multivesicular bodies mature from the trans-Golgi network/early endosome in Arabidopsis. Plant Cell 23: 3463–81.

163. Shevell D.E., Leu W.M., Gillmor C.S., Xia G., Feldmann K.A., and Chua N.H. (1994) EMB30 is essential for normal cell division, cell expansion, and cell adhesion in Arabidopsis and encodes a protein that has similarity to Sec7. Cell 77: 1051-1062.

164. Shibaoka, H. (1994). CORTICAL MICROTUBULES : Alterations in the Cross-linking Between Microtubules and the Plasma Membrane.

165. Song, K., Jang, M., Kim, S.Y., Lee, G., Lee, G.-J., Kim, D.H., Lee, Y., Cho, W., and Hwang, I. (2012). An A/ENTH Domain-Containing Protein Functions as an Adaptor for Clathrin-Coated Vesicles on the Growing Cell Plate in Arabidopsis Root Cells. Plant Physiol. 159: 1013–1025.

166. Sorefan, K., Girin, T., Liljegren, S.J., Ljung, K., Robles, P., Galván-Ampudia, C.S., Offringa, R., Friml, J., Yanofsky, M.F., and Østergaard, L. (2009). A regulated auxin minimum is required for seed dispersal in Arabidopsis. Nature 459: 583–586.

167. Sousa, R. and Lafer, E.M. (2015). The role of molecular chaperones in clathrin mediated vesicular trafficking. Front. Mol. Biosci. 2: 26.

168. Spitzer, C., Reyes, F.C., Buono, R., Sliwinski, M.K., Haas, T.J., and Otegui, M.S. (2009). The ESCRT-Related CHMP1A and B Proteins Mediate Multivesicular Body Sorting of Auxin Carriers in Arabidopsis and Are Required for Plant Development. The Plant Cell 21: 749–766.

169. Steinmann T., Geldner N., Grebe M., Mangold S., Jackson C.L., Paris S., Gälweiler L., Palme K., and Jürgens G. (1999). Coordinated Polar Localization of Auxin Efflux Carrier PIN1 by GNOM ARF GEF. Science 286: 316–318.

170. Su, W., Liu, Y., Xia, Y., Hong, Z., and Li, J. (2011). Conserved endoplasmic reticulum-associated degradation system to eliminate mutated receptor-like kinases in Arabidopsis. Proc. Natl. Acad. Sci. U. S. A. 108: 870–875.

171. Su, W., Liu, Y., Xia, Y., Hong, Z., and Li, J. (2012). The arabidopsis homolog of the mammalian os-9 protein plays a key role in the endoplasmic reticulum-associated degradation of misfolded receptor-like kinases. Mol. Plant 5: 929–940.

172. Suetsugu, N., Kagawa, T., Wada, M., and Corporation, T. (2005). An Auxilin-Like J-Domain Protein , JAC1 , Regulates Phototropin-Mediated Chloroplast Movement. 139: 151–162.

173. Sun, T., Zhang, Q., Gao, M., and Zhang, Y. (2014). Regulation of SOBIR1 accumulation and activation of defense responses in bir1-1 by specific components of ER quality control. Plant J. 77: 748–756.

174. Takahashi, K., Hayashi, K. -i., and Kinoshita, T. (2012). Auxin Activates the Plasma Membrane H+-ATPase by Phosphorylation during Hypocotyl Elongation in Arabidopsis. Plant Physiol. 159: 632–641.

175. Tanaka, H., Kitakura, S., De Rycke, R., De Groodt, R., and Friml, J. (2009). Fluorescence Imaging-Based Screen Identifies ARF GEF Component of Early Endosomal Trafficking. Current Biology 19: 391–397.

176. Tanaka, H., Kitakura, S., Rakusová, H., Uemura, T., Feraru, M.I., De Rycke, R., Robert, S., Kakimoto, T., and Friml, J. (2013). Cell Polarity and Patterning by PIN Trafficking through Early Endosomal Compartments in Arabidopsis thaliana. PLoS Genetics 9: e1003540.

177. Tanaka, H., Nodzyński, T., Kitakura, S., Feraru, M.I., Sasabe, M., Ishikawa, T., Kleine-Vehn, J., Kakimoto, T., and Friml, J. (2014). BEX1/ARF1A1C is Required for BFA-Sensitive Recycling of PIN Auxin Transporters and Auxin-Mediated Development in Arabidopsis. Plant and Cell Physiology 55: 737–749.

178. Tanaka, K., Fujimura-Kamada, K., and Yamamoto, T. (2011). Functions of phospholipid flippases. J. Biochem. 149: 131–143.

179. Teh, O. and Moore, I. (2007). An ARF-GEF acting at the Golgi and in selective endocytosis in polarized plant cells. Nature 448: 493–496.

180. Tejos, R., Sauer, M., Vanneste, S., Palacios-Gomez, M., Li, H., Heilmann, M., van Wijk, R., Vermeer, J.E.M., Heilmann, I., Munnik, T., and Friml, J. (2014). Bipolar Plasma Membrane Distribution of Phosphoinositides and Their Requirement for Auxin-Mediated Cell Polarity and Patterning in Arabidopsis. Plant Cell 26: 2114–2128.

181. Toshima, J.Y., Toshima, J., Kaksonen, M., Martin, A.C., King, D.S., and Drubin, D.G. (2006). Spatial dynamics of receptor-mediated endocytic trafficking in budding yeast revealed by using fluorescent alpha-factor derivatives. Proc. Natl. Acad. Sci. U. S. A. 103: 5793–5798.

182. Utsuno, K., Shikanai, T., Yamada, Y., and Hashimoto, T. (1998). AGR, an Agravitropic locus of Arabidopsis thaliana, encodes a novel membrane-protein family member. Plant and Cell Physiology 39: 1111–1118.

183. Van Leene, J. et al. (2014). An improved toolbox to unravel the plant cellular machinery by tandem affinity purification of Arabidopsis protein complexes. Nat. Protoc. 10: 169–187.

184. Vandenbussche, F., Petrasek, J., Zadnikova, P., Hoyerova, K., Pesek, B., Raz, V., Swarup, R., Bennett, M., Zazimalova, E., Benkova, E., and Van Der Straeten, D. (2010). The auxin influx carriers AUX1 and LAX3 are involved in auxin-ethylene interactions during apical hook development in Arabidopsis thaliana seedlings. Development 137: 597–606.

185. Viaene, T., Landberg, K., Thelander, M., Medvecka, E., Pederson, E., Feraru, E., Cooper, E.D., Karimi, M., Delwiche, C.F., Ljung, K., Geisler M., Sundberg E., and Friml J. (2014). Directional Auxin Transport Mechanisms in Early Diverging Land Plants. Current Biology, in press

186. Vieten A., Vanneste S., Wisniewska J., Benková E., Benjamins R., Beeckman T., Luschnig C., and Friml J. (2005). Functional redundancy of PIN proteins is accompanied by auxin-dependent cross-regulation of PIN expression. Development 132: 4521–4531.

187. Wabnik, K., Robert, H.S., Smith, R.S., and Friml, J. (2013). Modeling Framework for the Establishment of the Apical-Basal Embryonic Axis in Plants. Current Biology 23: 2513–2518.

188. Wang, C., Yan, X., Chen, Q., Jiang, N., Fu, W., Ma, B., Liu, J., Li, C., Bednarek, S.Y., and Pan, J. (2013). Clathrin Light Chains Regulate Clathrin-Mediated Trafficking, Auxin Signaling, and Development in Arabidopsis. The Plant Cell 25: 499–516.

189. Went, F.W. (1974). Reflections and speculations. Annual Review of Plant Physiology 25: 1–27.

190. Whitford R., Fernandez A., Tejos R., Pérez A.C., Kleine-Vehn J., Vanneste S., Drozdzecki A., Leitner J., Abas L., Aerts M., Hoogewijs K., Baster P., De Groodt R., Lin Y.C., Storme V., Van de Peer Y., Beeckman T., Madder A., Devreese B., Luschnig C., Friml J., and Hilson P. (2012). GOLVEN Secretory Peptides Regulate Auxin Carrier Turnover during Plant Gravitropic Responses. Developmental Cell 22: 678–685.

191. Widhalm, J.R., Ducluzeau, A.L., Buller, N.E., Elowsky, C.G., Olsen, L.J., and Basset, G.J.C. (2012). Phylloquinone (vitamin K1) biosynthesis in plants: Two peroxisomal thioesterases of lactobacillales origin hydrolyze 1,4-dihydroxy-2-naphthoyl-coa. Plant J. 71: 205–215.

192. Willige, B.C., Ahlers, S., Zourelidou, M., Barbosa, I.C.R., Demarsy, E., Trevisan, M., Davis, P.A., Roelfsema, M.R.G., Hangarter, R., Fankhauser, C., and Schwechheimer, C. (2013). D6PK AGCVIII Kinases Are Required for Auxin Transport and Phototropic Hypocotyl Bending in Arabidopsis. The Plant Cell 25: 1674–1688.

193. Willige, B.C., Isono, E., Richter, R., Zourelidou, M., and Schwechheimer, C. (2011). Gibberellin Regulates PIN-FORMED Abundance and Is Required for Auxin Transport-

Dependent Growth and Development in Arabidopsis thaliana. The Plant Cell 23: 2184–2195.

194. Wisniewska J., Xu J., Seifertová D., Brewer P.B., Ruzicka K., Blilou I., Rouquié D., Benková E., Scheres B., and Friml J. (2006). Polar PIN Localization Directs Auxin Flow in Plants. Science 312: 883–883.

195. Wisniewska, J., Xu, J., Seifertová, D., Brewer, P.B., Ruzicka, K., Blilou, I., Rouquié, D., Benková, E., Scheres, B., and Friml, J. (2006). Polar PIN localization directs auxin flow in plants. Science 312: 883.

196. Xu T., Dai N., Chen J., Nagawa S., Cao M., Li H., Zhou Z., Chen X., De Rycke R., Rakusová H., Wang W., Jones A.M., Friml J., Patterson S.E., Bleecker A.B., and Yang Z. (2014). Cell Surface ABP1-TMK Auxin-Sensing Complex Activates ROP GTPase Signaling. Science 343: 1025–1028.

197. Yamaoka, S., Shimono, Y., Shirakawa, M., Fukao, Y., Kawase, T., Hatsugai, N., Tamura, K., Shimada, T., and Hara-Nishimura, I. (2013). Identification and dynamics of Arabidopsis adaptor protein-2 complex and its involvement in floral organ development. Plant Cell 25: 2958–69.

198. Yang, H. and Murphy, A.S. (2009). Functional expression and characterization of Arabidopsis ABCB, AUX 1 and PIN auxin transporters in Schizosaccharomyces pombe. The Plant Journal 59: 179–191.

199. Zádníková P., Petrásek J., Marhavy P., Raz V., Vandenbussche F., Ding Z., Schwarzerová K., Morita M.T., Tasaka M., Hejátko J., Van Der Straeten D., Friml J., and Benková E. (2010). Role of PIN-mediated auxin efflux in apical hook development of Arabidopsis thaliana. Development 137: 607–617.

200. Zhang J., Vanneste S., Brewer P.B., Michniewicz M., Grones P., Kleine-Vehn J., Löfke C., Teichmann T., Bielach A., Cannoot B., Hoyerová K., Chen X., Xue HW., Benková E., Zažímalová E., and Friml J. (2011). Inositol Trisphosphate-Induced Ca2+ Signaling Modulates Auxin Transport and PIN Polarity. Developmental Cell 20: 855–866.

201. Zhang, J., Nodzynski, T., Pencik, A., Rolcik, J., and Friml, J. (2010). PIN phosphorylation is sufficient to mediate PIN polarity and direct auxin transport. Proceedings of the National Academy of Sciences 107: 918–922.

202. Zhang, X. and Oppenheimer, D.G. (2009). Irregular Trichome Branch 2 (ITB2) encodes a putative aminophospholipid translocase that regulates trichome branch elongation in Arabidopsis. Plant J. 60: 195–206.

203. Zhang, Y., Persson, S., Hirst, J., Robinson, M.S., van Damme, D., and Sanchez-Rodriguez, C. (2015). Change your Tplate, change your fate: Plant CME and beyond. Trends Plant Sci. 20: 41–48.

204. Zhao, X., Greener, T., Al-Hasani, H., Cushman, S.W., Eisenberg, E., and Greene, L.E. (2001). Expression of auxilin or AP180 inhibits endocytosis by mislocalizing clathrin:

evidence for formation of nascent pits containing AP1 or AP2 but not clathrin. J. Cell Sci. 114: 353–365.

205. Zhuang, X., Wang, H., Lam, S.K., Gao, C., Wang, X., Cai, Y., and Jiang, L. (2013). A BAR-domain protein SH3P2, which binds to phosphatidylinositol 3-phosphate and ATG8, regulates autophagosome formation in Arabidopsis. Plant Cell 25: 4596–615.

206. Zouhar, J. and Sauer, M. (2014). Helping Hands for Budding Prospects: ENTH/ANTH/VHS Accessory Proteins in Endocytosis, Vacuolar Transport, and Secretion. Plant Cell Online 26: 4232–4244.

207. Zourelidou, M., Absmanner, B., Weller, B., Barbosa, I.C., Willige, B.C., Fastner, A., Streit, V., Port, S.A., Colcombet, J., van Bentem, S. de la F., Hirt H., Kuster B., Schulze W.X., Hammes U.Z., and Schwechheimer C. (2014). Auxin efflux by PIN-FORMED proteins is activated by two different protein kinases, D6 PROTEIN KINASE and PINOID. Elife 3: e02860.

208. Zourelidou, M., Muller, I., Willige, B.C., Nill, C., Jikumaru, Y., Li, H., and Schwechheimer, C. (2009). The polarly localized D6 PROTEIN KINASE is required for efficient auxin transport in Arabidopsis thaliana. Development 136: 627–636.

209. Zuo, J., Niu, Q.W., and Chua, N.H. (2000). An estrogen receptor-based transactivator XVE mediates highly inducible gene expression in transgenic plants. Plant J. 24: 265–273.

210. Zwiewka, M. and Friml, J. (2012). Fluorescence Imaging-Based Forward Genetic Screens to Identify Trafficking Regulators in Plants. Frontiers in Plant Science 3.

211. Zwiewka, M., Feraru, E., Möller, B., Hwang, I., Feraru, M.I., Kleine-Vehn, J., Weijers, D., and Friml, J. (2011). The AP-3 adaptor complex is required for vacuolar function in Arabidopsis. Cell Research 21: 1711–1722.

212. Zwiewka, M., Nodzynski, T., Robert, S., and Vanneste, S. (2015). Osmotic stress modulates the balance between exocytosis and clathrin-mediated endocytosis in Arabidopsis thaliana. Mol Plant. 2015 Aug;8(8):1175-87